

Geological Storage of CO₂: Sensitivity and Risk Analysis

Meisam Ashraf



Dissertation for the degree of Philosophiae Doctor (PhD)

Department of Mathematics
University of Bergen

October 2013

Chapter 1

Introduction to the papers

1.1 Introduction

The main scientific part of this thesis consists of three papers. They come in a sequence to show the research progress within this PhD program. Paper I includes a detailed study on the flow responses and effect of relative permeability on the flow and it is submitted to the International Journal of Greenhouse Gas Control (IJGGC). Pressure is an important model response during injection operations. Therefore, a special study is dedicated to pressure analysis in the system. This is reported in Paper II, which is submitted to the IJGGC. Finally, Paper III reports modern stochastic techniques used to perform detailed quantitative sensitivity analysis and probabilistic risk assessments. This paper is accepted for publication in the IJGGC.

1.2 Summary of papers

Paper I: Impact of geological heterogeneity on early-stage CO₂ plume migration

Summary:

It is a conventional practice in the context of CO₂ storage study to simplify the geological modeling to achieve an easier force balance study in the medium. Assuming a homogeneous medium is the first step to quantify the temporal and spatial scales in CO₂ storage problems by a dimensionless analysis on the analytical solution of flow equation. However, in practice the real flow performance is very much influenced by geological heterogeneity.

We use a set of SAIGUP realizations selected to cover the variability of four sedimentological and structural parameters. The selected parameters are lobosity, barriers, aggradation angle, progradation direction. Each of these parameters varies over three levels, except the progradation direction, which includes up-dip and down-dip directions. Combining the available parameters makes 54 realizations.

30 years of injection and 70 years of early migration of CO₂ are simulated and flow responses related to the storage capacity and leakage risk objectives are defined and calculated from the simulation results. The responses are reported in scatter plots at the end of injection and at the end of early migration time.

This work is specific in examining how heterogeneity influences flow behavior by using a number of geological realizations. Flow responses defined in this work are specific to CO₂ studies and differ from the responses used in the original SAIGUP project to study oil recovery. We simulate the aquifer average pressure, model boundary fluxes, residual and mobile CO₂ saturation, and spatial distribution of connected CO₂ volumes. These responses can be considered to evaluate the site storage capacity and risk of CO₂ leakage to surface.

Comments:

This work initially was presented at the Edinburgh 2010 ACM conference, in a brief proceedings presentation, and more details of the work are reported in a proceedings for CMWR 2010 conference in Barcelona. The aim of this paper is to investigate the impact of geological heterogeneity on a typical CO₂ injection problem.

The main concern here is to include realistic geological heterogeneity knowledge

into flow simulation work-flow, which is specific to the CO₂ storage problem. Results of this work conclude that the range of variability in flow responses indicate the significance of geological heterogeneity in modeling the CO₂ flow. Geological features are ranked by for their impact on each of the defined flow responses and in particular, aggradation angle has shown a big impact in most of the responses.

This paper lacks the quantitative sensitivity analysis, which was added in later works.

Contribution of the candidate:

Major part of the work is done by the candidate. This includes:

- Defining the problem.
- Designing the simulation scenarios.
- Defining the simulation responses.
- Performing the simulations and processing the simulation results.
- Analyzing the results.
- Writing the report.

The candidate has received helps from the co-authors mainly on analyzing the simulation results and writing the report. This has been through discussion meetings and review comments on the draft report originally written by the candidate.

Paper II: Impact of geological heterogeneity on early-stage CO₂ plume migration: sensitivity study

Summary:

In this paper, we consider faults in addition to the four geological parameters used in Paper I. In the SAIGUP study, fault modeling is performed in an intensive variability over structural parameters and transmissibility across the fault. To keep the work less succinct and conclusive in studying the dynamics of flow, we fix the structural variability in its medium level and vary the transmissibility over three main levels: unfaulted, open faults and closed faults.

The flow responses analyzed are the same as defined in Paper I. In addition, we perform a linear sensitivity analysis for the flow responses with respect to the geological variations. The outcome of the sensitivity analysis shows that the flow behavior is highly sensitive to aggradation angle. Barriers and faulting will also influence the flow responses significantly. In this work, similar to Paper I, we clearly see the range variation in flow responses which demonstrates how important it is to model the geological features accurately.

Comments:

- *The SAIGUP realizations*

This paper is presented in ECMOR conference in Oxford, 2010. This is a complementary to proceedings works presented in ACM Edinburgh, 2009 and CMWR in Barcelona, 2010.

Topography is a major player in the gravity dominated flow behavior. The SAIGUP realizations include variability in topography of the geological layering via structural changes due to faults and also barriers in the model. These are good enough for early migration when the CO₂ and water segregate and plumes accumulate below cap-rock and start the longer migration. In the long-term migration, top surface geometry is an important geological parameter and larger models than the SAIGUP models with a better resolution of the top surface are needed to get good predictions of the long-term migration phase. This was considered in the next generation of geological studies performed following this study [1, 2] under the IGEMS research project.

- *Physical assumptions*

The work concentrates on how geological heterogeneity impacts the flow performance. We need to measure the volumetric sweep efficiency of CO₂ plumes to evaluate the residual trapping. The most important parameter is the rock transmissibility, rather than fluid properties. Including more physics in the modeling will add the computational costs specially when the flow modeling is used in a sensitivity analysis or risk assessment process. Therefore, we used simple fluid models for PVT.

To accelerate the flow, we used linear relative permeability curves. This increases the flow mobility in the low saturation values. However, in CO₂-water system the relative permeability curves are closer to a quadratic function. This is investigated in the next paper (Paper III). Hysteresis effects are modeled by changing the endpoints in the relative permeability curves and no scanning-curves is considered here. During injection, the main process is drainage. After injection, the imbibition process starts and mostly is a replacement of CO₂ by water due to gravity segregation. This justifies the usage of simple hysteresis model, and more detailed study can be done to investigate this influence in a quantitative manner.

- *Uncertainty considerations*

Our main motivation for using the SAIGUP data was the extensive work that was put into building realistic geological realizations. The geological parameters are changed in value between low and high levels. These values are assumed with the same probability, which is a reasonable start point for sensitivity analysis. In general, this probability might not be uniform, depending to the regional geology of the storage site.

Contribution of the candidate:

The study was a joint work between the candidate and the co-authors on the following steps:

- Defining the problem.

- Designing the simulation scenarios.
- Defining the simulation responses.
- Performing the simulations and processing the simulation results.
- Analyzing the results.
- Writing the report.

The candidate had a solid and major contribution in every step. Performing simulations and processing the simulation results were done solely by the candidate.

Paper III: Impact of geological heterogeneity on early-stage CO₂ plume migration: sensitivity study

Summary:

In this paper, we use the same setup that is used in Paper II. Five geological features are examined, which are lobosity, barriers, aggradational angle, progradational direction, and faults. Also, the same injection scenario is used: 30 years of CO₂ injection and 70 years of early migration. The injector is controlled by a constant rate and no pressure constraint is set to allow for all ranges of pressure, including those that are unrealistic. Moreover, we define an additional model output that is related to the risk of CO₂ leakage through any breakings in the cap-rock.

We examine the influence of simplifying assumptions considered in our work regarding linearity of relative permeability function. We perform a detailed flow analysis on various geological realizations using two different relative permeability relations: linear and quadratic functions. The non-linearity in relative permeability hinders the flow in the lower saturation values of the displaced phase, i.e., water phase. We discuss the influence of curvature on CO₂ flow dynamics within the aquifer. Finally, we perform a quantitative sensitivity analysis by using the flow simulation results. The sensitivity analysis results suggest that aggradational angle, fault criteria, and progradational direction are the most influential geological parameter in our study.

Comments:

Results show that using linear relative permeability function ends up in conservative conclusions with respect to CO₂ distributions in the domain in terms of storage safety. Since computational costs are much lower for linear relative permeability scenario than quadratic relative permeability, it sounds a good strategy to perform sensitivity analysis by using linear relative permeability function on flow responses that are based on CO₂ distribution in the domain.

However, dramatic pressure build-up can happen in the medium during injection in the quadratic relative permeability scenario. This suggests that for pressure studies we must use more realistic relative permeability functions. Following this work, a detailed pressure study with more realistic relative permeability curves is performed, which is reported in the next paper.

Within one geological realization, injection location can dramatically impact the injectivity of the well. In fact, this is an uncertain parameter in the CO₂ storage operations. Choosing to inject in the river channels or in the permeable homogeneous parts

near the shore will enhance the injectivity and the CO₂ sweep efficiency in the medium. On the other hand, injecting in the locations with low permeabilities and pore-volumes can significantly increase the injection pressure, while limiting the transport of CO₂ in the medium. Studying the impact of injection location can be performed by injecting in many different points in one realization and comparing the corresponding flow responses. However, this will considerably increase the number of detailed simulations in the study.

For the allowed time, we limited our study to a fixed point by injecting via one well in the flank part of the SAIGUP models. This location is selected after qualitative analysis of a detailed study on a homogeneous case. There, we aimed to fulfill the criterion of maximizing the CO₂ storage volume via increasing the vertical travel path towards the structural trap location under the cap-rock. One mitigating strategy for minimizing the effect of injection location can be to inject via several wells in different location in the medium.

Similar argument applies to the leakage risk study reported here. We use a leakage probability over the cap-rock that can dramatically influence the calculated leakage risk. We take this assumption to simplify the way we introduce the method.

Contribution of the candidate:

Major part of the work is done by the candidate. This includes:

- Defining the problem.
- Designing the simulation scenarios.
- Defining the simulation responses.
- Performing the simulations and processing the simulation results.
- Analyzing the results.
- Writing the report.

The candidate has received helps from the co-authors mainly on analyzing the simulation results and writing the report. This has been through discussion meetings and review comments on the draft report originally written by the candidate.

Paper IV: Geological storage of CO₂: heterogeneity impact on pressure behavior

Summary:

After observing the influence of relative permeability curvature on pressure response for CO₂ injection studies, in this paper we perform a detailed pressure study on the chosen geological realizations.

Pressure build-up is an important criterion that can determine the success and failure of CO₂ storage operations. Over-pressurized injections can induce new fractures and open the existing faults and fractures that increases the risk of leakage for the mobile CO₂ in the domain. On the other hand, the pressure disturbance imposed on the system travels within the domain beyond the scales of CO₂ distribution. If the CO₂ is injected into a saline aquifer connected to fresh water aquifers, the pressure pulse may result in

fresh water contaminations by the brine far from the injection point. We define specific pressure responses to examine the pressure disturbance in the system during injection.

Two injection scenarios are examined for the same 160 geological realizations setup. In the first scenario, the injector is set to a fixed volumetric rate to inject the CO₂ volume in 30 years into the domain, allowing for an unlimited pressure build-up. In the second scenario, a pressure constraint is set on the injector that results in various rate of injection in different geological realizations to inject the same amount of CO₂ volume considered in the first injection scenario.

Pressure response sensitivity study with respect to different geological features indicates the significance of aggradational angle, progradation direction, and faults during injection. A probabilistic pressure analysis is also performed based on the 160 simulations on the available realizations.

Contribution of the candidate:

Almost all parts of the work is done by the candidate. This includes:

- Defining the problem.
- Designing the simulation scenarios.
- Defining the simulation responses.
- Performing the simulations and processing the simulation results.
- Analyzing the results.
- Writing the report.

The candidate has received helps from the first adviser mainly on writing the report. This has been through review comments on the draft report originally written by the candidate.

Paper V: Geological storage of CO₂: global sensitivity analysis and risk assessment using the arbitrary polynomial chaos expansion

Summary:

In this paper, we perform a stochastic sensitivity and risk analysis. We obtain a high resolution global sensitivity and probabilistic study on the flow responses that are defined and discussed in the previous papers. We choose barriers, aggradational angle, and faults from the SAIGUP geological parameters. Faults are considered by changing the transmissibility value across them, which is a continuous parameter. One more parameter is added to the study which is common in the literature and models the external pressure support from other aquifers attached to the model (regional groundwater effect).

Flow simulation on high resolution variational geology demands a huge computational costs. To enhance the calculation speed, we use a data-driven method that does not need to solve the full physical flow equations. We approximate the flow solver by a response surface method that is a polynomial and relates the system output to the input with a minimal computational cost. We use the arbitrary polynomial chaos expansion

(aPC) to approximate the flow responses. The aPC method considers the uncertainty in the input variables.

A global sensitivity analysis is performed by employing Sobol indices that are based on variances of responses. The method is shown to be robust in problems of high levels of complexity and non-linearity.

And finally, we perform a Monte-Carlo process using the approximating polynomial on a high resolution input variations. This makes it possible to perform a high resolution probabilistic study on the flow responses. This way, extreme cases can be identified by probability of occurrence.

Comments:

To implement our stochastic technique, we choose geological parameters in this study that can be interpolated between two levels of their values. For example, it makes sense to use barriers coverage level of 25% between the low (10%) and medium (50%) levels used in the previous studies. Some of the geological parameters are discrete and can not be interpolated between two values. For instance, lobosity can only be varied over three points and we can not define a 1.5-lobe.

Having a large number of points in the input values interval requires intensive geological modelings to be used in the flow simulations. Using the data-driven polynomial, the approach only needs evaluating the polynomial in the defined values, and there is no need for full geological modeling except in the collocation points, i.e., point values that the polynomial coefficients must be calculated.

The work reported here is to demonstrate the work-flow of using the aPC for global sensitivity analysis and probabilistic risk assessment. A normal work-flow starts by defining the uncertainties in the input parameters and follows by building the geological models for the aPC collocation points that are based on those uncertainties. To perform this study on the SAIGUP models that are consistent with a uniform uncertainty in the geological parameters, with no loss of generality, we used uniform uncertainty distributions for our study. However, the aPC method is not limited to uniform uncertainty descriptions.

Geological features are ranked based on the sensitivity analysis results. The results are in agreement with dynamics of the flow in the aquifer. Aggradation angle is the most influential parameter, while the regional groundwater has the least influence in the model responses. The study is not limited to the assumed uncertainty of input parameters and the conclusion may change for a very different uncertainty description.

Contribution of the candidate:

Major part of the work is done by the candidate. This includes:

- Defining the problem.
- Designing the simulation scenarios.
- Designing the work-flow.
- Integrating the aPC MATLAB code into the work-flow.
- Performing the runs and processing the results.

- Performing the global sensitivity analysis.
- Performing the risk assessment.
- Analyzing the results and preparing plots.
- Writing the report.

The candidate received help from the co-authors and others involved in defining the problem and writing the report. The report has gone through extensive reviews, after it was originally written by the candidate. The core of the report, including the formulation of the method, the description of the modeling, the presentation of the results, and discussions on the results are originally written by the candidate. The review comments resulted in additional elaborations on the pressure issue and some discussions on the aPC technique when it is compared to other techniques in the literature. The candidate received support from the co-authors on the aPC directly related comments.

Chapter 2

Scientific results

Paper I

2.1 Impact of geological heterogeneity on early-stage CO₂ plume migration: pressure behavior study

M. Ashraf, K.A. Lie, H.M. Nilsen & A. Skorstad

Submitted to *International Journal of Greenhouse Gas Control (IJGGC)*

Impact of Geological Heterogeneity on Early-Stage CO₂-Plume Migration: Sensitivity Study

Meisam Ashraf Knut-Andreas Lie Halvor M. Nilsen Arne Skorstad

November 29, 2011

1 Introduction

Underground sequestration of CO₂ produced from localized sources like power plants and oil and gas recovery sites has been proposed as a possible solution to reduce the rate of anthropogenic CO₂ emission into the atmosphere [5, 2]. Much of the technology required to inject CO₂ into saline aquifers, unminable coal seams, and abandoned reservoirs is already available from the petroleum and mining industry. However, before large-scale storage operations can be initiated, answers to practical questions regarding operational safety and the fate of the injected CO₂ need to be answered. The main concern for policy makers and the general public is the risk of leakage, i.e., how likely it is that the injected CO₂ (or highly saline brine) will migrate into water resources, active petroleum reservoirs, or back to the surface via conductive features like fractures and faults, through ill-plugged wells [10], or through caprocks broken by the high pressure imposed to the system during the injection operation. Likewise, there is a concern about pressure buildup, which may extend much further than the injected CO₂ plume (the effluent of CO₂ into brine). In other words, the operator of a potential injection site needs to maximize storage volumes while minimizing leakage risks and effects on areas surrounding the injection point.

The flow of CO₂ in the subsurface is governed by a very complex interaction between physical forces acting on the reservoir fluids and properties of the reservoir rock itself. To determine the fate of the injected CO₂, it is necessary to develop effective (numerical) models that can be used to accurately describe the pertinent flow dynamics during injection and the subsequent migration period. Moreover, the numerical models must also properly account for geological heterogeneity—i.e., variations in hydraulic conductivity and fluid storage—and how this heterogeneity influences the flow dynamics. Geological heterogeneity is recognized as a major control mechanism within petroleum production [3] and an important constraint on many aspects of quantitative hydrogeology. For this reason, much effort has been devoted to understand and represent geological heterogeneity in flow models, see e.g., [4]. The understanding of the geology of a specific reservoir or aquifer is typically limited and the description of the geological heterogeneity will usually have large uncertainties attached. If flow simulations are to be used to assess risks associated with a storage operation, the numerical flow model must properly account for the impact of uncertainty in the geological description. Yet, academic studies of CO₂ injection commonly employ simplified or conceptualized reservoir descriptions, in which the medium is considered (nearly) homogeneous, and instead focus on developing complex flow models, discretization schemes, and solvers.

Within oil recovery, the impact of geological uncertainty on production forecasts has been thoroughly investigated in the SAIGUP project [8, 6, 9], in which an ensemble of synthetic but realistic models of shallow-marine reservoirs were generated and several thousand cases were run for different production scenarios. The results showed that realistic variations in the structural and sedimentological description has a strong influence on production responses. Simulation of CO₂ storage involves temporal and spatial scales and density ratios that are quite different from those encountered in oil recovery. Potential storage sites may also have geological characteristics that differ from those seen in producible oil reservoirs. For these reasons, one cannot expect that knowledge of how geological heterogeneity impacts flow predictions of oil-water systems can be carried directly over to CO₂-brine systems relevant for CO₂ injection scenarios. Nevertheless, we will herein consider a scenario in which CO₂ is injected into an abandoned shallow-marine reservoir and use geological realizations generated as part of the SAIGUP project to study the impact of geological heterogeneity on the early-stage

migration of the CO₂ plume. How heterogeneity impacts the injection operation will be studied in a separate work, in which we also discuss more realistic pressure constraints on the injection operation.

Our work is a continuation of an early study reported in [1], which focused on a few primary flow responses. Herein, we will also include flow responses that relate more directly to leakage risk. In addition, we evaluate how curvatures in the relative-permeability model influences plume migration; this as a complement to previous studies of endpoint and hysteresis effects, see e.g., [11, 7].

2 Model Setup

In this study, we will consider a storage operation in which supercritical CO₂ is injected into a shallow-marine reservoir underneath a sealing caprock that forms a type of structural trap that is often seen in petroleum reservoirs. To represent the aquifer geology, we use an ensemble of synthetic models developed in the SAIGUP study [8]. In this study, data were collected from many different sources to develop representative, parametrized models that span realistic parameter intervals for progradational shallow-marine depositional systems with limited tidal influence [6]. An ensemble of geostatistical realizations were then made from the parametrized model, each having a heterogeneity and geometrical complexity as seen in real-life models of petroleum reservoirs. In our study, we have selected the following five parameters that altogether give 160 realizations:

Lobosity – is defined by the plan-view shape of the shoreline. As a varying parameter, lobosity indicates the level at which the shallow-marine system is dominated by each of the main depositional processes. Two depositional processes are considered in the SAIGUP study: fluvial and wave processes. The higher the amount of sediment supply provided from rivers is relative to the available accommodation space in the shallow sea, the more fluvial dominant the process will be. As the river enters the mouth of the sea, it can divide into different lobes and branches. Wave processes from the sea-side smear this effect and flatten the shoreline shape. Less wave effect produces more pronounced lobe shapes around the river mouths. Very high permeability and porosity can be found in the channeling branches, while dense rock with low permeability fills the space between them. Reservoir quality decreases with distance from the shore-face. We expect that the level of lobosity can have a considerable effect on the CO₂ injection and plume size in the aquifer. In this study, models of three levels of lobosity are used: flat shoreline, one lobe and two lobes, as illustrated in the upper row of Figure 1.

Barriers – Periodic floods result in a sheet of sandstone that dips, thins, and fines in a seaward direction. In the lower front, thin sheets of sandstone are interbedded with mud-stones deposited from suspension. These mud-draped surfaces will potentially act as significant barriers to both horizontal and vertical flow, and are modeled by transmissibility multipliers corresponding to three levels of coverage for the barrier sheet: low (10%), medium (50%), and high (90%), as illustrated in the middle row of Figure 1.

Aggradation – In shallow-marine systems, two main factors control the shape of the transition zone between river and basin: amount of deposition supplied by the river and the accommodation space that the sea provides for these depositional masses. One can imagine a constant situation in which the river is entering the sea and the flow slows down until stagnation. The deposition happens in a spectrum from larger grains depositing at the river mouth to fine deposits in the deep basin. If the river flux or sea level fluctuates, the equilibrium changes into a new bedding shape based on the balance of these factors. The SAIGUP data models cases in which, for instance, the river flux increases and shifts the whole depositional system into the sea. The angle at which the transitional deposits are stacked on each-other because of this shifting, is called aggradation angle. Three levels of aggradation are modeled here: low, medium, and high angles. The three parameter choices are illustrated in the bottom row of Figure 1, where we in particular notice how a low aggradation angle gives continuous facies layering parallel to the dip direction of the model.

Progradation – denotes the direction of the depositional dip. Two types are considered here: up and down the dominant structural dip. Because the model is tilted a little, this corresponds to the lobe direction from flank to crest or vice versa.

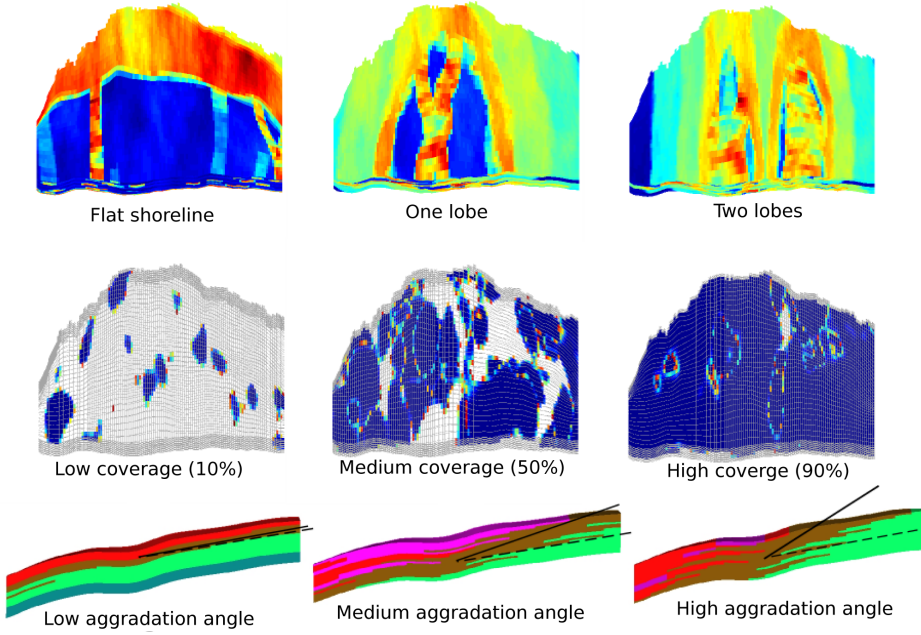


Figure 1: Illustration of geological parameters from the SAIGUP study: the top row shows three different lobosities for up-dip progradation (if the lobes flip over the long axis, we will have down-dip progradation); the middle row shows barriers representing different degrees of mud-draped coverage; and the bottom row shows aggradational angle.

Table 1: Geological features from the SAIGUP project included in this study. The last column reports markers used to distinguish different features in the plots.

Feature	Levels	Marker
Lobosity	flat, one-lobe, two-lobe	square, circle, diamond
Barrier	low(10%), medium(50%), high(90%)	small, medium, large
Aggradational angle	low(parallel layering), medium, high	blue, green, red
Progradation	up-dip, down-dip	first half, second half
Fault	unfaulted, open faults, closed faults	thin, medium, thick

Fault – are represented by three different parameters in the SAIGUP study: fault type, intensity, and transmissibility. Herein, we limit our study to compartment faults of medium intensity and consider three parameter choices: no faults, open faults, and closed faults.

Table 1 lists the markers (shape, size, color, thickness) that will be used to signify different parameters values in plots of simulation results later in the paper.

We will consider storage of forty million cubic meters of supercritical CO₂, which amounts to approximately 20% of the total pore volume in the aquifer and will be injected from a single well over a period of thirty years. After the injection period, seventy years of plume migration is simulated for all cases. If the medium was homogeneous, we would expect that the injection will create one big plume that moves upward because of the gravity force until it accumulates under the structural trap of the caprock, i.e., migrating from the injection point and upward to the crest of the aquifer. The idea is therefore to inject as deep as possible to increase the travel path and the volume swept by the plume before it reaches the crest. To this end, the injector is placed down in the flank and only completed in the three lowest layers of the aquifer. Hydrostatic boundary conditions are imposed on the sides, except at the faulted side on the crest, and no-flow boundary conditions are imposed on the top and bottom surfaces.

The injected CO₂ is assumed to be a supercritical fluid with density 700 kg/m³ and viscosity 0.04 cP. The supercritical fluid is modeled as a dead oil with a formation factor of 1.1 at 0 bar and 0.95 at 400 bar. Brine is assumed to be slightly compressible ($3.03 \cdot 10^{-6}$ psi⁻¹) with density 1033 kg/m³ and

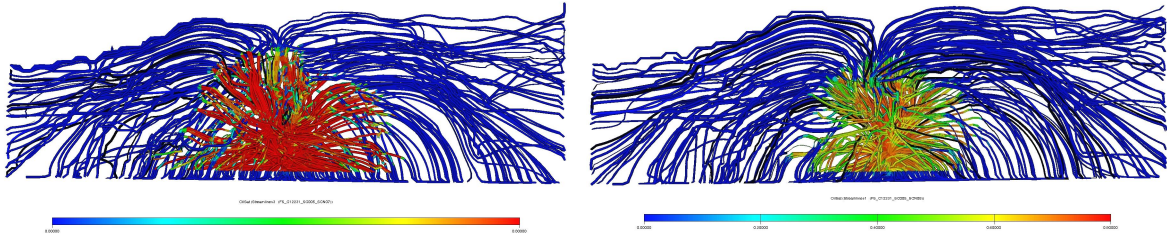


Figure 2: CO₂ saturation plotted on streamlines for linear relative permeabilities (left) and quadratic permeabilities (right).

viscosity 0.4 cP. The rock compressibility is set to $3 \cdot 10^{-7}$. For both fluids, we will use Corey-type relative permeability functions

$$k_{rCO_2} = (1 - S)^\alpha, \quad k_{rw} = S^\alpha, \quad \alpha = 1, 2$$

where S denotes the saturation of brine normalized for end points 0.2 and 0.8.

3 Basic Flow Responses

In this section we will give a qualitative discussion of how some basic flow responses like the wave speeds of the plume migration, average aquifer pressure, mobile and residually trapped volumes, and plume sizes are affected by variations in the geological parameters.

3.1 Effect of relative permeability curvature

How the geological heterogeneity impacts the plume migration will depend upon the fluid model. We therefore start by discussing the choice of relative permeability functions. Previous studies have mainly looked at hysteresis and effects from saturation endpoints, see e.g., [7]. However, the curvature of relative permeability function will also play a significant role and in the following we will therefore consider both linear and quadratic relative permeability curves. In oil recovery processes, the efficiency of flooding increases by the higher viscosity of displacing fluid. For example in water-flooding, increasing the water viscosity using additives is a way to increase the process efficiency. For CO₂ storage, on the other hand, we are interested in mixing brine and CO₂ to increase the rate of dissolution; a lower viscosity of CO₂ compared to brine helps this aim.

With linear relative permeability and a CO₂ viscosity of tenth of the brine viscosity, there will be no sharp displacement front in the system and CO₂ invades the brine zone in a spectrum of rarefaction waves from zero to the maximum possible saturation (0.8 in our case). On the other hand, with quadratic relative permeability functions, there will be a sharp displacement front with a saturation around 0.4 followed by rarefactions.

To illustrate the different behavior of linear and quadratic relative permeabilities, we have picked one of the SAIGUP models which includes one shoreline lobe, medium level of barriers, high aggradation angle, up-dip progradation, and open faults. Figure 2 shows the CO₂ distribution resulting from the two different relative permeability functions. Although the streamline paths appear to be almost identical, there are significant differences in the extent of the plume and the saturation profile inside. With linear relative permeability and a CO₂ viscosity of tenth of the brine viscosity, there will be no sharp displacement front in the system and CO₂ invades the brine zone as a rarefaction fan from zero to the maximum possible saturation. In the left plot of Figure 2, this is observed as a spectrum of saturations ranging from zero to 0.8 and then a bank of constant saturation down to the injector (the red color region around the well). With quadratic relative permeabilities, on the other hand, there will be a sharp displacement front followed by a rarefaction fan. The front (with a saturation around 0.4) is recognizable followed by rarefactions down to the injector in the right plot of Figure 2.

In the simulation we observe that a significantly larger volume of injected CO₂ escapes through the down boundary in the quadratic case. The reason is that the mobility will be higher in the linear case and the wave speed at the tip of the rarefaction fan is significantly faster than the wave speed of the

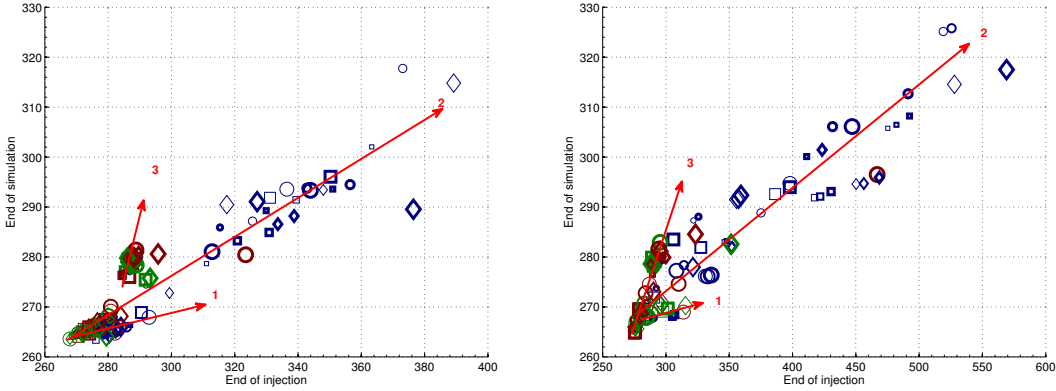


Figure 3: Cross-plot of average aquifer pressure at the end of simulation versus at the end of injection for linear (left) and quadratic (right) relative permeabilities.

displacement front for the quadratic case; compare the size of the two plumes in Figure 2. This means that the CO₂ plume will spread easier in the medium resulting in less flow through the boundary closest to the injector. Because of the lower mobility values in the quadratic case, more mass of CO₂ will be almost immobilized in the medium and the CO₂ plume will migrate very slowly compared with the linear case. Secondly, we observe higher pressures in the system during injection for quadratic permeabilities. The curvature of the quadratic curve gives lower mobility of CO₂ for small saturation values, and thence higher injection pressure is required to move the flow in the medium.

3.2 Pressure responses

The average aquifer pressure in general shows a sharp jump at the start of injection and a declining trend during injection and plume migration caused by pressure release through the open boundaries. (Specifying different boundary conditions would have resulted in different pressure trends). Figure 3 shows cross-plots of the average aquifer pressure at the end of injection and end of simulation for our two different choices of relative permeability functions. In both plots, one can recognize three different trends which have been indicated by three straight lines. The first trend, which has the lowest slope, represents cases with large pressure variation during injection and small range of pressure variation during the migration phase that follows after the end of injection. In these cases, the heterogeneity of the medium forms channels towards the open boundaries through which the injection pressure is released, resulting in low aquifer pressure at the end of simulation. The second trend, represents cases in which the heterogeneity affects injection, gravity segregation, and flow through open boundaries. In particular, we observe that most cases that have high injection pressure correspond to a low aggradation angle, for which low vertical permeability forces the injected CO₂ plume to move relatively slow in the lowest, poor-quality layers before migrating up towards the caprock. This increases the pressure in the domain during injection and keeps a higher pressure gradient to the open boundaries. In the third trend, the heterogeneity makes chambers and compartments in which the pressure increases during injection and then remains high. Cases with closed faults are of this class. The heterogeneity in these cases affects the gravity segregation process more than in the two other trends because of faults and a high level of barriers.

We also see the effect of curvature in the relative permeabilities by comparing the two plots. Higher range of pressure variations is observed during injection for the nonlinear relative permeability runs. Moreover, nonlinear relative permeability gives lower mobility which leads to higher pressure build-up during injection. This means that longer time is required for the pressure to be released through the open boundaries after injection and more cases therefore follow the second and third trend.

More details about the bottom-hole pressure will be given in a forthcoming paper, in which we also will discuss more realistic constraints on the injection operation.

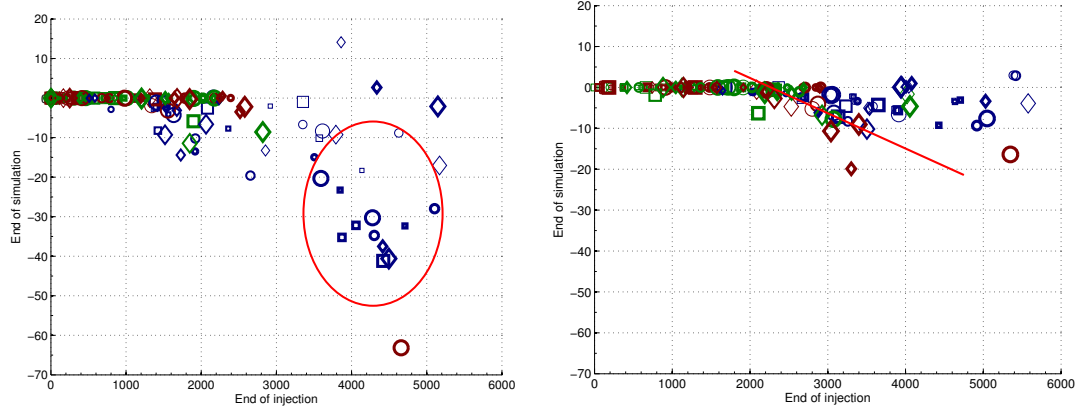


Figure 4: Cross-plot of CO₂ flux out over the down-dip boundary for linear (left) and quadratic (right) relative permeabilities. Positive values represent outward fluxes and negative values represent inward fluxes.

3.3 Plume migration

The direction in which the CO₂ plume moves in the medium will primarily impact the amount of residual (and structural) trapping, but as we will see later, also significantly change the risk for leakage through breaches and holes in the caprock. When evaluating the safety of a long-term storage operation, there are several potentially conflicting aspects that need to be considered with regard to plume migration. On one hand, we prefer the plume to spread out laterally to enhance residual trapping and mixing of CO₂ and brine, while on the other hand we want to confine the plume to the smallest volume possible to minimize the the risk of leakage and contamination into other aquifers, minimize the contact with potential leakage points and simplify monitoring operations. To investigate this aspect, we will study the sweep efficiency in local regions. On the other hand, if a big movable plume connects with a leakage pathway through the caprock, large volumes of CO₂ may escape, and for this reason, it may be better if the injected CO₂ splits into many small plumes. In our analysis, we will therefore also consider the number of plumes and their volumes.

3.3.1 Boundary fluxes

The sweep efficiency of the CO₂ plume, i.e., the percentage of the aquifer volume that has been in contact with CO₂, is positively correlated with the amount of residual trapping (and mixing of CO₂ and brine). Herein, we will consider the flux out of the open boundaries as an indirect measure of volumetric sweep efficiency. The model has open boundaries on three sides, which are modeled by imposing huge pore-volumes multipliers in the outer cells, while no-flow boundary conditions are imposed along the top faulted side. Using large pore-volume multipliers to represent an open boundary enables us to model flow both in and out of the domain, and this way, we can represent volumes of CO₂ leaving and later re-entering the aquifer. (In addition, this method will contribute to eliminate effects from Dirichlet type boundary conditions).

The lower boundary is closest to the injection point and hence the most likely place that injected CO₂ volumes will be lost. Figure 4 shows two cross-plots of the CO₂ across this boundary at the end of injection and the end of simulation. Towards the end of injection, most cases have positive flux values, which means that parts of the main plume connected to the injection point has been forced to leave the domain in the down-dip direction by the increased injection pressure. However, after injection stops, many cases have small negative fluxes, which means that a small volume of CO₂ reenters the domain. Once again, we observe that cases with low aggradation angle stand out from the rest. In these cases, the injected plume is almost entirely confined to the bottom of the model because of poor vertical communication. Hence, a large portion of the injected volume will be forced out of the domain in the down-dip direction. After the end of injection, gravity forces will gradually cause some of these lost volumes to move up-dip again and reenter the domain. We notice that cases with closed faults (shown in the red circle in the left plot of Figure 4) show a relatively higher return

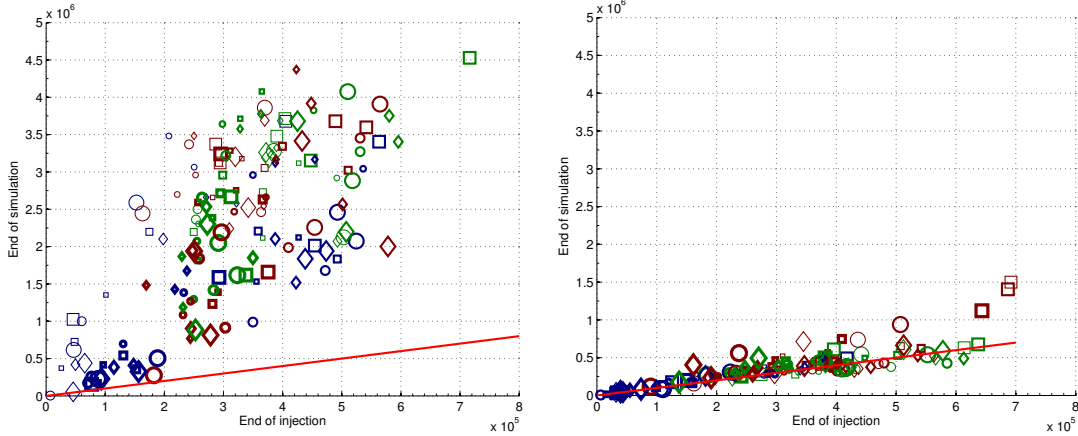


Figure 5: Residually trapped volumes for linear (left) and quadratic (right) relative permeabilities. Cases on the red lines have the same values at the end of injection and end of simulation.

flux for the linear relative permeability function. With nonlinear relative permeability function, some of the cases follow a linear trend (shown by the red line in the right-hand plot), in which the return flux is proportional to the outward flux.

3.3.2 Total mobile/residual CO₂

Residual trapping occurs when the CO₂ saturation is below the residual saturation value of 0.2. Although the residually trapped CO₂ is free to move in a molecular sense on the microscale, the corresponding bulk volume is considered immobile on the macro scale. To reduce the risk of leakage, it is therefore important to obtain an efficient volumetric sweep that will maximize the residual volumes and minimize the mobile volumes. Herein, we will define residually trapped volumes as volumes in which the CO₂ saturation is below the residual value of 0.2. Notice that with this definition, all mobile volumes (in which the saturation exceeds 0.2) will contain a residual portion of CO₂ that is not free to escape. This portion will eventually become residually trapped if the saturation of the mobile CO₂ decreases to the residual value.

Figure 5 shows cross-plots of the total residual volume at the end of injection and end of simulation. Drainage is the dominant flow process during injection. When injection ceases, the plume migration turns into a imbibition-dominated process which increases the residual trapping of CO₂. With linear relative permeability, the imbibition process takes place relatively fast, and the residual volume increases significantly from end of injection to end of simulation. Once again, low-aggradation cases form notable exception having small amounts of residual trapping. The reason is primarily that significant volumes have been lost over the down-dip boundary, and secondarily that the (vertical) sweep is limited because the CO₂ plume is confined to the lower layers of the reservoir during most of the simulation time.

With quadratic relative permeabilities, the migration process is significantly slower and many cases have almost the same residual volume at the end of injection and end of simulation. As already discussed, the curvature of the relative permeability function does not have a considerable influence on the flow paths (compare the streamline paths in Figure 2). Compared with the results in the left plot of Figure 5, we therefore ultimately expect a significant increase in residual trapping before the plume settles; this prognostication has been confirmed for a few (arbitrary selected) cases by computing the plume migration for more than ten thousand years. We also observe that in some cases the residual volumes *decrease* after injection ceases. This is caused by mobile CO₂ invading zones of residual CO₂, thereby turning residual volumes into mobile volumes according to the definition of residual trapping used herein. These cases are therefore likely to be influenced by hysteresis effects, which for simplicity have been disregarded in this study.

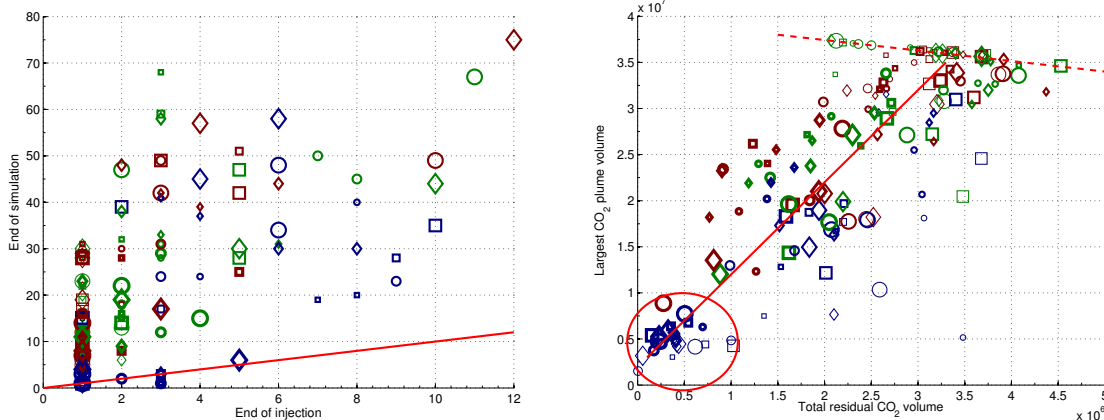


Figure 6: The cross-plot to the left shows the number of CO₂ plumes at the end of simulation versus the number of plumes at the end of injection for linear relative permeability function. The right plot shows the volume of the largest CO₂ plume versus the volume of residual CO₂ at the end of simulation.

3.3.3 Connected CO₂ volumes

In the next section, we will study the risk of leakage through the caprock. To this end, we will assume that all mobile CO₂ connected to a leakage point will escape through that point. Hence, it is preferable if the total mobile CO₂ volume is split into smaller plumes rather than forming a big mobile plume. Moreover, the surface area per volume increases by splitting the plume (assuming constant plume shape) and this helps residual trapping (and mixing of brine and CO₂).

During injection, the flow support from the well builds a connected mass of CO₂ shaping one or a few big plumes. When the injection ceases, the CO₂ starts distributing in the medium and plumes may split because of branches in the flow paths created by heterogeneity. The plot to the left in Figure 6 shows how the number of plumes increases significantly in most cases during the migration phase, except for a few low-aggradation cases for which the injected plumes stay intact or reform into a single plume.

The right plot in Figure 6 shows the volume of the largest CO₂ plume versus the residual trapping. Here, we see two major trends indicated by a solid and a dashed line. The solid line, having a positive slope, represents cases that lose CO₂ through the open boundaries, mainly through the one closest to the injection point. As a consequence, less CO₂ volume exists in the system and the size of the largest plume will be smaller. Hence, less volume will be swept while the plume migrates upward (if it does), which again means that less CO₂ is residually trapped. In particular, we notice the cases inside the ellipse which are the same cases that had large CO₂ volumes escaping through the down-dip boundary as shown in Figure 4. The dashed line with negative slope corresponds to cases for which almost all of the injected CO₂ stays inside the domain. These cases show a small range of variation for the largest plume size and are reflecting the effect of different heterogeneity features on the residual trapping process. Because equal volumes of CO₂ are injected in all cases, we notice that the bigger the largest plume is, the smaller the residual volume will be.

4 Analysis of Parameter Impact

The main purpose of the current study is to investigate how geological heterogeneity impacts the formation of a CO₂ plume during injection and during the early-stage migration after injection ceases. In this section, we will therefore perform a simple 'sensitivity analysis' that will tell us something of how the different geological parameters impact the flow responses discussed in the previous section. The five geological parameters impact the flow responses to different degrees; some parameters are more influential during injection, others take effect when the migration starts after injection has ceased, and some are influential both during injection and migration. Comparing the relative impact of the different parameters will indicate which of the parameters are most important to represent accurately when modeling a specific aquifer of the type considered herein.

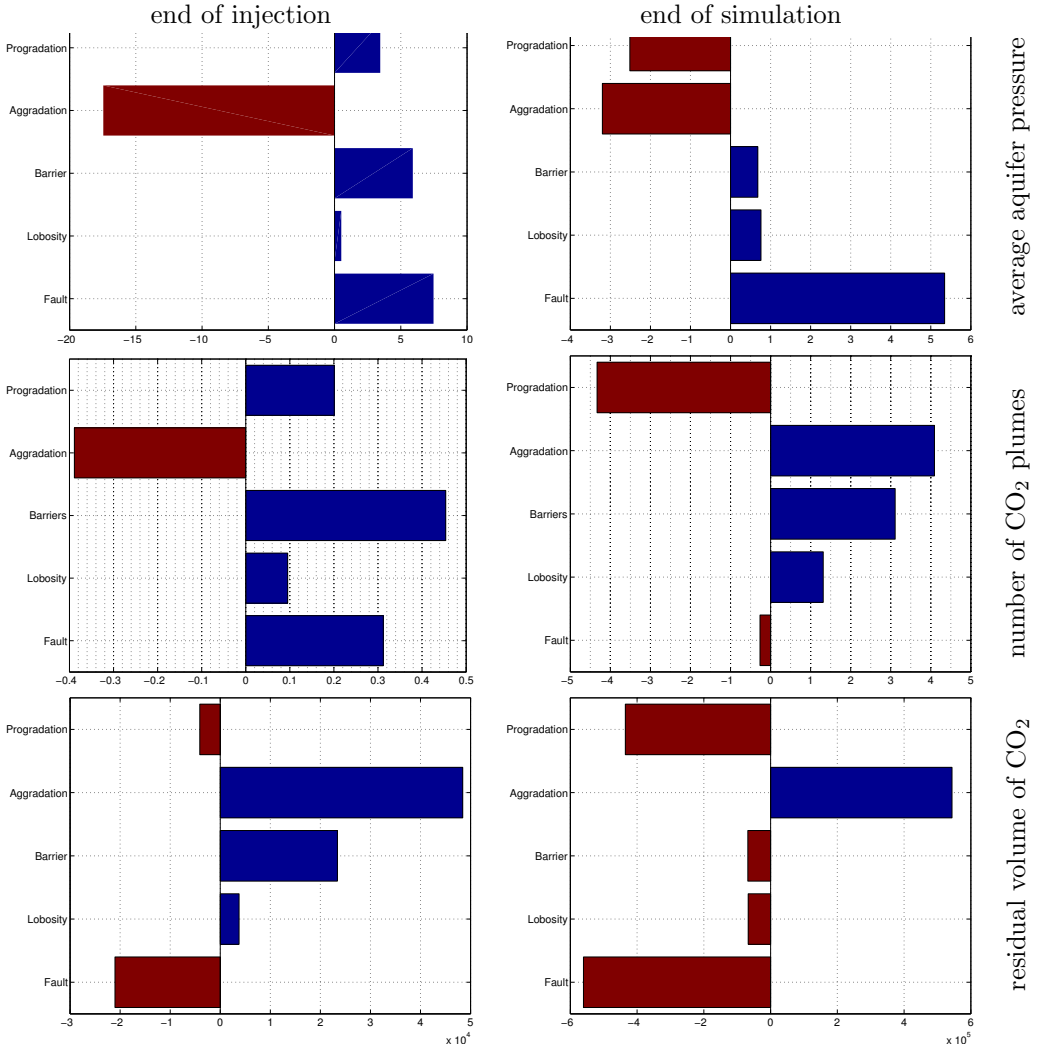


Figure 7: Sensitivities to different geological features at end of injection and end of simulation for the average aquifer pressure, number of CO₂ plumes, and residual volume of CO₂.

To quantify the relative impact of each geological parameter, we will define a normalized gradient for each feature. We will use barriers as an example to explain the analysis. There are three levels of barriers: low, medium and high. Suppose that we want to calculate the sensitivity of the number of plumes with respect to the level of coverage for the barrier sheets. We do this in two steps: first we average the number of plumes for cases of the same level of barriers. Having three levels of barrier, this results in three averaged plume numbers corresponding to each level of barriers. In the next step, we fit a line through these three points and calculate the inclination of this line which represents how the number of plumes increases if the barrier parameter increases one level. For other features like fault and lobosity, we follow the same procedure. We use three levels for each feature and fit a trend through these three points. For example, the first level of fault criteria relates to unfaulted cases, the second relates to open faults, and the third represents cases with closed faults.

Figure 7 shows the sensitivity for three different flow responses. In the upper row, we see that during injection the average aquifer pressure is most influenced by aggradation, while at the end of simulation the most influential feature is the fault specification. The lack of good vertical communication for low aggradation angles means that the CO₂ is confined to the lower (poor quality) layers and relatively high pressures must be imposed to inject the required amount of CO₂ into the aquifer. For higher angles, the CO₂ can flow more easily upward through channels with higher permeabilities and less pressure support is required. Hence, the negative gradient. After the injection ceases, the dominating force is gravity, the main flow direction is vertical, and the pressure is now mostly affected by faults. If the faults are closed, they will prevent the release of pressure through the open

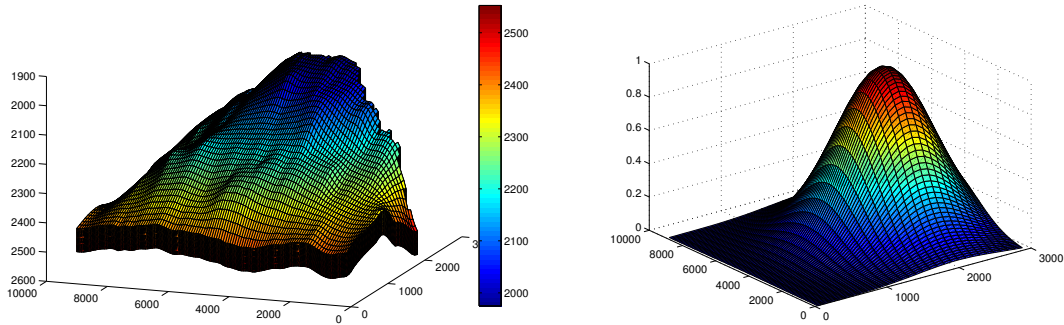


Figure 8: The left plot shows a sample grid geometry with depth values shown in meters. The right plot shows the Gaussian probability distribution for point leakage through the caprock. The distribution is centered at a point on the crest which is in the same slice as the injection point.

boundaries. We also observe that the effect of progradation switches from positive to negative after the injection is stopped: Injecting in the up-dip direction is easier than injecting down-dip, while a down-dip deposition opens up more conductive medium in front of the plume as it migrates towards the crest.

The second row in Figure 7 shows the sensitivity in the number of CO₂ plumes. During injection, the barriers coverage is the most influential parameter, because mud-draped surfaces enhance the lateral flow and force the plume to split rather than migrating towards and accumulating at the crest. Aggradation has a similar effect: the lower the angle is, the more the injected CO₂ spreads out laterally. At the end of simulation, progradation and aggradation are the dominant effects. In particular, higher aggradation angle improves the segregation across layers and thus increases the splitting of plumes through heterogeneities. The impact of the faults is more significant than the figure shows: open faults contribute to split plumes, while the unfaulted cases and the cases with closed faults introduce a small number of plumes. In average, the positive and negative contributions cancel out to almost zero. Finally, the bottom row in Figure 7 reports sensitivities for the total residual volume. Here, aggradation is the most influential parameter during injection and faults the most important parameter during the migration phase.

Similar analyzes have been conducted for other flow responses as well. Altogether, our sensitivity study shows that aggradation is the parameter that has most impact on the flow responses we have studied. Aggradation has either the largest or the second largest gradient during both injection and migration for almost all responses. The faulting has the second highest impact. Mostly effected by closed fault, the fault parameter influences the storage capacity and the extent to which a CO₂ plume accumulates under the caprock. Barriers play a dominating role for the splitting of plumes during injection, whereas the progradation affects the gravity segregation through conductive channels during the migration phase and the volume available to flow in the dip direction. Finally, lobosity has small impact compared to the other parameters and can therefore likely be ignored for the fluid responses considered above. However, lobosity has a considerable effect on the lateral movement and splitting of plumes during the migration period and may therefore have a more significant impact on the estimates of point leakage.

5 Leakage Risk

The SAIGUP study does not supply any information about the caprock and its geomechanical properties. We are therefore only able to conduct a conceptual study of the risk associated with point leakage through imperfections in the caprock. To this end, we assume that each point on the top surface has a prescribed probability for being a leakage point. As a simple example, we will assume that the probability for point leakage follows a standard 2D Gaussian distribution centered at a given point on the crest, see Figure 8. Moreover, we will assume that all mobile CO₂ (except for the residual portion) will escape through the caprock if a plume comes in contact with a leakage point. We have seen above that the heterogeneity and tilt of the medium will cause the injected CO₂ to be distributed

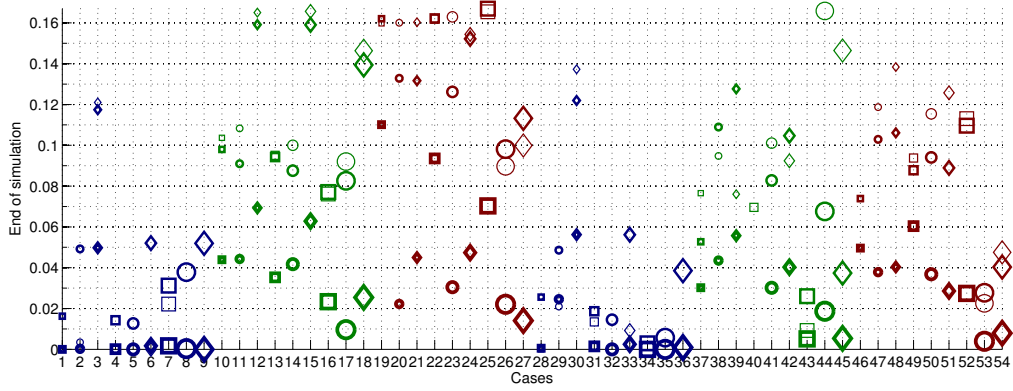


Figure 9: Leakage risk at end of simulation for linear relative permeabilities.

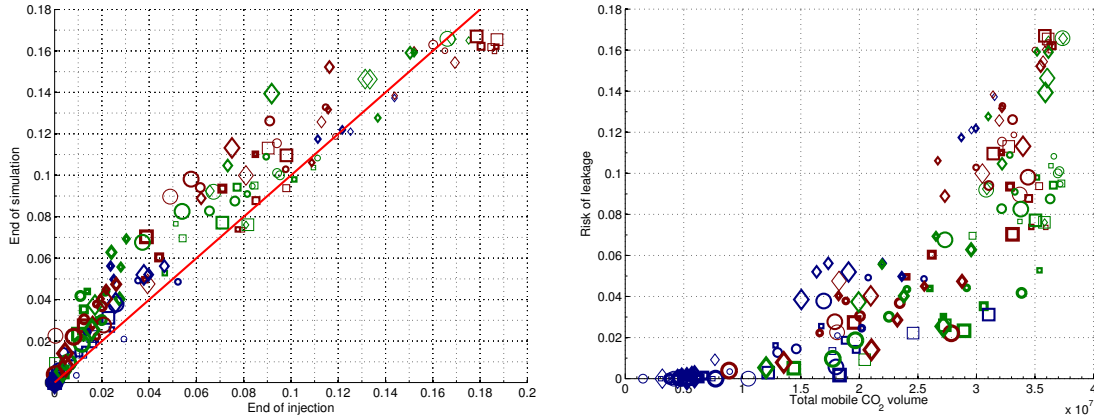


Figure 10: The left plot shows a cross-plot of leakage risk for linear relative permeability function. The right plot shows mobile CO₂ volume versus leakage risk at the end of simulation.

under the caprock as a number of plumes with variable sizes. For each cell along the top surface, we now define the risk as the probability of point leakage weighted by the size of the CO₂ plume that the cell is part of. We then sum the values for all the topmost cells, normalize this sum, and use the resulting single number as a measure of leakage risk. The worst possible case would be if all the injected CO₂ volume forms a mobile plume that contacts every point along the top surface; this gives a risk value equal to one. For all actual cases, however, the risk value will be less than one because not all of the CO₂ will be mobile (because of residual trapping and loss of volumes across the open boundaries), because the mobile volume may form more than one plume, or because not all the mobile volume has reached the top due to reduced vertical mobility.

Figure 9 shows the resulting leakage risks for all cases at the end of simulation computed using linear relative permeabilities. Similarly, the left plot in Figure 10 shows how the risk develops during the seventy year period from the end of injection to the end of simulation, whereas the right plot shows a cross-plot of the leakage risk versus the total volume of mobile CO₂. The plots lead to the rather obvious conclusion that improved vertical connection will increase the risk of leakage through possible imperfections in the caprock and that there is a positive correlation between the volume of mobile CO₂ in the system and leakage risk. However, we also observe that there are cases which have zero leakage risk. These are cases with low aggradation, for which the flow stays in the injected layers and moves laterally towards the open boundaries, resulting in a low amount of mobile CO₂ in the system. Furthermore, these cases have (almost) no cross-layered CO₂ movement, which means that (almost) no CO₂ reaches the top surface. In other words, the low-aggradation cases, which have seemed to be infeasible because of high injection pressure, larger lateral spread, and loss of volumes through the open boundaries in our discussion in the previous two sections, here appear as the most feasible with

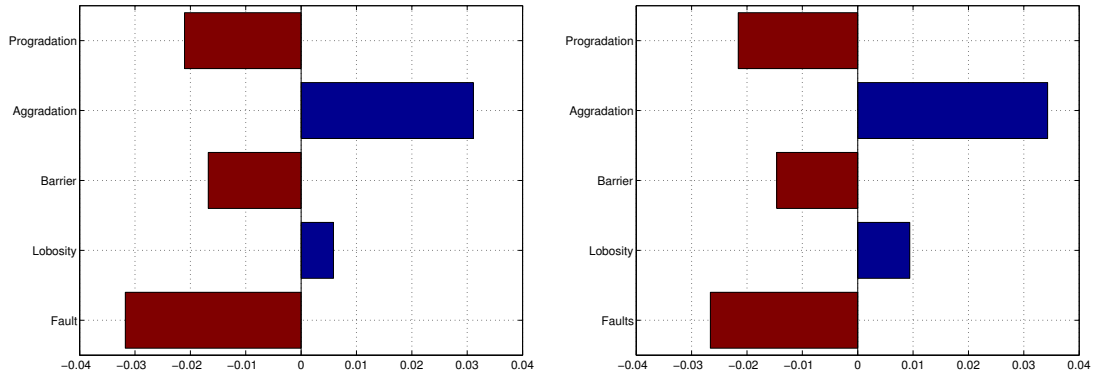


Figure 11: Sensitivity of the leakage risk with respect to the five geological parameters at the end of injection (left) and end of simulation (right).

respect to the chosen risk measure.

Figure 11 shows gradients for the leakage risk. Although less pronounced during injection time, the gravity force makes a major plume body attached to the crest both during the injection time and afterwards. Hence, we see that the leakage-risk sensitivity shows almost the same profile at end of injection and end of simulation. This can also be observed in Figure 10. The sensitivity is slightly less during injection compared to end of simulation, because more CO₂ will be below the caprock at end of simulation. This overtakes the effect of mobile volume reduction due to residual trapping process and the increase in the number of plumes at end of simulation, which both result in less risk of leakage.

Once again, aggradation angle and fault criteria are the two most influential features. Increasing the aggradation angle improves the vertical communication and contributes to increase the formation of CO₂ plumes below the caprock. Closed faults limit the movement of the plume and result in less accumulation below the caprock, whereas open faults generally increase the upward migration of plumes.

6 Conclusions

Herein, we have presented a study of how various geological parameters influence the injection and early-stage migration of CO₂ in progradational shallow-marine systems. One hundred and sixty equally probable realizations have been considered and several flow responses related to storage capacity and risk of point leakage have been calculated at the end of injection and after seventy years of gravity-dominated plume migration.

First of all, we have investigated the effect of relative permeability curvature by comparing the results of linear and quadratic relative permeability curves. The results show that linear relative permeabilities give significantly higher wave speeds that lead to earlier accumulation of CO₂ under the caprock, and will for this reason give conservative estimates of the plume migration and the risk associated with point leakage after a prescribed number of years.

Second, and more important, we have demonstrated and discussed how the heterogeneity induced by different geological parameters give large variations in flow responses. Each geological feature will influence the flow behavior and can result in local/global pressure build-up or pressure drop, enhance the flow direction, hinder the flow in the medium, or lead to loss of injected volumes over the open boundaries, and may induce different effects during the injection and plume migration. Specifically, we have demonstrated how variation in aggradation angle, fault criteria, and progradation direction significantly change the flow direction within the medium and hence impact the residual trapping and formation of movable CO₂ plumes under the caprock. Barriers are important during injection and must be modeled more carefully if the study focuses on injection operations.

Altogether, our study shows that geological heterogeneity has a major impact on the injection and formation of a CO₂ plume and the subsequent early-stage migration of this plume. A predictive study should therefore incorporate realistic estimates of geological uncertainty to provide reliable forecasts of operational risks and the long-term fate of injected CO₂.

References

- [1] M. Ashraf, K.-A. Lie, H. M. Nilsen, J. M. Nordbotten, and A. Skorstad. Impact of geological heterogeneity on early-stage CO₂ plume migration. In J. Carrera, editor, *Proceedings of the XVIII International Conference on Water Resources (CMWR 2010)*, Barcelona, Spain, 2010. CIMNE.
- [2] P. J. Cook, A. Rigg, and J. Bradshaw. Putting it back where it came from: Is geological disposal of carbon dioxide an option for australia. *Australian Petroleum Production and Exploration Association Journal*, 1, 2000.
- [3] S. P. Dutton, W. A. Flanders, and M. D. Barton. Reservoir characterization of a permian deep-water sandstone, East Ford field, Delaware basin, Texas. *AAPG Bulletin*, 87(4):609, 2003.
- [4] T. T. Eaton. On the importance of geological heterogeneity for flow simulation. *Sedimentary Geology*, 184(3-4):187–201, 2006.
- [5] B. Hitchon. *Aquifer disposal of carbon dioxide: hydrodynamic and mineral trapping: proof of concept*. Geoscience Pub., 1996.
- [6] J. A. Howell, A. Skorstad, A. MacDonald, A. Fordham, S. Flint, B. Fjellvoll, and T. Manzocchi. Sedimentological parameterization of shallow-marine reservoirs. *Petroleum Geoscience*, 14(1):17–34, 2008.
- [7] R. Juanes, E. J. Spiteri, F. M. Orr Jr, and M. J. Blunt. Impact of relative permeability hysteresis on geological CO₂ storage. *Water Resources Research*, 42:W12418, 2006.
- [8] T. Manzocchi, J. N. Carter, A. Skorstad, B. Fjellvoll, K. Stephen, J. A. Howell, J. D. Matthews, J. J. Walsh, M. Nepveu, C. Bos, J. Cole, P. Egberts, S. Flint, C. Hern, L. Holden, H. Hovland, H. Jackson, O. Kolbjørnsen, A. MacDonald, P. A. R. Nell, K. Onyeagoro, J. Strand, A. R. Syversveen, A. Tchistiakov, C. Yang, G. Yielding, and R. W. Zimmerman. Sensitivity of the impact of geological uncertainty on production from faulted and unfaulted shallow-marine oil reservoirs: objectives and methods. *Petroleum Geoscience*, 14(1):3–15, 2008.
- [9] J. D. Matthews, J. N. Carter, K. D. Stephen, R. W. Zimmerman, A. Skorstad, T. Manzocchi, and J. A. Howell. Assessing the effect of geological uncertainty on recovery estimates in shallow-marine reservoirs: the application of reservoir engineering to the saigup project. *Petroleum Geoscience*, 14(1):35–44, 2008.
- [10] J. M. Nordbotten, D. Kavetski, M. A. Celia, and S. Bachu. A semi-analytical model estimating leakage associated with CO₂ storage in large-scale multi-layered geological systems with multiple leaky wells. *Under Review at: Environmental Science and Technology*, 2008.
- [11] E. Spiteri, R. Juanes, M. Blunt, and F. Orr. Relative-permeability hysteresis: Trapping models and application to geological CO₂ sequestration. In *SPE Annual Technical Conference and Exhibition*, 2005.

Paper II

2.2 Geological storage of CO₂: heterogeneity impact on pressure behavior

M. Ashraf

Submitted to *International Journal of Greenhouse Gas Control (IJGGC)*

Geological storage of CO₂: heterogeneity impact on pressure behavior

December 7, 2012

Contents

1	Introduction	2
2	Geological parameters	3
3	Injection scenario	5
4	Pressure analysis	6
4.1	Injection time	8
4.2	Well and aquifer pressure	9
4.3	Pressurized region	11
4.4	Build-up region	12
4.5	Farthest pulse	13
5	Discussion	14
6	Conclusion	16

Abstract

Due to the high rates of industrial CO₂ emission, it is an operational objective to maximize CO₂ injection rate into underground geological formations. Forcing the injection wells with high volumetric rates can result in an overpressurized system with possible breakages in the formation integrity, which increases the risk of CO₂ leakage.

The goal of this study is to investigate the injection pressure considerations that are needed to avoid uncontrolled development of fractures in the medium. Herein, we study how the geological heterogeneity influences the pressure behavior of a typical CO₂ injection operation. Five variable geological features are considered as input for sensitivity analysis. These features span a realistic geological space.

Two injection scenarios are examined. In the first scenario, CO₂ is injected at a constant rate and the pressure in the well and the domain is allowed to build up unlimitedly. In the second scenario, a pressure constraint is set on the well, and the injection rate is changed to keep the pressure below the limit. Model responses related to pressure build-up and propagation within the system are defined and demonstrated for a selected case. Results for all cases are presented and discussed accordingly. We conclude by ranking the most influential geological parameters.

1 Introduction

The increasing level of green-house gases in the atmosphere, and in particular carbon dioxide, is believed to cause global climate changes. The industrial emission rate is expected to increase over the next decade, without taking necessary preventive actions. For example, according to the Energy Information Administration (EIA), the US carbon dioxide emissions are forecast to reach 6.41 billion tonnes by 2030. The Kyoto protocol proposed an emission cut which requires 1.75 billion tonnes of annual carbon dioxide reduction [10].

Geological storage of CO₂ is a proposed solution to fight global climate change. Clear operational criteria and policies must be made for the process to avert unwanted consequences. Concerns connected to putting a large mass of CO₂ into underground geological formations are not limited to the spatial distribution of the injected fluid. The pressure signals imposed through the injection point can travel beyond the scale of the CO₂ invaded zones. Although geological barriers can hinder the pressure exchange between different regions, pressure can transfer through low-permeable rocks where the CO₂ is trapped by capillarity.

In addition to the depleted oil and gas fields, deep geological aquifers are practical targets for geological storage of CO₂. If injecting into brine aquifers, the pressure waves can push brine into connected fresh water aquifers and contaminate them. Brine displacement issues are discussed in [4] by defining open, closed, and semi-closed aquifer boundaries. Brine might also leak through abandoned wells into other zones. Cailly et al. [3] discuss well design considerations to prevent any leakage through wells.

Geomechanical deformations are important during injection period. They can lead to changes in effective permeability and porosity. It is possible that the pressure build-up around injection wells will crack the rock with uncontrolled fracture extensions to the structural sealing layers. Faults can be activated due to high pressure in the system, providing a

leakage path across layers. In addition to increased spatial CO₂ spread, an intensive induced fracture network can result in local earthquakes.

Pressure constraints must be considered for injection operations to limit the pressure buildup. However, this comes with the cost of injection rate reduction. Rock quality within the injection region has significant impact on pressure build up and therefore, geological uncertainty plays a considerable role in assessing the success and feasibility of the operation.

Any risk of breakings in the formation integrity must be assessed to define the appropriate preventive measures. We need to perform pressure sensitivity analysis to identify the influential parameters in the model. Uncertainty reduction in the influential parameters enhances the accuracy of pressure behavior prediction.

Geological uncertainty is a major issue in pressure analysis. Most of the pressure-related studies in the literature provide either deterministic case studies or generic preventive measures based on theoretical studies [9, 13, 6, 14, 12, 11]. It is important to include realistic geological descriptions in any study related to uncertainty. For example, permeability variation on the grid should be in the form of realizations of geological realistic formations. To the best of our knowledge, this is the first pressure study in the context of CO₂ storage that considers the geological uncertainty in the form of structural variables rather than engineering parameters, such as permeability and porosity.

Within oil recovery context, the impact of geological uncertainty is thoroughly investigated in the SAIGUP project for shallow-marine depositional systems [5, 7, 8]. In the SAIGUP study, variations of geological features are examined in a set of field development strategies via several injection/production patterns. The study concludes that geological uncertainty has a dramatic influence on the oil recovery estimates. A number of geological realizations from the SAIGUP are used in [1, 2] to investigate the impact of geological uncertainty on injection and early migration of CO₂. Certain structural features are considered for those studies and flow responses are defined to measure the storage capacity, the trapping efficiency, and the leakage risk and the sensitivity of these responses to variations in geological parameters is investigated. Large variation in responses are observed. Aggradation angle and barriers are recognized to be the most influential in the CO₂ flow behavior[1, 2]. The focus in [1, 2] is to measure the spatial CO₂ distribution sensitivity to the variation of geological description.

This study is complementing [1, 2], in the sense that we herein analyze the sensitivity of pressure to the same geological parameters. In addition to the injection scenario used in [1, 2], we examine a different injection scenario with more realistic well control for the injection operation. A detailed study is given for the pressure behavior during injection time.

2 Geological parameters

In the SAIGUP study, a large number of realistic realizations were generated based upon a parametrization of a set of carefully selected geological features and a detailed sensitivity analysis study is performed for field oil recovery over number of development scenarios. Both the sedimentological and structural geological parameters have shown to dominate the uncertainty in total oil production. Hence, more accurate geological description enhances the

quality of flow simulations.

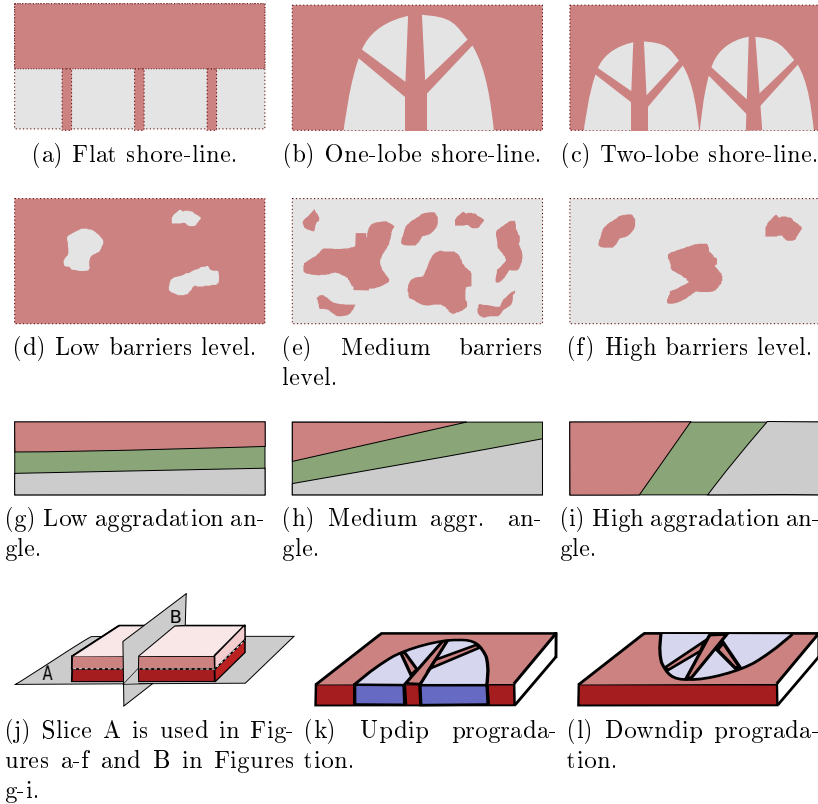


Figure 1: The studied geological features. a-c) Shoreline shape, gray is for poor quality rock and brown color resembles a good quality rock. d-f) Barriers level defined by transmissibility multiplier. Gray color is for zero and brown color shows one. g-i) Aggradation angle. k-l) Progradation direction.

Table 1: Marker codes used in the result plots. The code level corresponds to levels in Figure 1.

Code	Description	Code level	Feature level
Thickness	Fault	thin/medium/thick	unfaulted/open/close
Shape	Lobosity	square/circle/diamond	flat/one-lobe/two-lobe
Size	Barriers	small/medium/large	10% / 50% / 90%
Color	Aggradation	blue/green/red	low/medium/high
Case no. counting	Progradation	first half/second half	up-dip / down-dip

We have selected five geological parameters from the SAIGUP project to study the impact of heterogeneity on the pressure responses in a typical CO₂ injection problem. These parameters span realistic intervals for progradational shallow-marine depositional systems with limited tidal influence. The considered features with the grading levels in each one, are

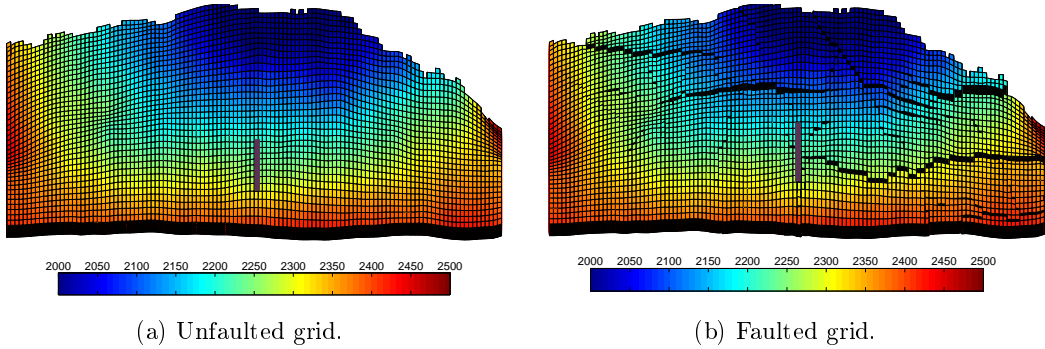


Figure 2: Models used in the study. Depth in meter is shown by color.

shown in Figure 1. In addition to the features shown in Figure 1, we also consider faulting levels: unfaulted, open faults, and close faults. In subsequent plots, each of these features are represented with codes such as shape, size and color which are explained in Table 1. For more details refer to [1].

3 Injection scenario

We define a CO₂ injection scenario to be implemented for all cases in which we use an injector down in the flank and hydrostatic boundary conditions on the sides, except the side near the crest (see Figure 2). No-flow boundary conditions are imposed on the top and bottom surfaces of the model. Model dimensions are: 9km × 3km × 80m. The well is completed only in the four layers in all cases. The idea is to inject as low as possible to increase the travel path and the volume swept by the plume. If the medium is homogeneous, following the injection we expect one big plume to be constructed and this plume to move up due to the gravity force until it accumulates under the structural trap beneath the cap-rock.

Slightly compressible supercritical CO₂ is considered and we seek to inject a volume of 40MM m³, which amounts to 20% of the total pore volume of the models. After the injection period, early plume migration is simulated in all of the studied cases and the simulation ends at 100 years. We use Corey-type quadratic functions for relative permeability, with end points 0.2 and 0.8 in both phases.

Low well injectivity can result in high pressure in the system. In this study, two injection strategies are implemented. In the first strategy (which is similar to the one used in [1]), the entire CO₂ volume is injected within 30 years at a constant volumetric rate. In the second strategy, we set an operational pressure constraint on the injector and continue injecting with appropriate rates to keep the pressure within the limit. We do some pressure response calculations to see the propagation of pressure pulses in the medium for both strategies.

In the pressure-constrained strategy, the injector operates with the priority of injecting a volumetric rate of 3650 m³/day. A pressure constraint of 400 bar is set on the injector. If the well bottom-hole pressure goes higher than that and violates this restriction (to maintain the target injection rate), the priority changes to keep the 400 bar by reducing the injection rate. The well continues operation switching between these priorities until a total CO₂ volume of

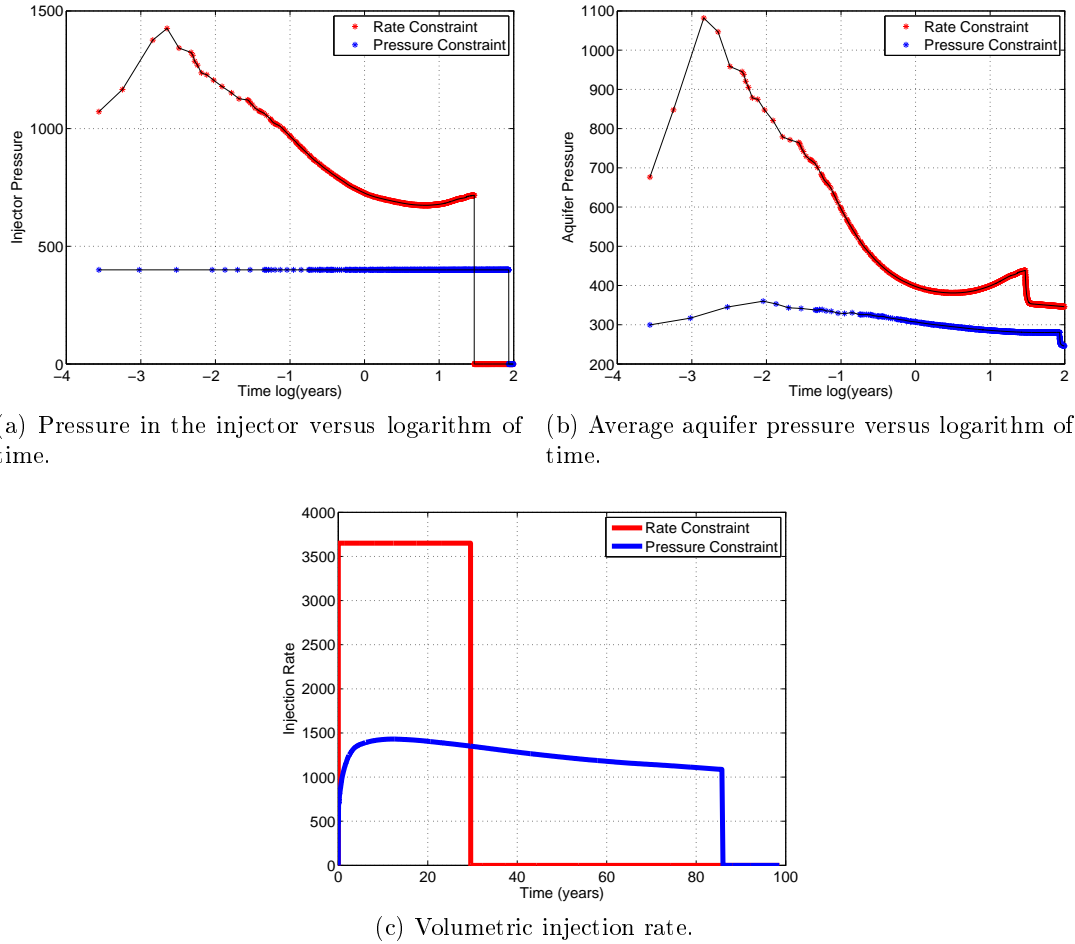


Figure 3: Aquifer and well pressure and injection rate in different injection scenarios shown for a test case.

40MM m³ is injected into the medium. As soon as the total injected volume reaches this number, the injector will be shut from the bore-hole and no injection happens for the rest of simulation time.

4 Pressure analysis

We start by discussing the pressure responses we will use in our study for one particular realization. Then we do the full analysis by considering all of the 160 specified realizations, which are made by combining the geological variable levels discussed earlier¹. Response plots are shown and discussed accordingly. Most of the reported results are chosen at 2.4 hours (0.1 day), i.e., at the beginning of injection. At that time, the system pressure response is higher compared to the later times when the pressure in the system drops to lower values

¹Combining all the features and levels makes 162 cases. However, two cases were missing in the original data set.

(Figure 3b). Also, upto this time the same amount of CO₂ is injected in all cases, which allows for a fair comparison between cases.

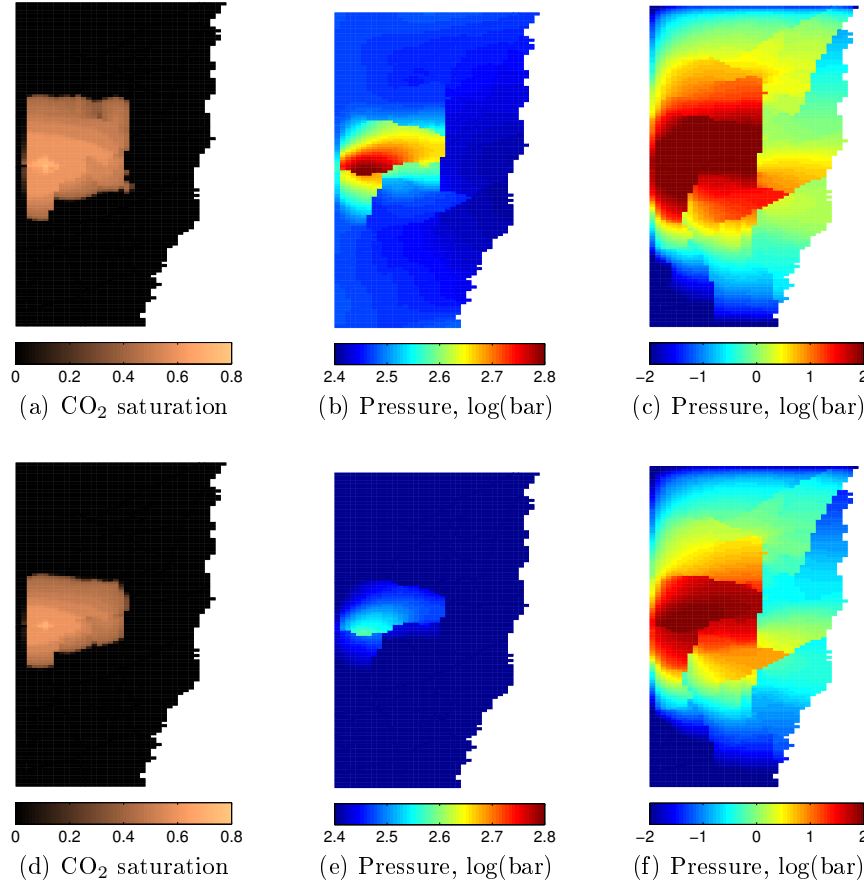


Figure 4: Responses at the middle of injection period (15 years). The first row corresponds to rate-constrained and the second row belongs to the pressure-constrained injection scenario. Figures c and f show the pressure build up from its initial value. Top view of last injection layer is shown in all figures.

Four types of responses are considered to be basis for the comparison between cases. One important question is how fast we can inject into a realization. To compare different cases, injection time is calculated considering a fixed total volume of injection in all models. Pressure behavior in the system is studied, by looking at aquifer average pressure and pressure drop across the well. An overpressure region is defined in which the volumetric spread of over-pressurized locations in the model is measured. Finally, the farthest place from the injection point that a pressure build up has reached is reported for each realization to see the impact of heterogeneity and channellings on how the pressure wave travels through the medium.

Figure 4 shows the pressure and saturation responses for the two injection scenarios in a selected case. This case has one lobe, parallel rock-type stratigraphy (i.e., low aggradation angle), and up-dip progradation. It is faulted with almost open faults and has high barrier

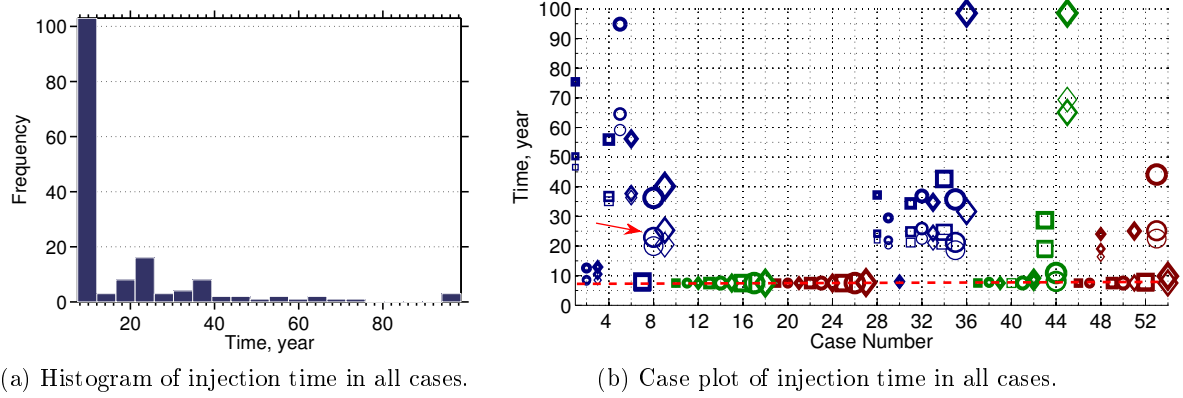


Figure 5: Time to inject quarter of the total specified CO₂ volume for all cases in the pressure-constrained scenario. The dashed red line in the right plot denotes the targeted injection time of 7.5 year, and the red arrow points to the case shown in Figure 4.

level. Responses for the rate constrained scenario are given in Figures 4a, 4b and 4c, and those for the pressure constrained scenario are given in Figures 4d, 4e and 4f.

The pressure build-up in Figures 4c and 4f tells about heterogeneity impact on maintaining the pressure locally rather than transferring it across the medium. Comparing Figures 4b and 4c with Figures 4e and 4f, we see that imposing a pressure constraint on the injector significantly reduces the pressure build-up in the medium (as should be expected). However, the pressure disturbance propagates widely through the system in both cases (Figures 4c and 4f), far beyond the CO₂ invaded zones in Figures 4a and 4d.

4.1 Injection time

In the pressure-constrained scenario, the less the injectivity of the well is, the longer it will take to inject into the medium, keeping the pressure below the critical limit. In some of the cases it takes longer than 100 years (i.e., longer than the considered total simulation time) to inject the specified CO₂ volume. To compare cases, we therefore calculate the time at which a quarter of the objective volume is injected. In all cases, this amount is injected within the total simulation time.

Figure 5 shows the injection time for all cases, using the pressure-constrained scenario. For many cases, the injector keeps the target rate, and thus, it completes the injection in 7.5 years (the dotted red line in the figure). The rest of the cases require longer injection time, due to the lower injectivity of the medium. This leads to pressure control in the injector, followed by a decrease in the injection rate.

Different codes used in the plot of Figure 5 are described in Table 1. Most of the cases with lower injection rates in the plot are colored blue, which translates to a low aggradational angle. Also cases with closed faults, denoted by thick markers, have (significantly) longer injection times.

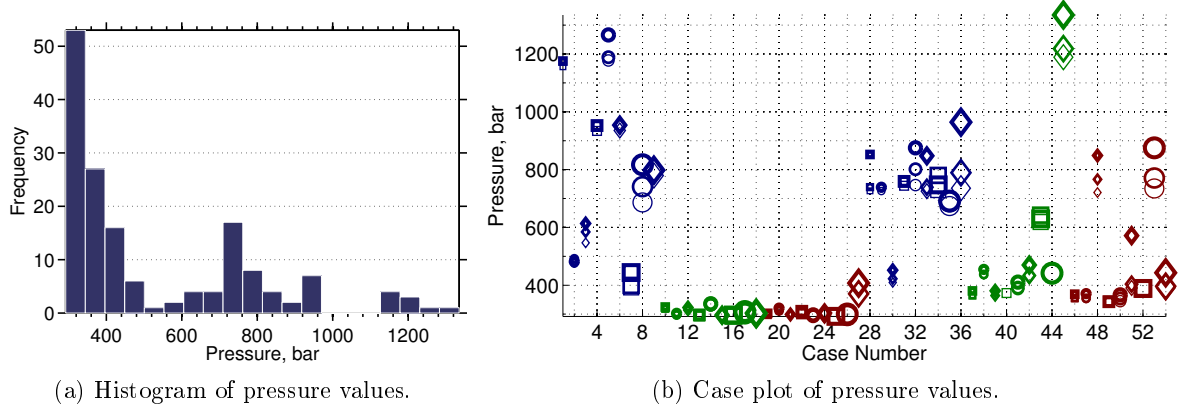


Figure 6: Average aquifer pressure for all cases in the rate-constrained scenario.

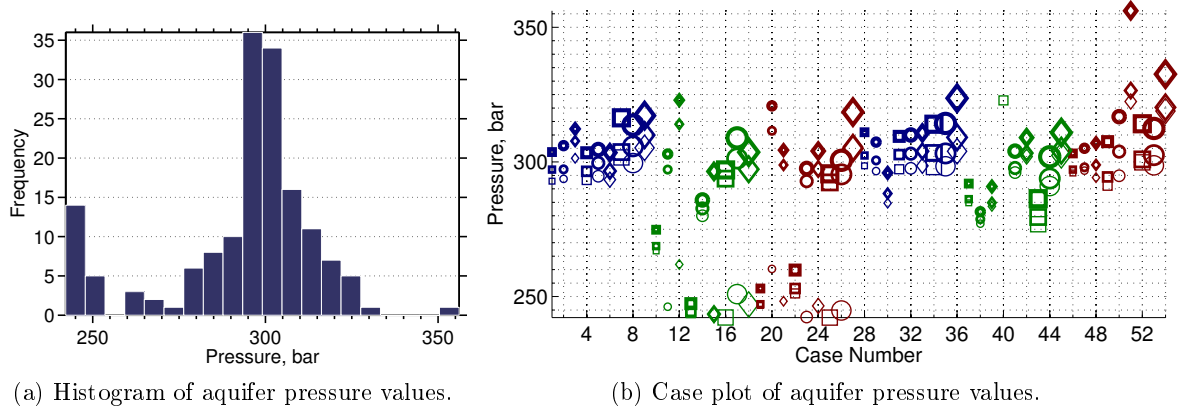


Figure 7: Aquifer average pressure for all cases in the pressure-constrained scenario.

time. Progradation effects are apparent on the higher aggradational cases: for some of the cases colored green and red in the second half of the plot in Figure 5, injection takes longer than the corresponding cases in the first half, which satisfy the targeted injection. This means that down-dip progradation, independent of aggradational angle level, can result in lower injectivity.

4.2 Well and aquifer pressure

To see the overpressure caused by different heterogeneities, we compare cases for their average pressure and well pressure drop. Histograms of average aquifer pressure are shown in Figures 6a and 7a for different injection scenarios and average aquifer pressure at 2.4 hours after the start of injection is plotted for all cases in Figures 6b and 7b. In the rate-constrained scenario, high ranges of average pressure are observed (Figure 6b). Effects of aggradational angle, progradation and faulting are visible in the plot. Three clusters can be identified in the histogram of Figure 6a with medium, high and extreme pressure values. In Figure 7a,

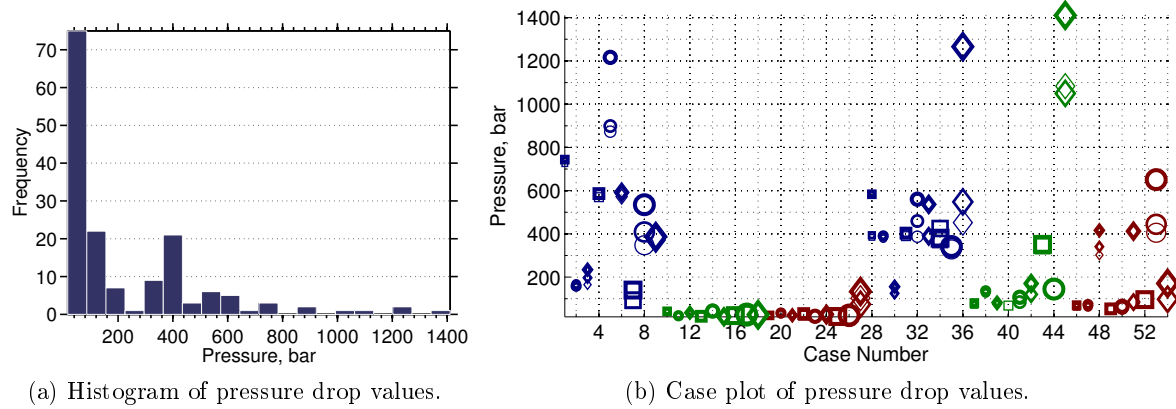


Figure 8: Average of injector pressure drop for all cases in the rate-constrained scenario.

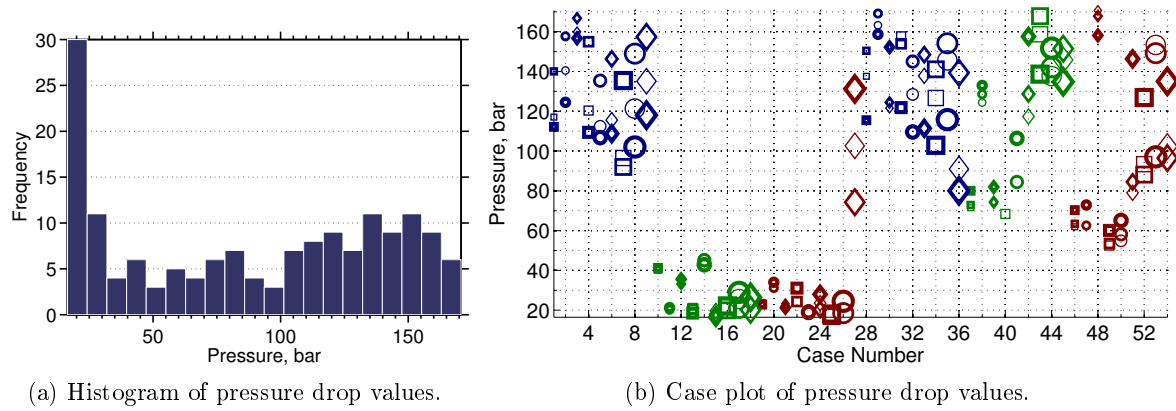


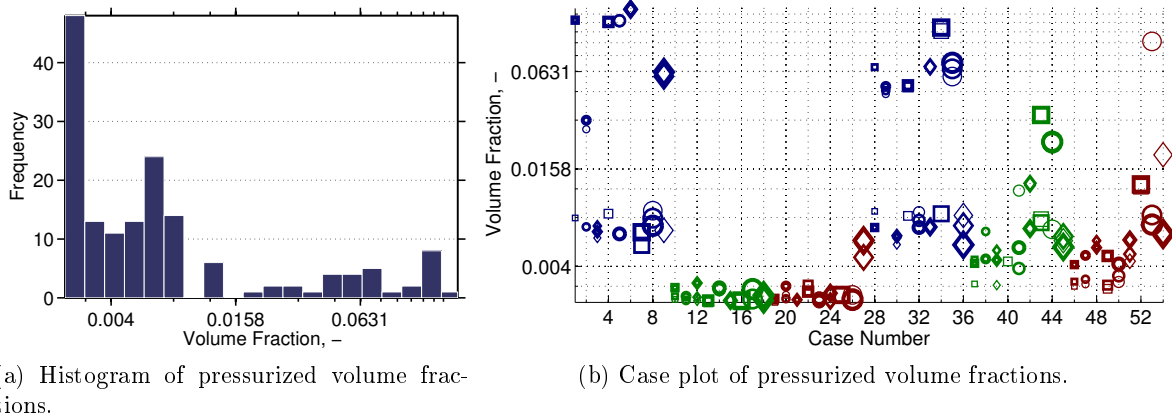
Figure 9: Average of injector pressure drop for all cases in the pressure-constrained scenario.

a small group of cases show lower pressures, while most of cases are distributed around the mean value (which reads 300 bar).

We define the average well pressure drop as the temporal average of the difference between the bottom-hole pressure and the average aquifer pressure.

Histograms of well pressure drop values are shown in Figures 8a and 9a. Higher values imply a poor injectivity of the medium. We see in Figure 8 that maintaining the target rate will in many cases require a huge pressure drop (up to 1400 bar in the worst cases) that would not be feasible nor possible to obtain. Pressure control on the injector reduces the range of pressure drop variation below 170 bar. The average injector pressure drop is plotted for all cases in Figures 8b and 9b.

Two regions can be identified in the medium, the region near the injection point; and the part of aquifer which is far from the injection point. The well-bore pressure is effected directly by heterogeneities in the near well-bore region, while the larger scale region influences the average aquifer pressure. Pressure drop variations in Figures 8a and 8b are influenced by the heterogeneity near the well-bore, where the reaction to injecting a fixed amount of CO₂



(a) Histogram of pressurized volume fractions.

(b) Case plot of pressurized volume fractions.

Figure 10: Pressurized volume fraction for all cases in the rate-constrained scenario.

starts by a local pressure build-up. Heterogeneity on the scale of aquifer plays a considerable role in the range of variations in Figures 9a and 9b. In the pressure-constrained scenario, local pressure is controlled by putting a constraint on the well. Hence, the pressure drop variations are controlled by the average aquifer pressure.

As we see in Figure 8b, low aggradation angle and down-dip progradations result in a poor injectivity and high pressure buildup in the injector. Vertical transmissibility drops dramatically for low aggradation angles [1]. This restricts the pressure transfer within the injection layer, and therefore the pressure builds up locally around the well. Moreover, in cases with down-dip progradation the low permeability rocks surrounding river branches near the injector result in a local pressure buildup.

A group of cases in Figure 9 have a relatively low pressure drop of less than 50 bar. These cases have a good injection quality, and the pressure is released through open boundaries easier than other cases. The rest of the cases show higher pressure drop because of the heterogeneities in the larger scale, far from the injector. These results are obtained for a fixed injection location to examine the heterogeneity impact on injectivity. Herein, we aim to honor the geological uncertainty. In practice, the injector must be drilled and completed in the best formation with highest possible injectivity.

Faults influence both local pressure build-up near the injector as well as the average aquifer pressure. Therefore, they have a visible trend in many cases in Figures 8b and 9b (for example, see the three cases denoted by red circles in the right end of Figure 8b). This is especially more apparent in cases with high level of barriers.

4.3 Pressurized region

Here, we study the overpressure distribution in the medium. An absolute pressure limit of 300 bar is set as threshold, such that all cells with a pressure higher than this value form a region that is called the pressurized region. The volumetric fraction of this region is defined by the ratio of pressurized volume to the total volume of all active cells in the model.

Histogram and case plot of the pressurized volume fraction at the start of injection are

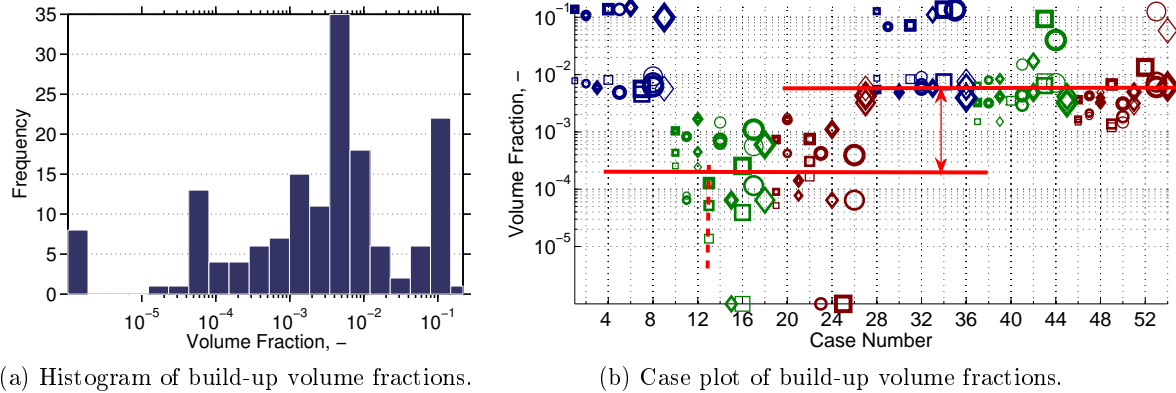


Figure 11: Build-up volume fraction for all cases in the rate-constrained scenario.

given in Figure 10. Here, we clearly see that low aggradation angle is very influential in the pressure buildup in the injection zone. A group of cases with low aggradation angle have a relatively large pressurized region in Figure 10b. However, also there are number of cases in Figure 10b that have a relatively low pressurized fraction. In these cases, the medium is conductive toward the open boundaries and the heterogeneity in the medium does not cause a major pressure buildup. Other observation in Figure 10b is the progradation effect; down-dip progradation, shows a rise in pressurized fraction for higher aggradation angles.

4.4 Build-up region

To study the pressure change, and how a pressure disturbance spreads through the medium, we use another metric. We calculate the pressure change by subtracting the initial pressure at each location from the current pressure. Different realizations are compared for the size of a region, which we call the buildup region, where the pressure increases from its initial value by 10 bar. The value 10 bar is chosen to make sure that the region has not reached the boundaries in any of the studied cases. The smaller the buildup region is, the less volume will be exposed to pressure change in the aquifer (Figure 11).

Higher pressure in the medium will obviously cause a larger buildup region. Impact of progradation on the pressure build-up is illustrated in Figure 11b. Up-dip progradation shows a relatively lower pressure buildup compared to down-dip progradation cases. We also see that aggradation dominates this effect, where cases with low aggradation angle show the same build-up pressure for both types of progradation directions (Note the blue colored markers that don't follow the lines in Figure 11b).

Several cases in Figure 11b show a trend for the fault parameter. The dashed line in the figure shows the trend of build-up pressure increase due to fault feature variations in three cases. Faulting changes the geometry of layers and puts different layers adjacent to each other. This enhances the connectivity in the medium. Local heterogeneities and closed

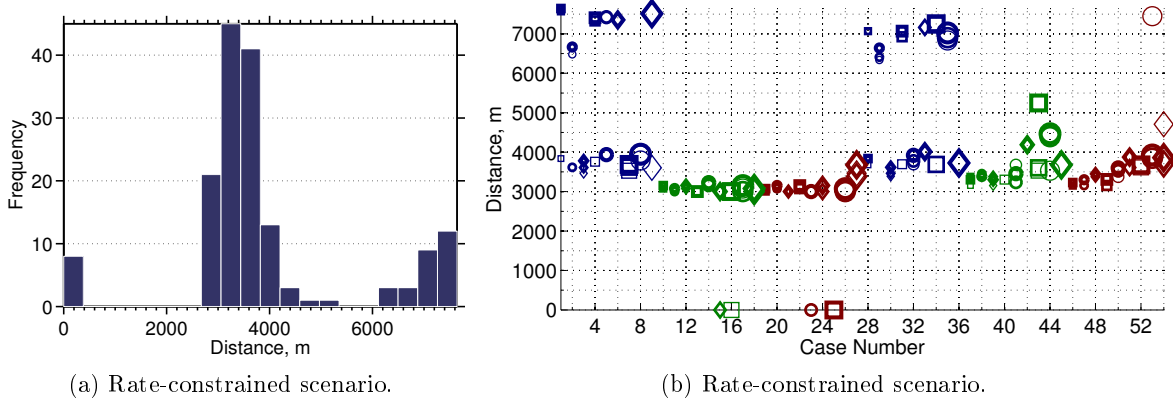


Figure 12: The farthest pulse of the pressure build-up distance from the injection point for all cases in the rate-constrained scenario.

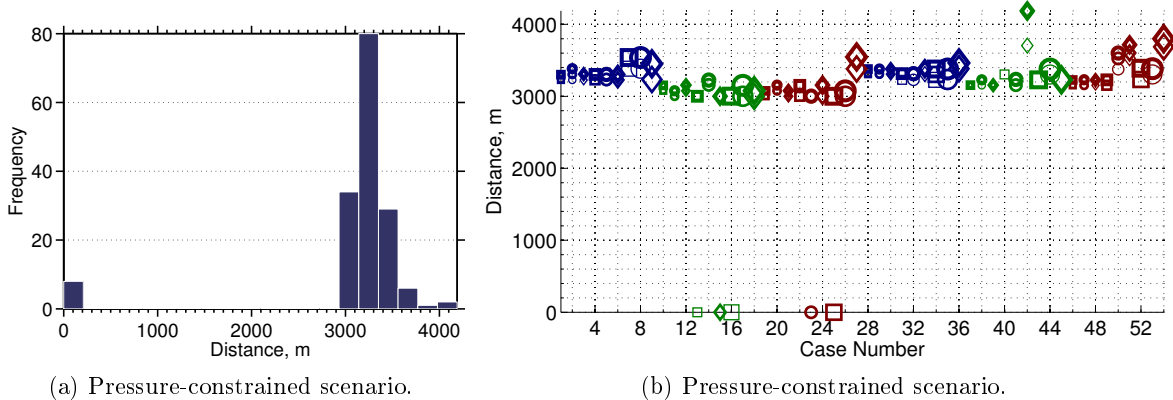


Figure 13: The farthest pulse of the pressure build-up distance from the injection point for all cases in the pressure-constrained scenario.

faults around the injector make a larger build-up region, because they cause higher pressure build-up in the domain. In these cases, the effect of heterogeneity of different scales, namely on the scale of near injector and far from injector, are combined causing a larger buildup fraction.

4.5 Farthest pulse

As discussed earlier, irregular geometries like faults and unconformities can lead to pressure spread in the domain. Looking at the volume fraction of pressurized and buildup regions helps in comparing cases for their pressure conductivity, but it does not show the extent of pressure spread in the medium. For that reason, we also look at the farthest cell from the injection point that falls within the buildup region defined earlier.

Figures 12 and 13 show the farthest pressure build-up distances from the injector in

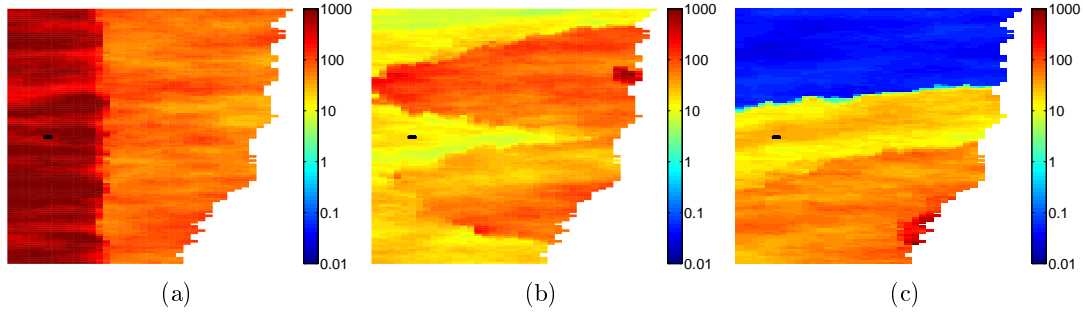


Figure 14: Permeability of three cases in unit millidarcies shown in color, and the Well location is illustrated with black color on each plot . Top view is shown in the plots.

different injection scenarios. In Figure 12a, three groups of cases can be identified: cases with zero distance of farthest pressure build-up pulse, cases with medium distances, and those with large distances from the injection point. Three specific cases are chosen as samples from each of the groups. In the first group, the pressure does not exceed the 10 bar threshold from its initial value in the medium. For these cases, the injector is placed in a permeable region and the medium is conductive towards open boundaries (Figure 14a). Hence, the imposed injection pressure does not build up, neither locally around the well nor globally in the aquifer scale. The second group in Figure 12a have a medium range of 3 – 4 km of distances from the injection point. Heterogeneity in these cases is not making a high pressure build-up around the injector and throughout the medium (Figure 14b).

In the third group, low permeability rocks in the injection layer cause a high pressure build-up around the injection point. If the injector zone is isolated by sealing heterogeneities, the pressure rises in a limited region. However, if the well is connected throughout the medium, and the heterogeneities in the aquifer scale contain relatively low permeability rocks, the pressure build up spreads wider in the aquifer. In Figure 14c, the injection point is located close to a low transmissibility rock. This rises the pressure level in the injector. Other parts of the aquifer are connected with poor quality rocks, resulting in a wide build-up region.

The farthest pulse distance ranges from 8 km to about 10 km in the extreme cases. By controlling the injection pressure, the maximum shrinks to less than 5 km (Figure 13a).

5 Discussion

So far, we reported the model responses that measure the pressure rise and pressure disturbance propagation in the domain. Pressurized volume fraction indicates the actual high pressures that may occur in an injection operation. Build-up volume fraction and farthest pulse are indicators of how the pressure disturbance is spread in the system. We are interested in limiting both the pressure increase and the area of well pressure influence in the aquifer.

In most of the results, aggradation angle, progradation direction and faults play a major role in the pressure behavior. For low aggradation angle, geological layers are made of rock types piled in a parallel stratigraphy. Thus, efficient vertical permeability is the harmonic

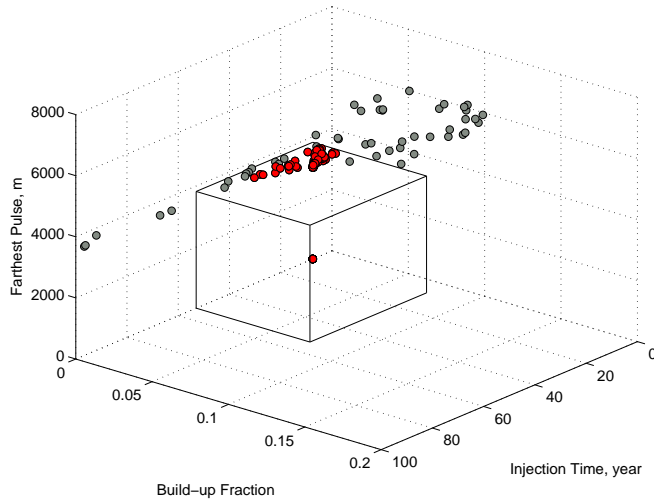


Figure 15: Pressure criteria implemented to filter the acceptable cases. Cases below the critical limits are plotted in red and cases exceeding the limits are plotted in gray.

average of these layers. If any of these layers contains a low permeability rock, this will result in a low vertical permeability. Injecting into a limited space sealed vertically, increases the pressure in the injection point.

Progradation direction can dominate the pressure behavior. It is very important to locate the injector in a high permeability zone is connected to other parts of the domain via permeable channels. Injecting into the river side of a shallow-marine depositional system, may end up into locating the injection point in a low quality rock between river branches joining the sea. This rises the pressure significantly near the injection point and can result in a high well-bore and aquifer pressure.

Structural deformations due to faulting process can increase the connectivity in the medium. If the transmissibility in the aquifer scale is high, the injection pressure releases through the open boundaries. However, if the injection area is surrounded by low quality medium, the pressure rises in the aquifer and the connectivity enhanced by fault geometries spread the build-up region in the domain. On the other hand, sealing faults result in high pressure within closed zones around the injection point. However, they may limit the pressure disturbance propagation in the domain.

From an operational perspective, pressure limits must be set to keep the operations within safe margins. One approach to study the safety of an operation could be setting critical limits on the pressure responses measured here. This limit is used to filter cases with desirable/acceptable pressure behavior. The critical margins are inferred from the realistic operational requirements. In our practice, we assume these margins to be 53 years for the injection time, 0.0787 for the pressurised volume fraction, 0.0745 for the build-up volume fraction, and 3822 m for the farthest pulse distance from the injection point. These values are picked from the middle points of range of variations in the results. By these assumptions, 49 cases out of total number of 160 cases exceed the critical limits.

Figure 15 shows the cases filtered by the pressure criteria. In Figure 15, the pressurized volume fraction is also considered in the filtration, though it is not shown in the plot axes.

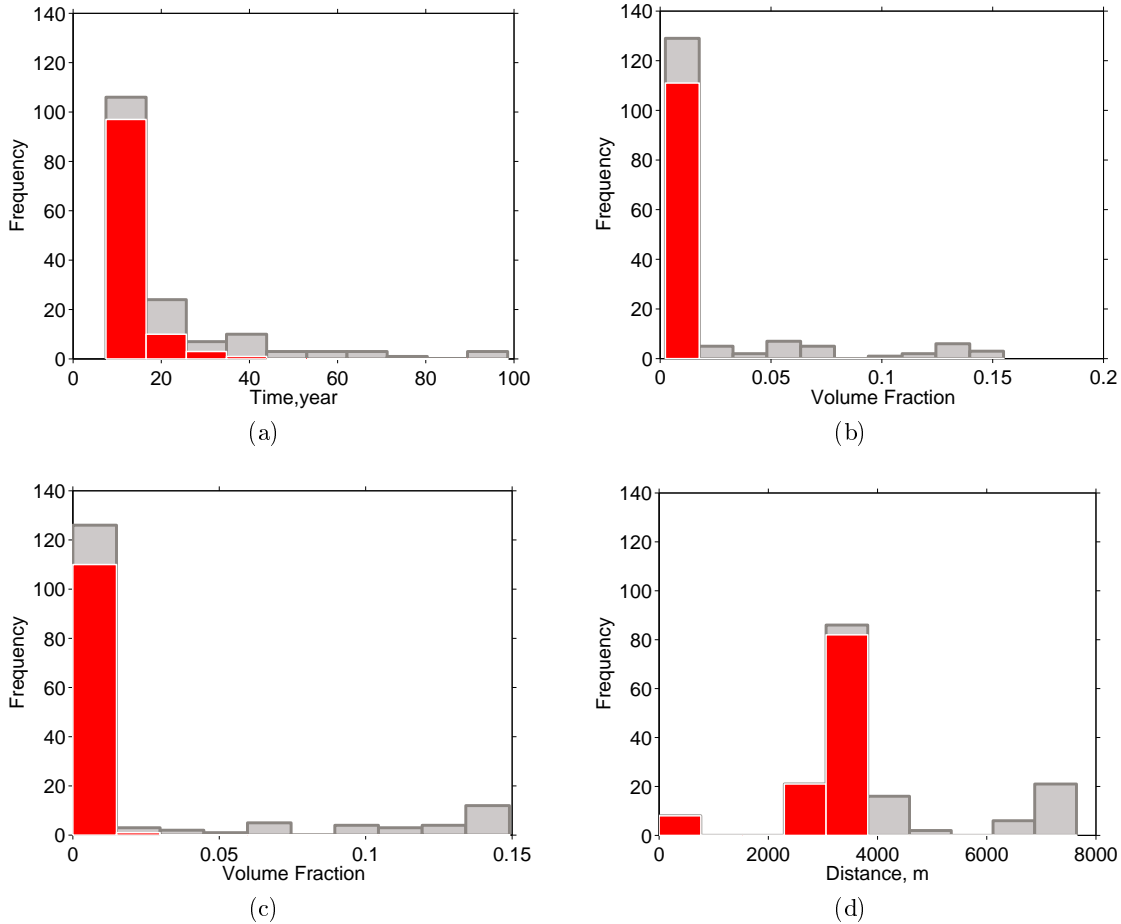


Figure 16: The histogram of filtered cases (colored in red) compared with the histogram of all cases for different pressure responses: a) Injection time, b) Pressurised volume fraction, c) Build-up volume fraction, and d) Farthest pulse distance from the injection point.

The plot shows that most of the cases that pass the filtering are concentrated in a region of low build-up fraction values. Figure 16 reports the histogram of filtered cases in comparison with the histogram of all studied cases for each response.

6 Conclusion

This work is a part of comprehensive sensitivity studies to assess the impact of geological heterogeneity on CO₂ injection and early migration. The aim of this study is to define preventing measures that can be used to avoid high pressures and the damages accompanied by them during the injection operations. Simulation responses related to the pressure behavior in the system are defined and calculated for two CO₂ injection scenarios. Geological variations in shallow-marine depositional systems are examined by using large number of realizations representing a spectrum of sedimentological and structural parameters. Operational critical values are considered for the defined preventive measures.

Most of the studied responses, show relatively a higher sensitivity to aggradation, progradation and faulting. Low aggradation angle keeps the flow restricted in a limited space. In cases with low rock quality in injection layers, pressure builds up in the well-bore. Injecting in down dip progradation, normally ends up in a higher pressure buildup and lower injectivity. In the down dip progradation, the majority of the region around injection point is made of low quality rock. Faults change the geometrical structure of the medium and they put different layers in contact. Pressure disturbance can leak through faults to larger distances from injection point. Closed faults can significantly reduce the injectivity quality.

The work-flow of pressure study demonstrated here can be used in a specific studies in the context of geological uncertainty. The work-flow can be used for other depositional systems and different values for operational limits can be used, which might lead to outcomes different than the results reported here.

References

- [1] M. Ashraf, K.A. Lie, Nilsen, and A. Skorstad. Impact of geological heterogeneity on early-stage CO₂ plume migration: Sensitivity analysis. In *ready for submission*, 2012.
- [2] M. Ashraf, K.A. Lie, H.M. Nilsen, J.M. Nordbotten, and A. Skorstad. Impact of geological heterogeneity on early-stage CO₂ plume migration. In *CMWR*, 2010.
- [3] B. Cailly, P. Le Thiez, P. Egermann, A. Audibert, S. Vidal-Gilbert, and X. Longaygue. Geological storage of CO₂: A state-of-the-art of injection processes and technologies. *Oil & Gas Science and Technology*, 60(3):517–525, 2005.
- [4] A. Cavanagh and N. Wildgust. Pressurization and brine displacement issues for deep saline formation CO₂ storage. *Energy Procedia*, 4:4814–4821, 2011.
- [5] J.A. Howell, A. Skorstad, A. MacDonald, A. Fordham, S. Flint, B. Fjellvoll, and T. Manzocchi. Sedimentological parameterization of shallow-marine reservoirs. *Petroleum Geoscience*, 14(1):17–34, 2008.
- [6] T. Le Guenan and J. Rohmer. Corrective measures based on pressure control strategies for CO₂ geological storage in deep aquifers. *International Journal of Greenhouse Gas Control*, 2010.
- [7] T. Manzocchi, J.N. Carter, A. Skorstad, B. Fjellvoll, K.D. Stephen, JA Howell, J.D. Matthews, J.J. Walsh, M. Nepveu, C. Bos, et al. Sensitivity of the impact of geological uncertainty on production from faulted and unfaulted shallow-marine oil reservoirs: objectives and methods. *Petroleum Geoscience*, 14(1):3–11, 2008.
- [8] J.D. Matthews, J.N. Carter, K.D. Stephen, R.W. Zimmerman, A. Skorstad, T. Manzocchi, and J.A. Howell. Assessing the effect of geological uncertainty on recovery estimates in shallow-marine reservoirs: the application of reservoir engineering to the SAIGUP project. *Petroleum Geoscience*, 14(1):35–44, 2008.

- [9] J.P. Nicot. Evaluation of large-scale CO₂ storage on fresh-water sections of aquifers: an example from the Texas Gulf Coast Basin. *International Journal of Greenhouse Gas Control*, 2(4):582–593, 2008.
- [10] C. Oldenburg. Comments on Economides and Ehlig-Economides,"Sequestering carbon dioxide in a closed underground volume" SPE 124430, October 2009. 2010.
- [11] J. Rutqvist, J. Birkholzer, F. Cappa, and C.-F. Tsang. Estimating maximum sustainable injection pressure during geological sequestration of CO₂ using coupled fluid flow and geomechanical fault-slip analysis. *Energy Conversion and Management*, 48(6):1798–1807, 2007.
- [12] J. Rutqvist and C.F. Tsang. A study of caprock hydromechanical changes associated with CO₂ injection into a brine formation. *Environmental Geology*, 42:296–305, 2002. 10.1007/s00254-001-0499-2.
- [13] L.G.H. van der Meer. Investigations regarding the storage of carbon dioxide in aquifers in the Netherlands. *Energy Conversion and Management*, 33(5-8):611–618, 1992.
- [14] L.G.H. van der Meer. The conditions limiting CO₂ storage in aquifers. *Energy Conversion and Management*, 34(9-11):959–966, 1993.

Paper III

2.3 Geological storage of CO₂: Application, feasibility and efficiency of global sensitivity analysis and risk assessment using the arbitrary polynomial chaos.

,
M. Ashraf, S. Oladyshkin, W. Nowak

Proceedings of the European Geosciences Union (EGU) General Assembly 2012, April, Vienna, Austria, Geophysical Research Abstracts., Vol. 14, EGU2012-9243. Published in International Journal of Greenhouse Gas Control (2013).

Geological storage of CO₂: global sensitivity analysis and risk assessment using the arbitrary polynomial chaos expansion

Meisam Ashraf^{a,b}, Sergey Oladyshkin^c, Wolfgang Nowak^c

^a*Department of Mathematics, University of Bergen, 5028 Bergen, Norway*

^b*SINTEF ICT, Department of Applied Mathematics P.O. Box 124 Blindern, N-0314 Oslo, Norway*

^c*SRC Simulation Technology, Institute for Modelling Hydraulic and Environmental Systems (LH2), University of Stuttgart, Pfaffenwaldring 61, 70569 Stuttgart, Germany.*

Abstract

Geological storage of CO₂ is a proposed interim solution for mitigating the climate change. The considerable costs and potential hazards of the technique require feasibility studies to assess all possible risks involved in the process. Modeling CO₂ storage requires working with large time and space scales, which in practice are accompanied by huge geological uncertainties.

The overall goal of this study is to demonstrate the application and feasibility of global sensitivity analysis with Sobol indices and probabilistic risk assessment via the very recent arbitrary polynomial chaos expansion (aPC) method. We model a typical CO₂ injection scenario implemented in realistic geological realizations. A number of uncertain parameters control the structural heterogeneities with assumed probability distributions. These parameters include the effect of barriers, the aggradation angle, fault transmissibility and regional groundwater effects. They represent realistic types of structural features that have not been analyzed before in this context and manner.

Within the aPC, a so-called response surface is representing how the model output changes with respect to the uncertain parameter values by multi-variate polynomials for all output quantities of interest. We choose the aPC, because the resulting response surface is significantly faster than the full original model, and so facilitates global sensitivity analysis and probabilistic risk assessment even for

Email addresses: meisam@resman.no (Meisam Ashraf),
Sergey.Oladyskin@iws.uni-stuttgart.de (Sergey Oladyshkin),
Wolfgang.Nowak@iws.uni-stuttgart.de (Wolfgang Nowak)

large problems.

Quantification of input parameter uncertainty is not the primary concern of this work, as it can change from one place to another. Therefore, no generalized conclusions on the reality of geological uncertainties can be drawn from this study.

Keywords:

CO₂ storage, Global sensitivity analysis, Probabilistic risk assessment, Uncertainty quantification, Arbitrary polynomial chaos, Sobol indices

1. Introduction

In the context of climate change mitigation, geological storage of CO₂ has been proposed as interim solution. The idea has been challenged during the last decades for its costs and potential hazards [1, 2]. A large number of studies has been performed in the industry and research communities to evaluate the safety and feasibility of CO₂ storage, addressing issues such as the status and barriers of CO₂ storage [3], screening and ranking of geological storage sites [4], large-scale impacts of CO₂ injection in deep saline aquifers [5], new solution methodologies for CO₂ leakage [6], the capture project [7], and leakage estimates [8]. Furthermore, many pilot projects have been installed, like In Salah [9], Ketzin [10], and Johansen [11]. A discussion on the experiences from the existing pilot projects is reported in [12].

Yet, there is a big demand for studies which demonstrate the appropriateness of the storage operation. Transparent scientific results are required to communicate the facts and evidences about feasibility and possible risks within public and industry. The large involved time and space scales, however, cause substantial computational issues in such studies (e.g., [13]), and the modeling procedure is accompanied by a huge extent of geological uncertainties (e.g., [14, 15, 16, 17]).

In an approach to quantify the impact of geological heterogeneity on model predictions of multiphase flow in geological formations, a large number of shallow marine depositional realizations has been generated and used in the sensitivity analysis of the impact of geological uncertainties on production forecasting (SAIGUP), see [18, 19, 20]. There, the impact of variable geological parameters has been quantified for oil recovery in different field development scenarios. The main general conclusion of that study is that realistic features of geological uncertainty in modeling (other than typical hydrological parameters) can lead to considerable uncertainties in prediction. Ashraf et al. [21, 22] used a number of SAIGUP realizations to study the impact of geological heterogeneity on the

injection and early migration of CO₂ in a shallow-marine aquifer with a complex, heterogeneous geological structure. That study transferred the significance of some of the geological structural features to the case of CO₂ injection.

In practice, modeling complicated physical phenomena in the subsurface requires stochastic approaches. Uncertainty can exist in different levels, from the formulation of dependency rules in the model to uncertainty about appropriate values for the model input parameters. Uncertainty coming from any source in the modeling procedure propagates through the model to the predicted responses. Ranking the important model parameters based on their influence on the model responses can support a better understanding of the system, and it can result in a better design of subsequent studies on the stochastic nature of the process. Hence, identifying and evaluating the sensitivities and uncertainties of model parameters and their impact on prediction uncertainties and projected risks is a significant task. Sensitivity analysis is known to be the right approach to identify the significance of uncertainty sources within the modeling process [23] and to improve the understanding of model behavior [24]. For example, the European Commission and the United States Environment Protection Agency recommend using sensitivity analysis in the context of extended compact assessment for policy making [25].

Uncertainty sources within the CO₂ storage problem can be classified in different types as geological, physical and operational uncertainties. This work is devoted to geological uncertainties. However the same procedure can be applied to extend the work for other types as well. Here, we use a set of SAIGUP realizations to perform a sensitivity analysis and to assess the risks caused by uncertainties in a choice of parameters that govern the geological structure of the featured shallow-marine deposit.

The goal of this study is to test and demonstrate the applicability of a recent set of methods to a realistic scenario. We choose a stochastic response surface method to project the model response to parameter changes onto high-dimensional polynomials via the arbitrary polynomial chaos expansion (aPC) [23, 26]. Highly similar ideas to the aPC have also been proposed in other scientific areas [27, 28, 29, 30]. As we review in Section 2, the involved orthogonal polynomial basis can be constructed for arbitrary probability distributions of the uncertain parameters. This data-driven approach provides fast convergence [23] in comparison to the classical polynomial chaos expansion (e.g., [31, 32, 33]). Moreover, it avoids the subjectivity of data treatment that would arise when being forced to fall back onto a limited number of theoretical distributions that can be tolerated with previous generalized versions of polynomial chaos expansions [34, 35]. The reduced

model represented by the response surface is significantly faster than the original complex one, and thus provides a promising starting point for global sensitivity analysis, uncertainty quantification, and probabilistic risk assessment.

In the current paper, we use global sensitivity analysis rather than a local one, because local analysis fails to cover the non-linear variation of model responses over the entire range of probability distributions of the input parameters. A practical approach in global sensitivity analysis is to work with the impact of uncertain parameters on prediction variances, because this shows a good success in nonlinear problems [36]. In the current study, we use Sobol indices [24] for sensitivity analysis, which are indeed working with variances. The fact that the aPC based response surface is based on orthonormal polynomials with exploitable known properties [37] substantially simplifies this analysis.

Finally, we perform risk analysis by applying a Monte-Carlo procedure to the response surface. The approximating polynomial is fast enough to be used for a large number of Monte-Carlo realizations. This makes it possible to cover the entire range of variations in the model input described by the assigned probability distributions, and thus provides accurate estimates for the risk in the system. We conclude with a discussion of the results.

The global sensitivity analysis and uncertainty quantification studies for CO₂ storage existing in the literature are concerned with classic hydrological uncertain parameters like porosity, pore volume and permeability as global constants (see for example [15, 26, 38]). To the best of our knowledge, the current study is the first one that implements the proposed mathematical analysis tools on realistic geological structural parameters at reservoir scale. The parameters we consider are the level of barriers presence, aggradation angle, fault transmissibility, and regional groundwater effects. The considered features are the structural and depositional features that dictate the distribution of hydrological parameters such as permeability and porosity, both in terms of value and spatial distribution. These are among the most uncertain geological parameters identified with the SAIGUP study (except the regional groundwater effect, which is specific to this study).

2. Response surface via arbitrary polynomial chaos expansion

Working with uncertain parameters in complex, non-linear and dynamic systems puts a high demand on stochastic tools to analyze the system and to propagate uncertainties through the system. Conceptually straightforward numerical Monte Carlo (MC) techniques are computationally demanding since the statistical accuracy of their predictions depends on the number of realizations used. The

Monte-Carlo estimation error (measured as standard deviation) for output statistics typically decreases only with the square root of the number of realizations used. Using a stochastic response surface is a promising approach in this respect.

Obviously, a response surface can be constructed in different ways, e.g. it can be constructed directly on a dense Cartesian grid of input parameters at extremely high computational efforts. In the current paper, we apply an alternative methodology which demands only a minimum number of model evaluations to construct the response surface. This approach is based on the theory of polynomial chaos expansion (PCE) introduced in [31]. Generally, all PCE techniques can be viewed as an efficient approximation to full-blown stochastic modeling (e.g., exhaustive MC). The basic idea is to represent the response of a model to changes in variables through a response surface that is defined with the help of an orthonormal polynomial basis in the parameter space. In simple words, the dependence of model output on all relevant input parameters is approximated by a high-dimensional polynomial. The resulting polynomials are functions of the model parameters. This projection can be interpreted as an advanced approach to statistical regression.

The PCE offers an efficient and accurate high-order way of including non-linear effects in stochastic analysis (e.g., [39, 40, 41]). One of the attractive features of PCE is the higher-order in uncertainty quantification, e.g., [32, 33, 42], as well as its computational speed when compared to other methods for uncertainty quantification performed on the full model, such as MC [43]. Due to its elegant reduction of models to polynomials, it allows performing many tasks analytically on the expansion coefficients. Alternatively, it allows performing excessive MC on the polynomials since they are vastly faster to evaluate than the original model.

Unfortunately, the original PCE concept [31] is optimal only for Gaussian distributed input parameters. To accommodate for a wide range of data distributions, a recent generalization of PCE is the arbitrary polynomial chaos (aPC [26]). Compared to earlier PCE techniques, the aPC adapts to arbitrary probability distribution shapes of input parameters and, in addition, can even work with unknown distribution shapes when only a few statistical moments can be inferred from limited data or from expert elicitation. The arbitrary distributions for the framework can be either discrete, continuous, or discretized continuous. They can be specified either analytically (as probability density/cumulative distribution functions), numerically as histogram or as raw data sets. This goes beyond the generalization of PCE in methods such as the generalized polynomial chaos (gPC) or the multi-element gPC (ME-gPC) [34, 35]. The aPC approach provides improved convergence in comparison to classical PCE techniques, when applied

to input distributions that fall outside the range of classical PCE. A more specific discussion and review of involved techniques will follow in Sections 2.1 to 2.3.

With an introduction to response methods via the aPC, we describe here the theoretical background that we use in our modeling procedure. The related techniques for sensitivity and risk analysis used in this work are explained in Sections 4 and 5.

2.1. Definitions and polynomial chaos expansion

Suppose that we approximate a problem by a functional Υ , which represents the model responses Γ for the input variables Θ :

$$\Gamma \approx \Upsilon(\Theta). \quad (1)$$

Like all PCE methods, the aPC is a stochastic approach to approximate the response surface. Considering the uncertainty in the input variables, the aPC constructs a set of polynomial basis function and expands the solution in this basis. Thus, the response vector Γ in Eq. (1) can be approximated by [23]:

$$\Gamma \approx \sum_{i=1}^{n_c} c_i \Pi_i(\Theta). \quad (2)$$

Here, n_c is the number of expansion terms, c_i are the expansion coefficients, and Π_i are the multi-dimensional polynomials for the variables $\Theta = [\theta_1, \dots, \theta_n]$, and n is the considered number of modeling parameters. If the model response $\Gamma(\Theta)$ depends on space and time, then so do the expansion coefficients c_i .

The number n_c of unknown coefficients c_i results from the number of possible polynomials with total degree equal to or less than d . This number depends on the degree d of the approximating polynomial, and the number of considered parameters n :

$$n_c = \frac{(d+n)!}{d!n!}. \quad (3)$$

2.2. Data-driven orthonormal basis

All polynomials Π_i in expansion (2) are orthogonal, i.e., they fulfill the following condition:

$$\int_{I \in \Omega} \Pi_l \Pi_m p(\Theta) d(\Theta) = \delta_{lm}, \quad (4)$$

where I is the support of Ω , δ is the Kronecker symbol, and $p(\Theta)$ is the probability density function for the input parameters. We obtain the orthonormal basis

with the moments-based method proposed in [23, 26]. Orthonormality has the advantage that many subsequent analysis steps are accessible to relatively simple analytical solutions.

Knowledge on variability never is so perfect such that we could express the probability of model parameter values in a unique distribution function. Available data are mostly scarce, and fitting a density function to observed frequencies is often biased by subjective choices of the modeler. Oladyshkin et al. [26] argued that, with aPC, it is possible to use available probabilistic information with no additional formal knowledge requirements for their probability distributions, only based on the statistical moments of the available data. They showed that, it is possible to calculate estimates for the mean, variance, and higher order moments of the model response $\Gamma(\Theta)$ even with incomplete information on the uncertainty of input data, provided in the form of only a few statistical moments up to some finite order.

2.3. Non-intrusive determination of the coefficients

The next task is to compute the coefficients c_i in Eq. 2. Generally, all PCE techniques can be sub-divided into intrusive [44, 45, 46] and non-intrusive [43, 47, 48, 49] approaches, i.e., methods that require or do not require modifications in the system of governing equations and corresponding changes in simulation codes. The challenge in choosing between the methods is to find a compromise between computational effort for model evaluations and a reasonable approximation of the physical processes by the interpolation.

For our study, we prefer the probabilistic collocation method (PCM: see [26, 43, 49]) from the group of non-intrusive approaches like sparse quadrature [50, 51, 52, 53]. In a simple sense, PCM can be interpreted as a smart (mathematically optimal) interpolation and extrapolation rule of model output between and beyond different input parameter sets. It is based on a minimal and optimally chosen set of model evaluations, each with a defined set of model parameters (called collocation points). For this reason, the collocation approach became more popular in the last years. Also, the collocation formulation does not require any knowledge of the initial model structure. It only requires knowledge on how to obtain the model output for a given set of input parameters, which allows treating the model like a “black-box”. The distinctive feature of non-intrusive approaches is that any simulation model can be considered a “black-box”, i.e. commercial software can be used without any modifications required.

According to [54], the optimal choice of collocation points corresponds to the roots of the polynomial of one degree higher ($d + 1$) than the order used in the

chaos expansion (d). This choice adapts the position of collocation points to the involved distribution shape, and is based on the theory of Gaussian integration (e.g., [55]). For one-dimensional problems (i.e., when analyzing only one uncertain model parameter), it allows exact numerical integrations of order $2d$ given $d + 1$ values of the function to be integrated.

For multi-parameter analysis, the number of available points from the corresponding Gaussian integration rule is $(d + 1)^n$, which is larger than the necessary number M of collocation points. The minimum value of M is equal to the number of coefficients n_c in Expansion (2), according to Eq. (3). The full tensor grid can be used only for low-order (1^{st} , 2^{nd}) analysis of few parameters. For higher-order analysis of many parameters, the tensor grid suffers from the curse of dimensionality (a full tensor grid in n dimensions requires $(d + 1)^n$ points, which rises exponentially in n)[56]. In that case, a smart choice of a sparse subset from the tensor grid becomes necessary. Then, PCM chooses the minimum required number of collocation points, equal to the number of coefficients n_c , from the full tensor grid according to their probability weight, i.e. according to their importance as specified by the available probability distribution of Θ . This simply means to select the collocation points from the most probable regions of the input parameter distribution (see [43]).

The weighted-residual method in the random space is defined as [49]:

$$\int (\Gamma - \sum_{i=1}^{n_c} c_i \Pi_i(\Theta)) w(\Theta) p(\Theta) d\tau = 0, \quad (5)$$

where $w(\Theta)$ is the weighting function and $p(\Theta)$ is the joint probability density function of Θ . Please note that choosing $w_i = \Pi_i$ in Eq. 5 results in the method discussed by [32] and [33]. In PCM, the weighting function is chosen as the delta function:

$$w(\Theta) = \delta(\Theta - \Theta_c). \quad (6)$$

Θ_c is the set of collocation points. Substituting from Eq. (6) into Eq. (5) gives the following:

$$\Gamma_c - \sum_{i=1}^{n_c} c_i \Pi(\Theta_c) = 0, \quad (7)$$

where Γ_c are the response values corresponding to the collocation values Θ_c . We solve Eq. (7) to find the coefficients c_i .

Hence, in total, n_c detailed runs are required to determine the n_c unknown coefficients. The roots of the data-driven polynomial basis (see Section 2.2) define

the positions of the collocation points specific to the distribution of input parameters at hand and, thus, indicate the optimal parameter sets for model evaluation, using all available information about the input parameters. In our study, we have $n = 4$ uncertain parameters and we use a polynomial of degree $d = 2$. This means that only $n_c = 15$ detailed runs are necessary to obtain the expansion coefficients and approximate the response surface.

3. CO₂ storage problem

Here, we describe the injection scenario for which we analyze sensitivities, uncertainties, and risks in Sections 4 and 5. The same flow responses are studied here as in [21, 22]. These are aquifer pressure, CO₂ mobile and residual volumes and leakage risk as described below. Then, we describe the uncertain parameters considered in the study followed by a discussion on the uncertain structural aspects of the considered geological settings.

3.1. Modeling scenario

A typical scenario of CO₂ injection is defined in which a volume of $40 \times 10^6 \text{ m}^3$ is injected via one well during an injection period of 30 years. This volume corresponds to 20% of the total aquifer pore volume. After stopping injection, simulation continues for 70 years to study the early migration of the CO₂ plume. For brevity, we omit the detailed model equations here and refer the interested reader to [23, 26].

In our scenario, we feature an aquifer system that is formed by shallow-marine deposits. There is one closed boundary on the top side of the model and the other sides are assumed to be open (Figure 1). All the open boundaries are modeled as Dirichlet boundaries, two of which with hydrostatic pressure distribution (the right and bottom boundaries in Figure 1). The remaining left boundary is also hydrostatic, but modified in order to account for the regional groundwater effect (see below).

The cells on the faces of the open boundaries are equipped with a very large pore volume multiplier, such that they numerically represent a much larger volume and effectively enlarge the domain. This helps to minimize the boundary effects of a computational domain that would otherwise be relatively small compared to the injected CO₂ volume (about 20% of the total pore volume, see above). The pore volume multiplier technique allows for a physically reasonable pressure build-up close to the boundary. Moreover, this allows the CO₂ that has left the domain to re-enter by gravity segregation after the injection has stopped.

A summary of the used parameter values is given in Table 1. The hydrological parameters like permeability and porosity vary within individual realizations due to the considered geological structure (see Figure 2 for the histograms of porosity and permeability in one selected realization). They also differ between the different realizations, as they are changed to represent different geological features. Although the geological realizations of this model vary in some geological features, but the same total pore volume, grid, and fault geometry is considered. The injection well is screened in the lower part of the model.

3.2. Analyzed model predictions

We seek to maximize the CO₂ storage volume and minimize the risk of leakage. These quantities are measured by various simulation outputs that are described in Table 2 and discussed in the following.

Aquifer pressure is considered as the spatial average of the pressure distribution in the domain, weighted by the pore volume of each rock type. Monitoring or predicting the pressure response is important to avoid over-pressurized injection operations.

Residual CO₂ volume is the volume of trapped CO₂ that is left in the small pores in an imbibition process. This volume is crucial for the long-term storage capacity of reservoirs.

Mobile CO₂ volume is the volume of CO₂ that can move in a continuous phase in the medium. It is considered as one of the important flow responses, because only mobile CO₂ volumes can lead to leakage through any failure in the sealing cap-rock or ill-plugged well.

Finally, we consider **leakage risk** through cap-rock failure. Cap-rock integrity is a major concern for the safety of CO₂ storage operations. An over-pressurized injection can lead to fractures that may extend up to the cap-rock, penetrate through the cap-rock, or activate pre-existing faults and fractures, and finally lead to CO₂ leakage. In addition, the capillary barrier effect of the cap-rock can be overcome by a local pressure build-up. Thus, the probability of cap-rock failure can depend on the geomechanical properties of the cap-rock and of the medium, on the topography of the cap-rock, and on the pressure build-up resulting from the CO₂ injection and migration. More details about failure mechanisms and failure criteria can be found in the literature (e.g., [57, 58, 59]). However, geomechanical modeling and knowledge about pre-existing features that can be activated during injection would be required to take these processes into account.

Here, we demonstrate how cap-rock integrity can be considered in the workflow of sensitivity analysis and uncertainty assessment in a simplified manner.

To avoid detailed studies of multiphase flow coupled with geomechanical simulations and fracture mechanics, we follow a pragmatic approach. The idea is to assign a spatial probability distribution of cap-rock failure over the area of the cap-rock layer, such that each point of the cap-rock has its own failure probability. In principle, this probability could be assigned in correspondence with the current pressure distribution and with geological features such as varying cap-rock thickness, material properties, faults and fractures. For the means of demonstration, we simply assign a spatial Gaussian function as a scenario assumption to provide the cap-rock failure probability for each point of the cap-rock (see Figure 3). Leakage risk is defined as the probability of leakage (due to cap-rock failure) times the amount of escaping CO₂ in case of leakage. Thus, we spatially integrate the product between cap-rock failure probability and the volume of mobile CO₂ below each point of the cap-rock over the entire area of the cap-rock.

3.3. Uncertain parameters

The most apparent uncertainty in CO₂ storage is the lack of geological knowledge. Large geological scales and diversity of rock properties make it impossible to obtain the whole descriptive picture for a study. A geological study will therefore be accompanied by huge levels of uncertainty. Many studies have shown the significance of geological heterogeneity on underground flow performance (e.g., [60, 61]). To obtain a descriptive image of a feature, like faults and depositional structure, such that uncertainty can be reduced, we must provide adequate data. The process of data collection from underground layers is very costly, therefore it is important to know the ranking of influence each feature has on the flow in order to optimize the cost of data acquisition in modeling.

From the geological parameters that are relevant for shallow-marine deposits used in [21, 22], we pick three parameters: the degree to which barriers may block horizontal and vertical flow, aggradation angle, and fault transmissibility. In addition to these, we consider the regional groundwater effect as an uncertain parameter in our study. Here, we give a brief description on each one, followed by the probabilities assigned to these parameters.

Barriers: During the formation of shallow-marine deposits, periodic floods result in a sheet of sandstone that dips, thins, and fines in a seaward direction. In the lower front, thin sheets of sandstone are inter-bedded with the mud-stones deposited from suspension. These mud-draped surfaces are potential significant barriers to both horizontal and vertical flow. In the SAIGUP realizations, these barriers were modeled by transmissibility multipliers in specific layers of the for-

mation. The position of the barriers is generated by creating an elliptic cone-shaped surface that follows the plan-view shoreline shape of the facies, characterized from real world data [18]. We define the degree of barrier presence by the areal percentage of zero-valued transmissibility multipliers. Figure 5 shows a medium level of barriers.

Aggradation angle: in shallow-marine systems, two main factors control the shape of the transition zone between river and basin: the amount of deposition supplied by the river and the accommodation space that the sea provides for these depositional masses. Deposition happens in a spectrum from larger grains depositing earlier on the land side, to fine deposits happening in the deep basin. If the river flux or sea level fluctuates, equilibrium changes into a new bedding shape based on the balance of these factors. In the SAIGUP study, progradational cases are considered, in which river flux increases and shifts the whole depositional system into the sea. The angle at which transitional deposits are stacked on each other because of this shifting is called the aggradation angle. Three levels of aggradation are shown in Figure 4: low, medium and high. The study reported in [21, 22] showed that aggradation can have a dramatic influence on the injection and migration process.

Fault transmissibility: Huge uncertainties can be involved when modeling the presence of faults. Faults are discrete objects that are modeled by changing the geometry of the simulation grid. The transmissibility for flow across faults changes during the process of faulting. This causes a spectrum of transmissibilities, from a sealing fault with no flow across it, to a fault that has not produced any barriers to the flow within its opening space.

Within a simulation grid, the influence of faults on the local and global flow behavior depends on a number of parameters including fault length, orientation, intensity and transmissibility. The well location with respect to the faults can change the overall behavior of injected CO₂ plume significantly. In the SAIGUP models, different levels of fault orientations, transmissibility, areal intensity, and well patterns are considered. For this study, we consider all fault modeling parameters at their medium level and consider to vary only the fault transmissibility. These variations, however, do not affect the definition of the no-flow boundary, which is motivated by the presence of an impermeable fault.

The used geology realizations contain compartmentalized fault systems comprising approximately equal densities of strike-parallel and strike-perpendicular faults based on a portion of the Gullfaks field [18, 62]. Figure 6 shows the fault pattern and location of the injector considered for the study.

It is shown in [63] that the transmissibility multiplier provides a numerically

more robust representation of faults within reservoir simulation than conventional permeability multipliers. We consider the fault transmissibility multipliers to range between zero and one. A multiplier value of one corresponds to a fault permeability equal to the harmonic average of cell permeabilities across the fault, i.e., to a fault without any influence on flow [63].

Regional groundwater effect: Geological modeling always comes with the uncertainty of how large the aquifer is and how it is connected to other underground aquifers. This is a direct consequence of the need to define boundary conditions to limit the computational domain, which cannot always coincide with meaningful physical boundaries in large-scale systems. However, connections to active external aquifers can be accounted for by adapting the values for the boundary conditions accordingly. Some connections might even change throughout the year, depending on rainfall. The flux across model boundaries might influence the CO₂ plume dynamics during and after injection. To simulate such effects, we changed the left boundary pressure by adding an uncertain additional pressure value Δp that varies between 0 and 100 bars.

As a scenario assumption, this pressure value is added at the start of injection, i.e., the pressure distribution is not at a steady state when the simulation starts, and this triggers a corresponding transient brine flow. We do so in order to analyze the effect of transient groundwater effects on the system. This may seem an arbitrary choice, but assuming a steady-state would also be arbitrary to some extent.

The overall process for sensitivity analysis, uncertainty propagation, and risk assessment starts by specifying probability information for the uncertain parameters. Next, one has to design and choose the simulation cases required to obtain the expansion coefficients in the approximating polynomial. However, in our study, we had access to the set of SAIGUP geological realizations and simulation results that had been designed without the considerations possible with the aPC. The computing time for each SAIGUP realization was about 2 hours on a 2.4GHz Intel Xeon CPU, and we decided to recycle these highly expensive simulations in our study. The large computing times are a key motivation to build a cheaper surrogate model for further analysis. Hence, we assume the histograms of uncertain parameters such that they result in collocation points that coincide with the SAIGUP designed values. Therefore, the histograms used in this study are almost uniform, as shown in Figure 7. In fact, these input distributions could also be handled with the gPC method already mentioned in the introduction, and would correspond to the use of Legendre polynomials. In our case, we use the aPC to avoid the step of modeling the input distributions as exactly uniform. Consequently, the polynomials resulting from the aPC approach are very close to Legendre polynomials.

The aPC, however, could be used for any type of histograms and so provides the freedom in other studies to adapt to arbitrary input statistics.

The main concern here is not a unique probability description of the input geological parameters, but rather we perform an uncertainty analysis practice, relying on a scenario assumption of probability distributions. Thus, no general geological conclusion is expected from this study, and results might change by feeding the work-flow with a different probability description.

4. Sensitivity analysis

In this section, we tackle global sensitivity analysis with Sobol indices based on the aPC technique, following the line of work on aPC by [23, 26, 37]. The big advantage of global aPC-based sensitivity analysis is that one can obtain global sensitivity information at computational costs that are hardly larger than those for local analysis. The reason is the following: local methods use infinitesimally small spacing between parameter sets for model evaluation to get numerical derivatives evaluated at a single point. The aPC-based method places the parameter sets for model evaluation at an optimized spacing in parameter space. This can be interpreted as fitting secants (or polynomials for non-linear analysis) to the model response. These secants (polynomials) approximate the model over the entire parameter space in a weighted least-square sense (compare with the best unbiased ensemble linearization approach described by [64]). This is more beneficial compared to computing a tangent or local second derivatives (compare FORM, SORM methods, e.g., [65]) that approximate the model well just around one point in the parameter space.

The system featured here is non-linear due to two reasons: First, the involved multi-phase flow equations [26] form a coupled system of non-linear partial differential equations, and second, these equations are non-linear in their coefficients. The latter is even more significant if parameters are spatially heterogeneous.

In the following, we briefly summarize the Sobol sensitivity indices technique for quantifying the relative importance of each individual input parameter in the final prediction. Then, we implement the method for our geological CO₂ storage problem, based on the aPC response surface.

The model responses featured here for global sensitivity analysis (this section) and for the probabilistic risk analysis (see Section 5) are listed in Table 2 and have been discussed in Section 3.1. In the sense of global sensitivity analysis [66], not only should the analysis technique be global, but also should the analyzed quantities be global. In the latter, global refers to the fact that they are relevant for the

engineer, are crucial in decision processes, etc. For example, an overall leakage risk is more informative in final decisions than the leakage rate at a specific point, and a total stored volume of CO₂ is more informative for volumetric efficiency considerations of the reservoir than the CO₂ saturation at individual points.

4.1. Sobol sensitivity indices

The method is well described in the literature [24, 36, 66, 67]. More recent works are concerned about expediting calculation pace by computing Sobol indices analytically from polynomial chaos expansions [26, 33, 37, 68, 69]. The idea behind the combination of PCE techniques with Sobol indices is to replace the analyzed system with an approximating function which leads to mathematical and numerical benefits in the sensitivity analysis.

Using polynomials for this approximation is convenient, because it is easy to analytically obtain the output variances from the statistics of the input variables of the polynomials. In our case, the solution is approximated by orthogonal polynomials with ascending polynomial degree. We expand the variance of model output into individual components originating from all possible combinations of input parameters. Assume that we break the system output into components as follows:

$$\Gamma = \Gamma_0 + \sum_i \Gamma_i + \sum_i \sum_{j>i} \Gamma_{ij} + \dots \quad (8)$$

A single index (here: i) shows dependency to a specific input variable. More than one index (e.g.: i and j) shows interaction of two or more input variables. If we consider the input vector Θ to have n components θ_i for $i = 1, \dots, n$, then $\Gamma_i = f_i(\theta_i)$ and $\Gamma_{ij} = f_{ij}(\theta_i, \theta_j)$. In practice, we stop at a finite number of terms in Eq. (8). The first order sensitivity index, the so called Sobol index, is defined statistically as follows [66]:

$$S_i = \frac{V[E(\Gamma | \theta_i)]}{V(\Gamma)}, \quad (9)$$

where $E(\Gamma | \theta_i)$ is the conditional expectation of output Γ for a given value of θ_i and V is the variance operator. In plain words, S_i is the fraction of total variance $V(\Gamma)$ that can be explained by the parameter θ_i . Since θ_i can be fixed at any value in its uncertainty interval, each of those values produces a distinct expectation. In Eq. (9), the variance of those expectations is divided by the unconditional variance

of output (i.e., with no input variable fixed). For more than one index, a higher-order Sobol index can be defined as:

$$S_{ij} = \frac{V[E(\Gamma | \theta_i, \theta_j)] - V[E(\Gamma | \theta_i)] - V[E(\Gamma | \theta_j)]}{V(\Gamma)}. \quad (10)$$

Here, $V[E(\Gamma | \theta_i, \theta_j)]$ is the variance of output expectations after fixing θ_i and θ_j . This index represents the significance of variation in output generated from the joint uncertainty in several input variables, i.e., from the interaction of uncertain parameters. If we add all indices that contain a given variable θ_i , the sum is called the total Sobol index:

$$S_{Ti} = S_i + \sum_{j \neq i} S_{ij} + \sum_{j \neq i} \sum_{k \neq i} S_{ijk} + \dots \quad (11)$$

The total Sobol index is a sensitivity measure to rank parameters according to their influence on the model results. When this index is close to zero, the corresponding parameter has a negligible role in the variation of the system response. In that case, the uncertainty in that parameter does not introduce a considerable uncertainty in the response, and the parameter could be omitted from further analyses.

In practice, we evaluate the Sobol indices analytically from the expansion coefficients of the aPC as described by [37].

4.2. Sensitivity analysis

We calculate the total Sobol indices for the geological CO₂ storage problem that is described earlier. The results are based on an aPC expansion of order two that is obtained by fifteen detailed simulations. The choice of order two is supported by the results of [43], where the authors found in a similar CO₂ storage problem that second order may be the cheapest non-linear expansion, but still sufficiently accurate for this type of purpose. Recently, [37] provided the results of a numerical convergence analysis for aPC-based Sobol analysis. They report that increasing the expansion order beyond 2 introduces only small changes to the sensitivity values for their considered system, and does not change the ranking of the analyzed parameters anymore. A study similar to the current study without aPC needed one hundred and sixty runs to perform a sensitivity analysis with a different method [22]. The pattern of sensitivity reported here is similar to what is produced in that study, but at dramatically reduced costs.

4.3. Results

The flow behavior in the domain is influenced by the type and intensity of different heterogeneities. This influence can be traced in the CO₂ pressure and saturation distributions over time. During injection, viscous forces imposed by the injector dominate the force balance. Viscous forces act in the form of spatial pressure gradients in all directions. After 30 years, the injection stops, and gravity starts playing the major role in the flow dynamics, acting in the vertical direction [21, 22].

Barriers and aggradation angle have different impacts on the flow during each flow regime, i.e., injection or after injection. Low fault transmissibility hinders the flow and keeps the pressure in compartments. Geometry distortion in the geological layers because of the faulting processes plays a considerable role in the splitting of CO₂ plumes within the domain. Water flux from lateral boundaries due to the regional groundwater effect enhances the spread of CO₂ and leads the mass of CO₂ toward the other open boundaries.

Figure 8 shows the sensitivity of different responses to the uncertain parameters. Total Sobol indices are plotted at specific times. End of simulation refers to the year 100, i.e., 70 years after injection stops. This time duration is long enough for the flow to stabilize at a stationary condition for the majority of the model runs.

As already observed in [21, 22], the aggradation angle plays a significant role in the flow behavior. In cases with low aggradation angle, the stratigraphy of rock types is a pattern of parallel layering. For higher aggradation angles, rock-types are distributed between more modeling layers. The effective vertical permeability changes from the harmonic average (in Figure 9a) toward the arithmetic average (in Figure 9c), as the aggradation angle increases from 0 to 90 degrees. The harmonic average might be much smaller than the arithmetic average, in particular when there are vertically impermeable rock-types in the medium. The shallow marine depositional system contains some rock-types with almost zero transmissibility in the vertical direction. Therefore, a low aggradation angle can hinder the flow from traveling upward across layers in the domain and force it to stay trapped in some lower layers, as seen for many of the low aggradation angle realizations in our study. The relatively large sensitivities to the level of barrier presence is based on the same effects.

Our results show a relatively weak sensitivity of responses with respect to the water influx from one side of the model. This sensitivity is in particular low during injection, when the high pressure imposed from the well dominates the dynamics of flow in the medium (Figure 8a). The sensitivity patterns for the mobile and

residual CO₂ volume are similar in Figures 8b and 8c, because the mobile and residual CO₂ volume add up to the total injected CO₂ volume, with the exception of the CO₂ volume that has left the domain. Hence, they are highly dependent on each other.

More detailed results are shown in Figures 10a to 10d. Total Sobol indices are plotted for each response during the entire time interval. When the flow regime switches from injection to a gravity-dominated system, we observe a jump or sharp drop in some of the sensitivity plots (Figures 10a and 10c at 30 years).

The sensitivity of the aquifer pressure with respect to the presence of barriers jumps up, right after stopping the injection. This happens because barriers slow down the pressure release through open boundaries, resulting in local pressure build-ups.

The sensitivity of the residual CO₂ volume with respect to barriers presence drops soon after injection. This is reasonable since the residual trapped volume is more a function of lateral flow in the medium, compared to the vertical flow in the relatively small thickness of the aquifer.

5. Risk analysis

The risk R of a process is quantitatively defined as the extent of consequence C caused by the process, multiplied by the probability P of that consequence to happen:

$$R = P \times C. \quad (12)$$

The consequence can be defined by direct measures in the simulation responses, or it can be related to consequences caused in the environment outside the considered system. For example, in the case of CO₂ injection into deep aquifers, the amount of CO₂ which stays mobile and undissolved in the medium for a time after injection can be considered as a consequence, bearing the potential of leakage up to the surface if exposed to a geological leakage point. The consequence could also be defined by a criterion for external consequences, like the rate of climate change (either locally or globally) due to CO₂ leakage, the costs of pumping CO₂ that does not remain in the subsurface, or via the related costs for CO₂ emission certificates.

The other part is the probability of these consequences to happen. This depends on the stochastic behavior of the process which results in the respective outcomes.

We use the polynomial-based reduced model for risk analysis, because it is fast enough to perform a Monte-Carlo analysis with a large number (here: 10000)

of realizations on the polynomials. Thanks to the higher-order approximation via the aPC, the principal non-linear physical behavior of CO₂ storage is included in the analysis, and detailed probabilistic risk assessment becomes feasible. We analyze here the same quantities as in Section 4, i.e., average pressure, the volume of mobile or immobile CO₂, and leakage risk. For definitions, see Section 3.1.

5.1. Quantification of expected values in CO₂ storage

Average response values can be calculated analytically from the polynomial (e.g., [26]) or via the Monte-Carlo post-process as mentioned above. Figures 11a to 11d show some of the calculated expectations as functions of time. In Figure 11a, the mobile CO₂ volume increases linearly in the medium because of the constant injection rate during the first thirty years. After injection, the mobile volume of CO₂ is reduced due to the trapped volume in residual form and the migration of CO₂ across open boundaries.

Figure 11b shows the expected values for the volume of residually trapped CO₂ as a function of time. The plot shows the significance of imbibition during the plume migration period, when water replaces CO₂ that is moving upward because of gravity segregation. During injection, CO₂ invades the aquifer and drainage is dominant. Therefore, the expected residual CO₂ plot shows a smaller slope during injection than what it shows later in time.

When injection starts, a pressure pulse travels through the medium at a finite velocity because of the slight compressibility of brine. The initially built-up pressure releases through open boundaries over time and the average pressure drops in the aquifer (Figure 11c). Under realistic injection settings, an average (spatial and statistical) pressure rise of up to 400 bars (from 270 to 670 bars in the first simulation time step, not visible in Figure 11c) would be very unrealistic and would not be allowed to occur. This high pressure rise occurs because large pressure values have to be exceeded in the injection cell before CO₂ becomes mobile at saturations above the residual value.

Also, during early injection time, the pressure is larger than at the end of injection. There are a few realizations where the contributions from the external aquifer support, a dense barrier system close to 100% areal coverage, an adverse aggradation angle of the formation and extremely low fault transmissibilities interact to effectively block the CO₂ flow close to the well. This has strong effects on pressure when the rock at the injector position happens to be poorly permeable, leading to a very poor injectivity. An adapted CO₂ injection strategy would react by lowering the injection rate, by choosing a different injection position, or by even abandoning the entire site.

Based on the results of the current study, it is possible to identify such adverse combinations and guide site investigation strategies to pay attention to such situations. In a follow-up study (ready for submission), we are currently investigating an active injection strategy controlled by an upper allowable pressure limit.

However, the initial sharp pressure increase is released very quickly. This happens, when first parts of the CO₂ plume have found flow pathways into regions with better rock properties, providing the possibility to relax the pressure build-up, and also to let the CO₂ escape towards the boundaries.

The expected leakage risk is plotted in Figure 11d, and increases in value as the injected CO₂ travels upward and accumulates beneath the sealing cap-rock.

5.2. Results of CO₂ storage risk assessment

In this section, the probability distributions (rather than expected values) of system responses during and after injection are studied. Results from the MC analysis of the response surface are given as histograms of output values and also as cumulative distribution functions (CDF) for probabilities (Figures 12 and 13).

Figures 12a to 12c show the histograms of responses obtained from the Monte-Carlo process at the end of injection. A long tail is observed for lower residual and mobile CO₂ values in Figures 12b and 12c. The long tail means a large range of possible low values. Pressure shows a long tail for higher values. This means that even high critical values still have substantial probabilities to be exceeded, indicating that the possibility of geomechanical damage to sealing layers will have to receive a large attention. We observe an issue of mass conservation in Figure 12b, where a few realizations show more mobile CO₂ in the domain than the total injected volume (which is about 40×10^6 m²). This is a typical issue for a large class of statistical methods that interpolate or extrapolate simulation results in the parameter space, because their setup is not based on the mass conservation equation. In this specific case, the mass conservation issue is caused by approximating the response surface via polynomials, with vanishing residuals only at the collocation points. The polynomials are evaluated at many randomly chosen parameter sets drawn from the histograms shown in Figure 7, which do not coincide with the collocation points.

Finally, we report how the corresponding probabilities change over time in Figures 13a to 13c. High pressure buildup is considerable during the early injection time, and it is negligible after injection during plume migration (Figure 13a). An over-pressurized injection can induce fracturing in the medium, extending to the sealing layers. Any fractures caused in the structural traps can expose the mobile CO₂ to leakage paths. Therefore, higher pressure values can be interpreted

as high risk in early time. The injection scenario in this study is set to a fixed injection rate. To avoid risky pressures during the start of injection, the injector can be set on pressure control instead, by changing the injection rate in order to keep the injection pressure limited.

6. Conclusion

In this paper, we used the arbitrary polynomial chaos expansion (aPC) method in a sensitivity analysis and risk assessment process. The goal was to demonstrate the application and feasibility of aPC-based methods in the context of realistic CO₂ injection scenarios. We implemented this method for a typical CO₂ storage problem. Four uncertain parameters with assumed uncertainty distributions are considered. Injection and early migration of CO₂ is studied. The flow sensitivity to geological heterogeneity is evaluated and quantified using Sobol indices. Risk analysis is performed on the defined problem. Flow dynamics are discussed and corresponding interpretations and explanations of the sensitivity and risk results are provided.

The performance of the aPC method has been satisfactory. It is very fast, compared to other stochastic methods for low-parametric systems, and this speed-up allows us to perform an extensive Monte-Carlo process on the aPC-based response surface to calculate the probability of response values throughout simulation time. This study was a first-time application of the aPC to study a realistically complex type of geological structural uncertainty. Based on our assessment of aPC feasibility, we can strongly encourage the use of aPC for sensitivity and risk analysis in complex situations.

The results have shown that the most influential parameter for most of the responses is the aggradation angle of deposition layers of the considered shallow-marine aquifer. The least relevant parameter is the regional groundwater effect, especially during injection time. We re-iterate that the aim of this study was to demonstrate a practice of using arbitrary polynomial chaos expansion for the sensitivity and risk analysis of a typical CO₂ storage problem. Since, in general, the levels of involved input uncertainty are not unique, the physical and geological conclusions of this study are restricted to the probability assumptions taken here and should not be generalized to systems that are very different.

7. Acknowledgements

The authors would like to acknowledge the sponsors of the MatMora project defined in the University of Bergen in partnership with SINTEF-ICT and the Uni-

versity of Stuttgart, and the German Research Foundation (DFG) for financial support of the project within the Cluster of Excellence in Simulation Technology (EXC 310/1) at the University of Stuttgart. We would also like to thank the three anonymous reviewers for their constructive comments.

References

- [1] M. Lenzen, Global warming effect of leakage from CO₂ storage, *Critical Reviews in Environmental Science and Technology* 41 (24) (2011) 2169–2185.
- [2] P. Viebahn, J. Nitsch, M. Fischedick, A. Esken, D. Schüwer, N. Supersberger, U. Zuberbühler, O. Edenhofer, Comparison of carbon capture and storage with renewable energy technologies regarding structural, economic, and ecological aspects in Germany, *International Journal of Greenhouse Gas Control* 1 (1) (2007) 121–133.
- [3] S. Bachu, CO₂ storage in geological media: Role, means, status and barriers to deployment, *Progress in Energy and Combustion Science* 34 (2) (2008) 254–273.
- [4] S. Bachu, Screening and ranking of sedimentary basins for sequestration of CO₂ in geological media in response to climate change, *Environmental Geology* 44 (3) (2003) 277–289.
- [5] J. Birkholzer, Q. Zhou, C. Tsang, Large-scale impact of CO₂ storage in deep saline aquifers: A sensitivity study on pressure response in stratified systems, *International Journal of Greenhouse Gas Control* 3 (2) (2009) 181–194.
- [6] J. Nordbotten, M. Celia, S. Bachu, H. Dahle, Semianalytical solution for CO₂ leakage through an abandoned well, *Environmental Science & Technology* 39 (2) (2005) 602–611.
- [7] D. Thomas, Carbon Dioxide Capture for Storage in Deep Geologic Formations-Results from the CO₂ Capture Project, Vol. 1, Elsevier Science Ltd, 2005.
- [8] M. Celia, S. Bachu, J. Nordbotten, S. Gasda, H. Dahle, Quantitative estimation of CO₂ leakage from geological storage: Analytical models, numerical models and data needs, in: Proceedings of 7th International Conference on Greenhouse Gas Control Technologies.(GHGT-7), 2004.

- [9] F. Riddiford, I. Wright, C. Bishop, T. Espie, A. Tourqui, Monitoring geological storage the in salah gas CO₂ storage project, in: Proceedings of the 7th International Greenhouse Gas Technologies Conference, Vancouver, BC, 2004.
- [10] A. Förster, B. Norden, K. Zinck-Jørgensen, P. Frykman, J. Kulenkampff, E. Spangenberg, J. Erzinger, M. Zimmer, J. Kopp, G. Borm, et al., Baseline characterization of the CO2SINK geological storage site at Ketzin, Germany, *Environmental Geosciences* 13 (3) (2006) 145–161.
- [11] G. Eigestad, H. Dahle, B. Hellevang, F. Riis, W. Johansen, E. Øian, Geological modeling and simulation of CO₂ injection in the Johansen formation, *Computational Geosciences* 13 (4) (2009) 435–450.
- [12] K. Michael, A. Golab, V. Shulakova, J. Ennis-King, G. Allinson, S. Sharma, T. Aiken, Geological storage of CO₂ in saline aquifers—a review of the experience from existing storage operations, *International Journal of Greenhouse Gas Control* 4 (4) (2010) 659–667.
- [13] H. Class, A. Ebigbo, R. Helmig, H. Dahle, J. Nordbotten, M. Celia, P. Audigane, M. Darcis, J. Ennis-King, Y. Fan, et al., A benchmark study on problems related to CO₂ storage in geologic formations, *Computational Geosciences* 13 (4) (2009) 409–434.
- [14] F. Walton, J. Tait, D. LeNeveu, M. Sheppard, Geological storage of CO₂: A statistical approach to assessing performance and risk, in: Proceedings of the 7th International Conference on Greenhouse Gas Control Technologies (GHGT-7), 2004.
- [15] S. Brennan, R. Burruss, M. Merrill, P. Freeman, L. Ruppert, A probabilistic assessment methodology for the evaluation of geologic carbon dioxide storage, *US Geological Survey Open-File Report* 1127 (2010) 31.
- [16] E. Wilson, T. Johnson, D. Keith, Regulating the ultimate sink: Managing the risks of geologic CO₂ storage, *Environmental Science and Technology* 37 (16) (2003) 3476–3483.
- [17] A. Hansson, M. Bryngelsson, Expert opinions on carbon dioxide capture and storage—a framing of uncertainties and possibilities, *Energy Policy* 37 (6) (2009) 2273–2282.

- [18] J. Howell, A. Skorstad, A. MacDonald, A. Fordham, S. Flint, B. Fjellvoll, T. Manzocchi, Sedimentological parameterization of shallow-marine reservoirs, *Petroleum Geoscience* 14 (1) (2008) 17–34.
- [19] T. Manzocchi, J. Carter, A. Skorstad, B. Fjellvoll, K. Stephen, J. Howell, J. Matthews, J. Walsh, M. Nepveu, C. Bos, et al., Sensitivity of the impact of geological uncertainty on production from faulted and unfaulted shallow-marine oil reservoirs: objectives and methods, *Petroleum Geoscience* 14 (1) (2008) 3–11.
- [20] J. Matthews, J. Carter, K. Stephen, R. Zimmerman, A. Skorstad, T. Manzocchi, J. Howell, Assessing the effect of geological uncertainty on recovery estimates in shallow-marine reservoirs: the application of reservoir engineering to the SAIGUP project, *Petroleum Geoscience* 14 (1) (2008) 35–44.
- [21] M. Ashraf, K. Lie, H. Nilsen, J. Nordbotten, A. Skorstad, Impact of geological heterogeneity on early-stage CO₂ plume migration, in: CMWR, 2010.
- [22] M. Ashraf, K.-A. Lie, H. M. Nilsen, A. Skorstad, Impact of geological heterogeneity on early-stage CO₂ plume migration: sensitivity study., in: Proceedings of ECMOR XII, 2010.
- [23] S. Oladyshkin, W. Nowak, Data-driven uncertainty quantification using the arbitrary polynomial chaos expansion, *Reliability Engineering & System Safety* 106 (2012) 179–190.
- [24] I. Sobol, Global sensitivity indices for nonlinear mathematical models and their Monte Carlo estimates, *Mathematics and Computers in Simulation* 55 (1-3) (2001) 271–280.
- [25] E. Commission, European Commission's Communication on Extended Impact Assessment, Brussels, Office for Official Publications of the European Communities, 2002.
- [26] S. Oladyshkin, H. Class, R. Helmig, W. Nowak, A concept for data-driven uncertainty quantification and its application to carbon dioxide storage in geological formations, *Advances in Water Resources* 34 (2011) 1508–1518. doi:10.1016/j.advwatres.2011.08.005.

- [27] J. Witteveen, S. Sarkar, H. Bijl, Modeling physical uncertainties in dynamic stall induced fluid–structure interaction of turbine blades using arbitrary polynomial chaos, *Computers & Structures* 85 (11) (2007) 866–878.
- [28] J. Witteveen, H. Bijl, Modeling arbitrary uncertainties using Gram-Schmidt polynomial chaos, in: Proceedings of the 44th AIAA Aerospace Sciences Meeting and Exhibit, number AIAA-2006-0896, Reno, NV, Vol. 117, 2006.
- [29] R. Ghanem, A. Doostan, On the construction and analysis of stochastic models: characterization and propagation of the errors associated with limited data, *Journal of Computational Physics* 217 (1) (2006) 63–81.
- [30] C. Soize, R. Ghanem, Physical systems with random uncertainties: chaos representations with arbitrary probability measure, *SIAM Journal on Scientific Computing* 26 (2) (2004) 395–410.
- [31] N. Wiener, The homogeneous chaos, *American Journal of Mathematics* 60 (1938) 897–936.
- [32] R. G. Ghanem, P. D. Spanos, *Stochastic Finite Elements: A Spectral Approach*, Springer-Verlag, New York, 1991.
- [33] O. Le Maître, O. Knio, *Spectral methods for uncertainty quantification: with applications to computational fluid dynamics*, Springer, 2010.
- [34] X. Wan, G. Karniadakis, Multi-element generalized polynomial chaos for arbitrary probability measures, *SIAM Journal on Scientific Computing* 28 (3) (2007) 901–928.
- [35] D. Xiu, G. Karniadakis, The Wiener–Askey polynomial chaos for stochastic differential equations, *SIAM Journal on Scientific Computing* 24 (2) (2002) 619–644.
- [36] U. Reuter, M. Liebscher, Global sensitivity analysis in view of nonlinear structural behavior, in: Proceedings of the 7th LS-Dyna Forum, Bamberg, 2008.
- [37] S. Oladyshkin, F. P. J. de Barros, W. Nowak, Global sensitivity analysis: a flexible and efficient framework with an example from stochastic hydrogeology, *Advances in Water Resources* 37 (2012) 10–22.

- [38] A. Kovscek, Y. Wang, Geologic storage of carbon dioxide and enhanced oil recovery. i. uncertainty quantification employing a streamline based proxy for reservoir flow simulation, *Energy Conversion and Management* 46 (11) (2005) 1920–1940.
- [39] D. Zhang, Z. Lu, An efficient, high-order perturbation approach for flow in random media via Karhunen-Loeve and polynomial expansions, *Journal of Computational Physics* 194 (2004) 773–794.
- [40] J. Foo, G. Karniadakis, Multi-element probabilistic collocation method in high dimensions, *Journal of Computational Physics* 229 (5) (2010) 1536–1557.
- [41] N. Fajraoui, F. Ramasomanana, A. Younes, T. A. Mara, P. Ackermann, A. Guadagnini, Use of global sensitivity analysis and polynomial chaos expansion for interpretation of non-reactive transport experiments in laboratory-scale porous media, *Water Resources Research* (doi:10.1029/2010WR009639).
- [42] R. Ghanem, P. D. Spanos, Polynomial chaos in stochastic finite elements, *Journal of Applied Mechanics* 57 (1990) 197–202.
- [43] S. Oladyshkin, H. Class, R. Helmig, W. Nowak, An integrative approach to robust design and probabilistic risk assessment for CO₂ storage in geological formations, *Computational Geosciences* 15 (3) (2011) 565–577. doi:10.1007/s10596-011-9224-8.
- [44] R. Ghanem, P. Spanos, A stochastic Galerkin expansion for nonlinear random vibration analysis, *Probabilistic Engineering Mechanics* 8 (1993) 255–264.
- [45] G. Matthies, H., A. Keese., Galerkin methods for linear and nonlinear elliptic stochastic partial differential equations, *Computer Methods in Applied Mechanics and Engineering* 194 (2005) 1295–1331.
- [46] D. Xiu, G. E. Karniadakis, Modeling uncertainty in flow simulations via generalized polynomial chaos, *Journal of Computational Physics* 187 (2003) 137–167.

- [47] A. Keese, H. G. Matthies, Sparse quadrature as an alternative to MC for stochastic finite element techniques, *Proc. Appl. Math. Mech.* 3 (2003) 493–494.
- [48] S. Isukapalli, S., A. Roy, G. Georgopoulos, P., Stochastic response surface methods (srsms) for uncertainty propagation: Application to environmental and biological systems, *Risk Analysis* 18 (3) (1998) 351–363.
- [49] H. Li, D. Zhang, Probabilistic collocation method for flow in porous media: Comparisons with other stochastic methods, *Water Resources Research* 43 (2007) 44–48.
- [50] I. Babuška, F. Nobile, R. Tempone, A stochastic collocation method for elliptic partial differential equations with random input data, *SIAM Journal on Numerical Analysis* 45 (3) (2007) 1005–1034.
- [51] D. Xiu, J. Hesthaven, High-order collocation methods for differential equations with random inputs, *SIAM Journal on Scientific Computing* 27 (3) (2005) 1118–1139.
- [52] T. Gerstner, M. Griebel, Dimension–adaptive tensor–product quadrature, *Computing* 71 (1) (2003) 65–87.
- [53] V. Barthelmann, E. Novak, K. Ritter, High dimensional polynomial interpolation on sparse grids, *Advances in Computational Mathematics* 12 (4) (2000) 273–288.
- [54] J. Villadsen, M. L. Michelsen, Solution of differential equation models by polynomial approximation, Prentice-Hall, 1978.
- [55] M. Abramowitz, A. Stegun, I., *Handbook of Mathematical Functions with Formulas, Graphs, and Mathematical Tables*, New York: Dover, 1965.
- [56] F. Nobile, R. Tempone, C. Webster, A sparse grid stochastic collocation method for partial differential equations with random input data, *SIAM Journal on Numerical Analysis* 46 (5) (2008) 2309–2345.
- [57] P. Zweigel, L. Heill, Studies on the likelihood for caprock fracturing in the sleipner CO₂ injection case, Tech. rep., Sintef Petroleum Research Report (2003).

- [58] E. Aker, E. Skurtveit, L. Grande, F. Cuisiat, Ø. Johnsen, M. Soldal, B. Bohloli, Experimental methods for characterization of cap rock properties for CO₂ storage, *Multiphysical Testing of Soils and Shales* 303–308.
- [59] J. Rohmer, D. Seyed, Coupled large scale hydromechanical modelling for caprock failure risk assessment of co₂ storage in deep saline aquifers, *Oil & Gas Science and Technology–Revue de l’Institut Français du Pétrole* 65 (3) (2010) 503–517.
- [60] S. Dutton, W. Flanders, M. Barton, Reservoir characterization of a Permian deep-water sandstone, East Ford field, Delaware basin, Texas, *AAPG bulletin* 87 (4) (2003) 609–628.
- [61] T. Eaton, On the importance of geological heterogeneity for flow simulation, *Sedimentary Geology* 184 (3-4) (2006) 187–201.
- [62] T. Manzocchi, J. Matthews, J. Strand, J. Carter, A. Skorstad, J. Howell, K. Stephen, J. Walsh, A study of the structural controls on oil recovery from shallow-marine reservoirs, *Petroleum Geoscience* 14 (1) (2008) 55–70.
- [63] T. Manzocchi, J. Walsh, P. Nell, G. Yielding, Fault transmissibility multipliers for flow simulation models, *Petroleum Geoscience* 5 (1) (1999) 53–63.
- [64] W. Nowak, Best unbiased ensemble linearization and the quasi-linear Kalman ensemble generator, *Water Resources Research* 45 (W04431). doi:10.1029/2008WR007328.
- [65] S. Jang, Y., N. Sitar, D. Kiureghian, A., Reliability analysis of contaminant transport in saturated porous media., *Water Resources Research* 30 (8) (1994) 2435–2448.
- [66] A. Saltelli, *Global sensitivity analysis: the primer*, Wiley, 2007.
- [67] A. Saltelli, Global sensitivity analysis: an introduction, in: Proc. 4th International Conference on Sensitivity Analysis of Model Output, pp. 27–43.
- [68] T. Crestaux, O. Le MaíLtre, J. Martinez, Polynomial chaos expansion for sensitivity analysis, *Reliability Engineering & System Safety* 94 (7) (2009) 1161–1172.
- [69] B. Sudret, Global sensitivity analysis using polynomial chaos expansions, *Reliability Engineering & System Safety* 93 (7) (2008) 964–979.

Table 1: Aquifer model information.

Parameter	Value	Unit
Number of active cells in the model	78720	-
Resolution X,Y,Z	$40 \times 120 \times 20$	-
Scale X,Y,Z	$3000 \times 9000 \times 80$	m
Injection rate	3650	m^3/day
Initial pressure	266.5	bar
Critical CO ₂ and water saturations	0.2	-
CO ₂ viscosity	0.04	cp
Water viscosity	0.4	cp
Rock compressibility	0.3e-6	1/bar

Table 2: Important model responses and their brief description. For more information, see [21, 22].

Response	Description
Aquifer pressure	Volume average of pressure, weighted by porosity
Mobile CO ₂	Volume of CO ₂ in places with saturation above critical value
Residual CO ₂	Volume of CO ₂ in places with saturation below critical value
Leakage risk	A risk value for the leakage through the cap-rock.

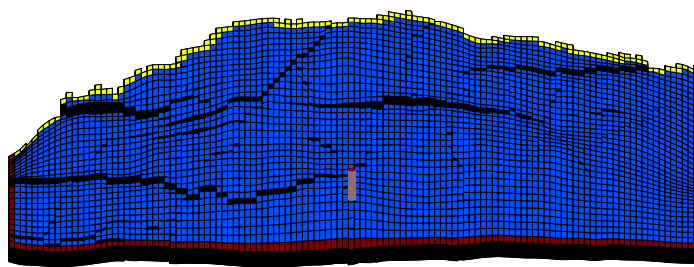


Figure 1: Boundary conditions and the well location in the designed injection scenario. Red color corresponds to the open boundaries and yellow color shows the closed side on the crest.

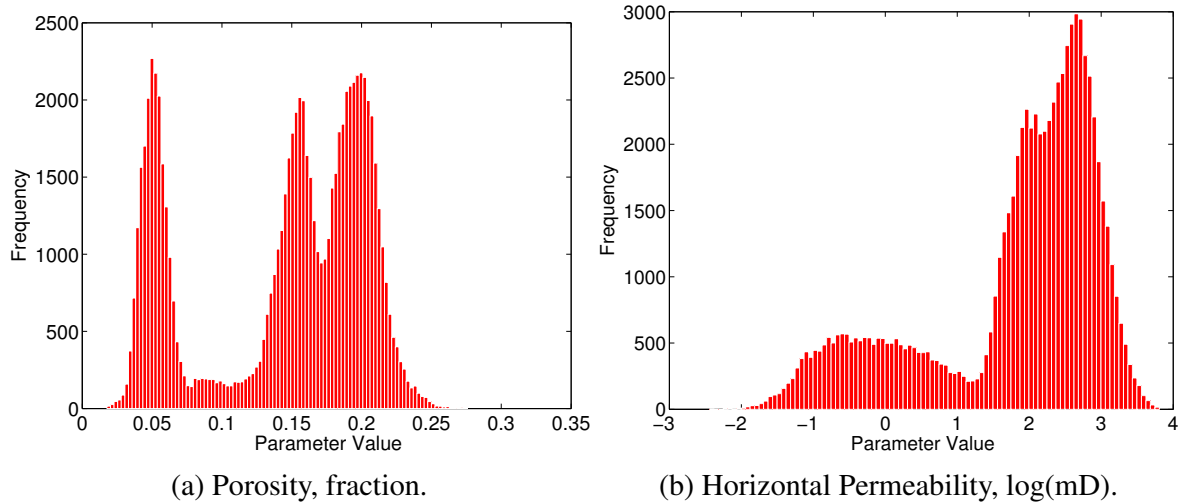


Figure 2: The histograms of hydrological parameters shown for a realization with low levels of heterogeneity. The vertical permeabilities are approximately one order of magnitude lower than the horizontal permeabilities.

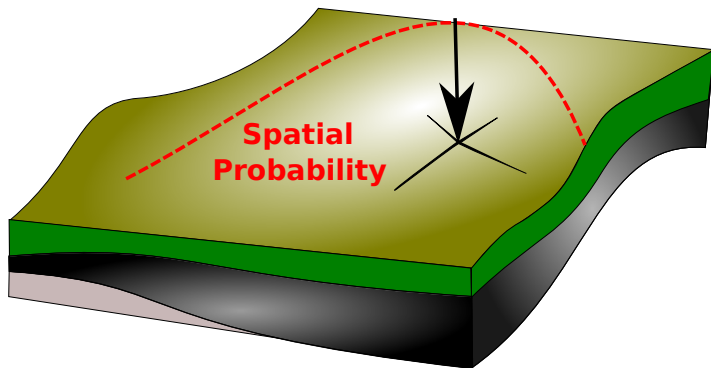


Figure 3: CO₂ leakage risk is computed as the product of a cap-rock failure probability and the amount of mobile CO₂ beneath the cap-rock, integrated over the entire surface area of the cap-rock. Here, we use a Gaussian function as simple scenario assumption for the cap-rock failure probability (indicated schematically by the color shading and the dashed red line with the black coordinate system).

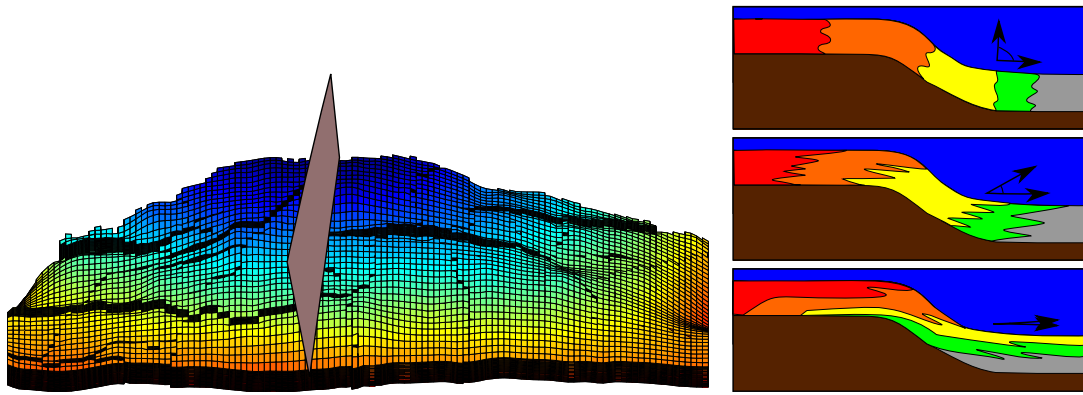


Figure 4: The river flows from left to right toward the sea on the model vertical section shown here (left figure). Aggradation angle is demonstrated in three levels (right figure); from top: low, medium and high aggradation angle. Between deposition and now, the entire system was rotated by tectonic effects such that the original river flow direction is oriented upward, not downward.

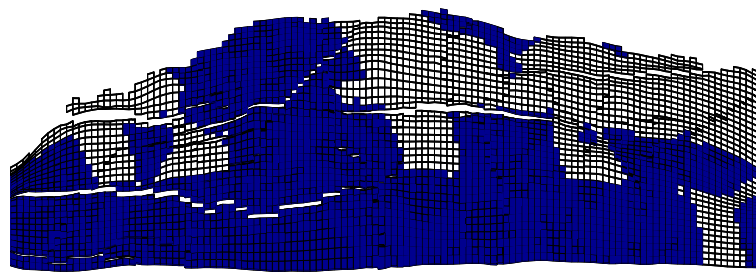


Figure 5: The figure shows 50% of zero transmissibility multipliers in a specific model layer representing a medium level of barriers. One layer of the model is shown in the figure.

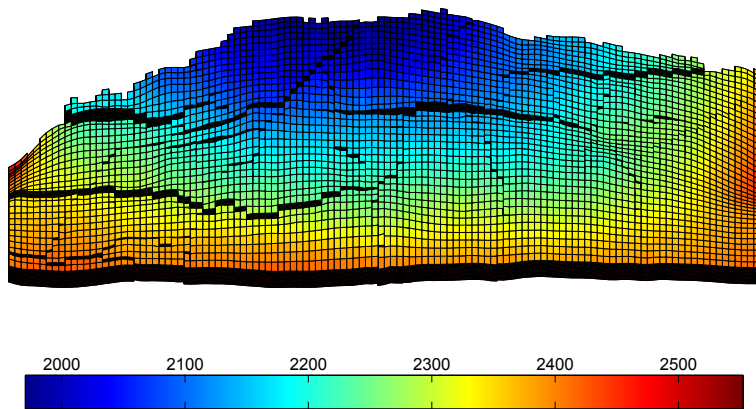


Figure 6: Fault orientation and intensity of the model used in the study. Depth in meter is shown by color on the grid.

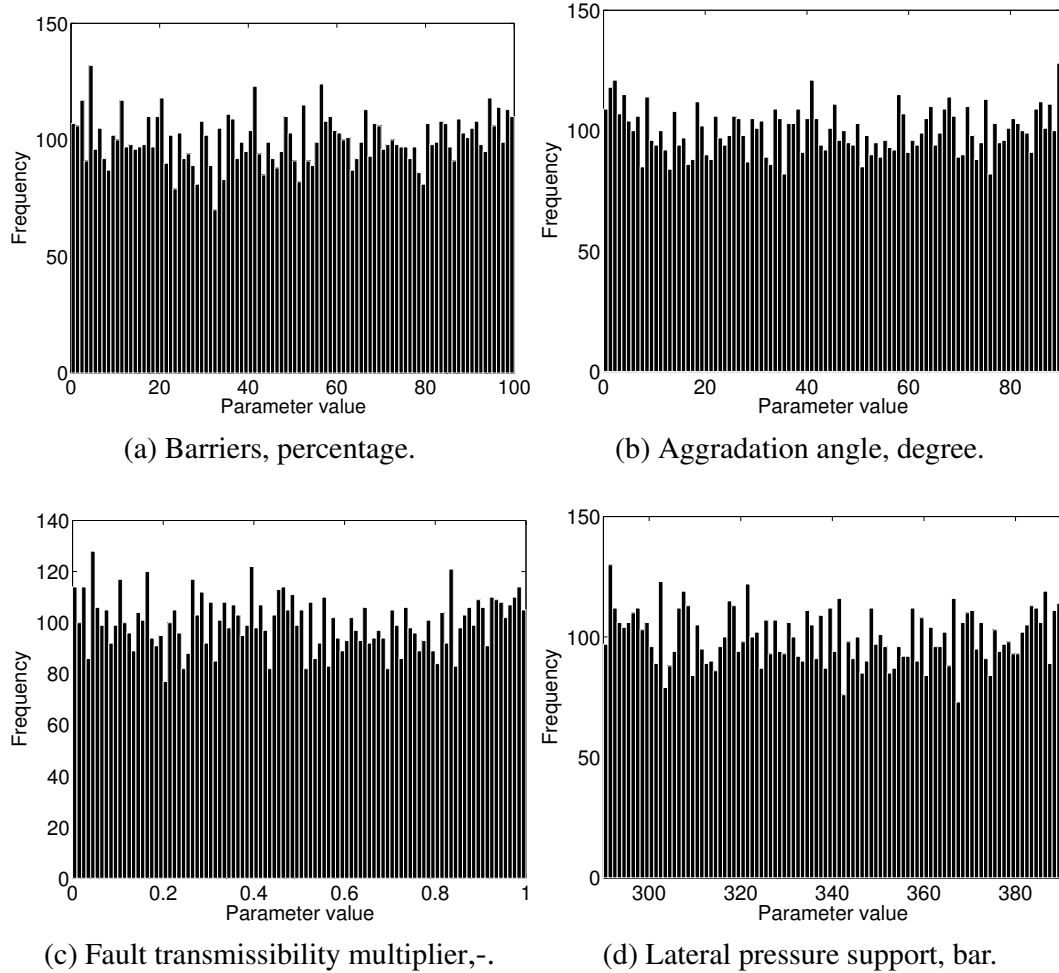


Figure 7: The histograms of geological variables used in this study are sampled from uniform distributions.

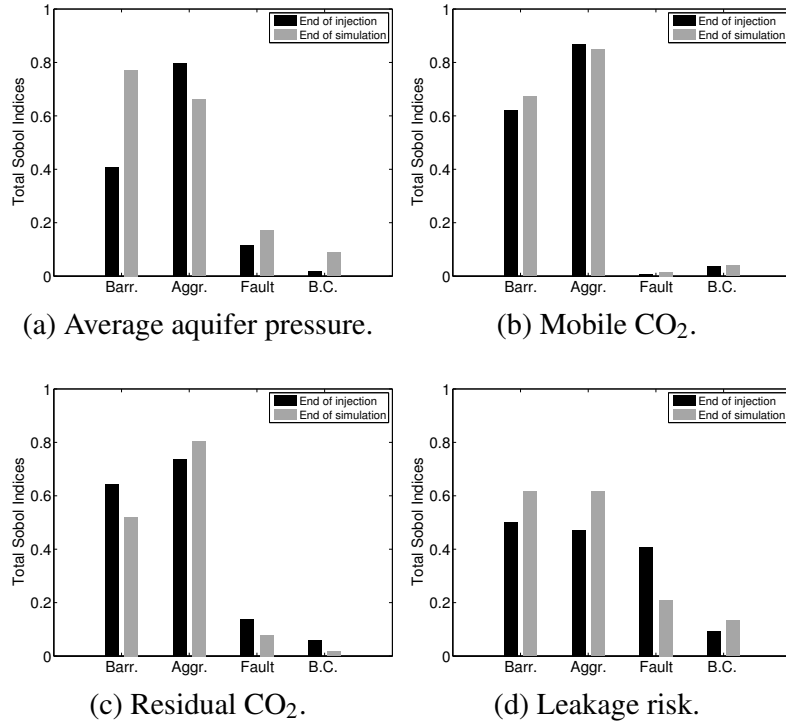


Figure 8: Sensitivity analysis for different responses (a: average aquifer pressure, b: mobile CO₂, c: residual CO₂, and d: leakage risk) with respect to the uncertain parameters. In the figures above, Barr. is for barriers, Aggr. for aggradation angle, Fault for fault transmissibility, and B.C. for regional groundwater effect.

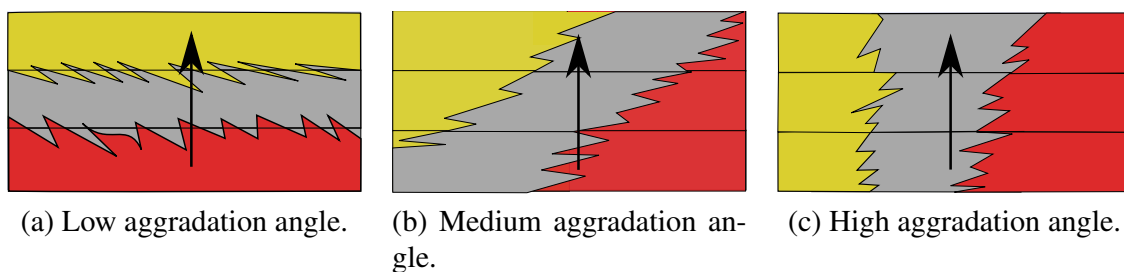


Figure 9: Illustration of how the aggradation angle affects the effective vertical conductivity.

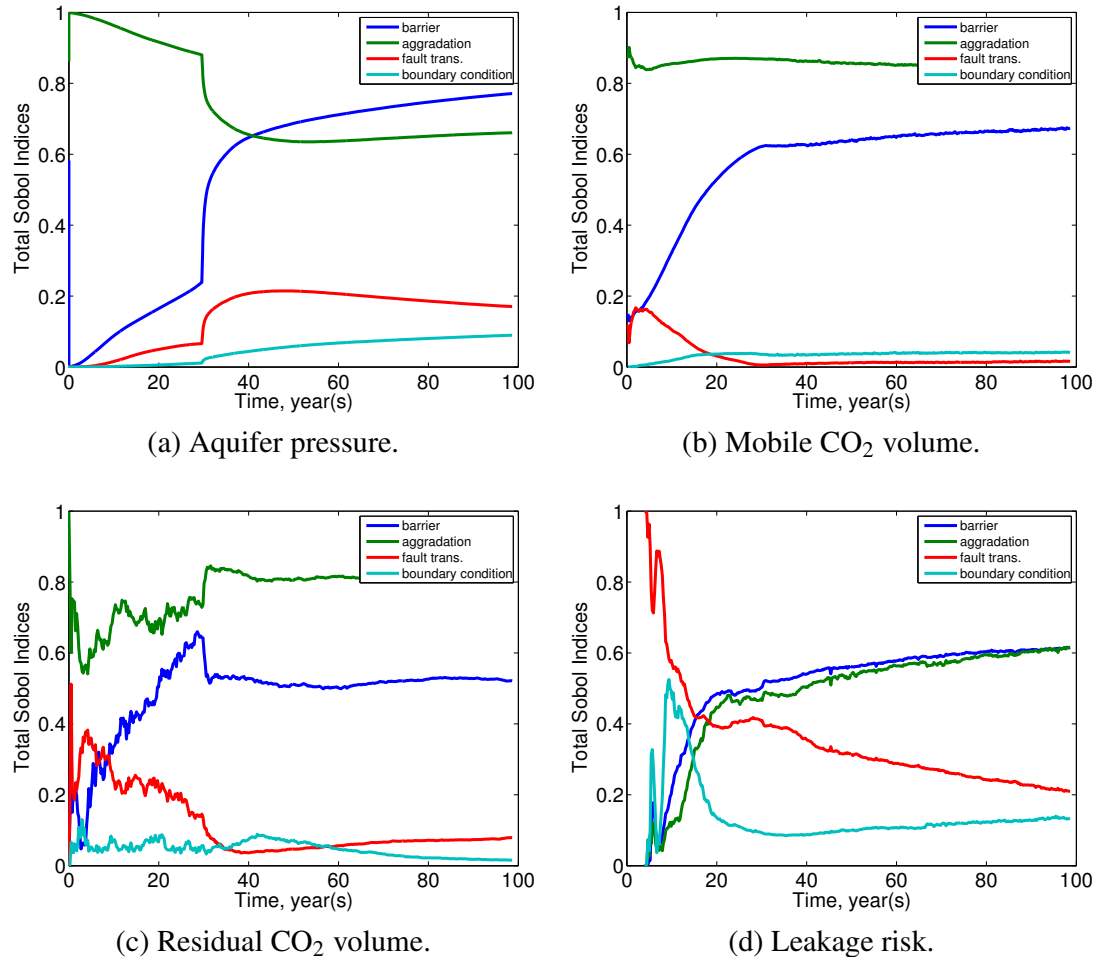


Figure 10: Sensitivities (expressed by total Sobol indices) plotted versus time for different responses.

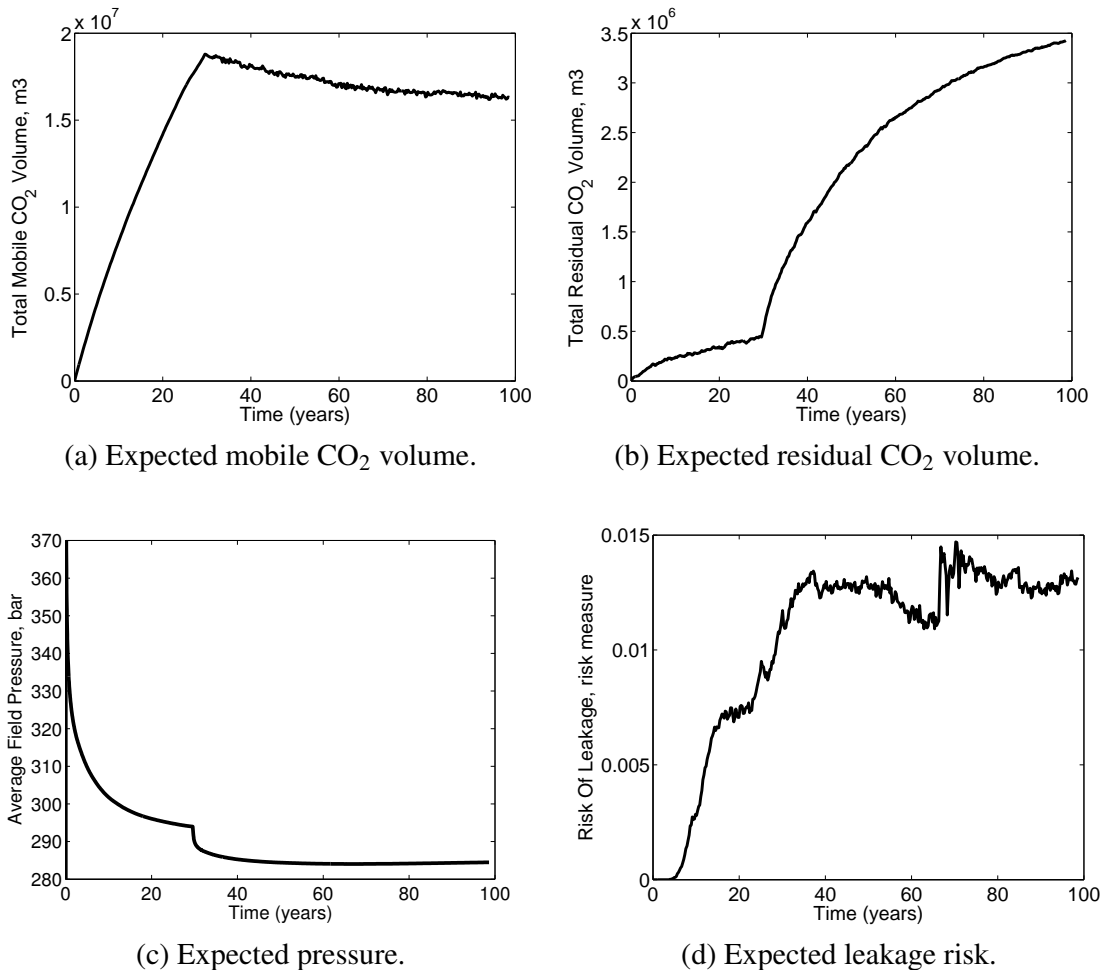


Figure 11: Expectation for response values versus time. The pressure value for initial time step in Figure c goes up to 670 bars.

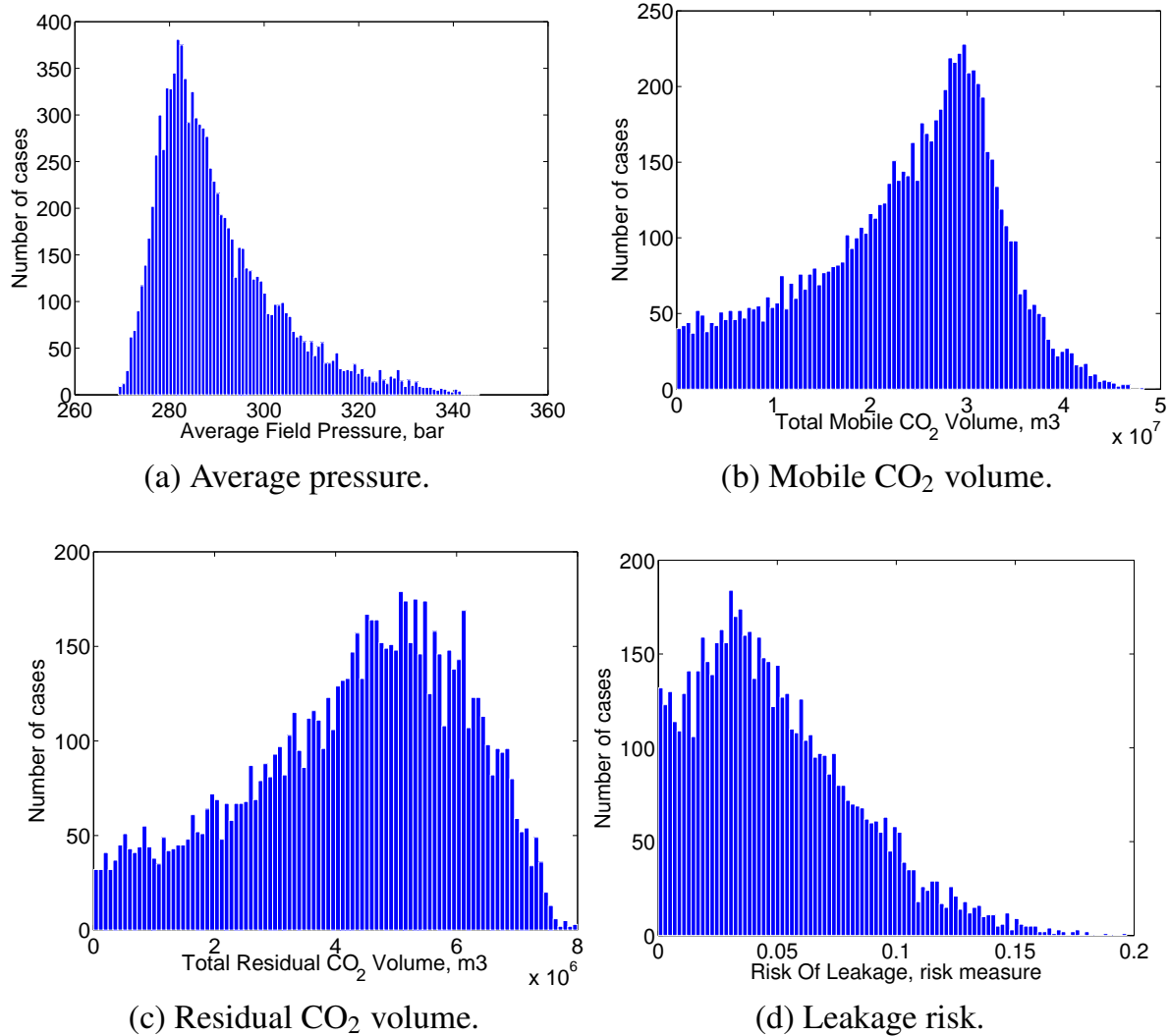


Figure 12: Histograms of selected response values.

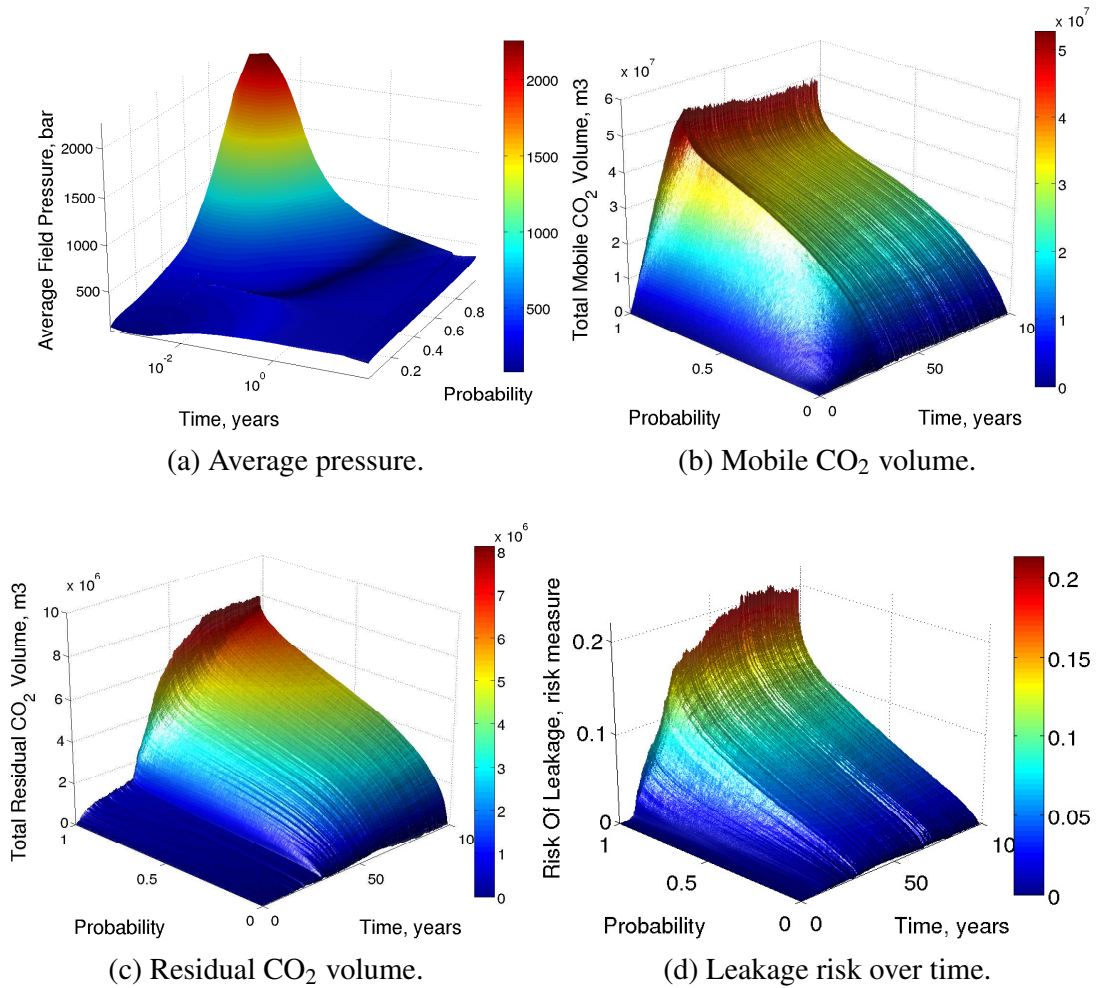


Figure 13: Evolution of the cumulative distribution function of different response values over time.

Appendix A

**Additional manuscripts not evaluated as part of
thesis**

Paper A

A.1 Impact of geological heterogeneity on early-stage CO₂ plume migration

Ashraf, M., Lie, K.A., Nilsen, H.M., Nordbotten, J. M., and Skorstad, A.

presented and published in the proceedings of the Computational Methods in Water Resources (CMWR) conference in Barcelona, 2010.

IMPACT OF GEOLOGICAL HETEROGENEITY ON EARLY-STAGE CO₂ PLUME MIGRATION

Meisam Ashraf^{*,§,1}, Knut-Andreas Lie^{*,§,2}, Halvor M. Nilsen^{§,3}, Jan M. Nordbotten^{*,4}, Arne Skorstad^{†,5}

*Department of Mathematics, University of Bergen, NO-5008 Bergen, Norway

§SINTEF ICT, Department of Applied Mathematics, NO-0314 Oslo, Norway

†Norwegian Computing Center, NO-0314 Oslo, Norway

¹Meisam.Ashraf@uni.no, ²Knut-Andreas.Lie@sintef.no, ³HalvorMoll.Nilsen@sintef.no
⁴Jan.Nordbotten@math.uib.no, ⁵Arne.Skorstad@nr.no

Key words: CO₂ storage, heterogeneity, sensitivity, shallow marine

Summary. In an effort to determine the influence of geological heterogeneity on CO₂ storage efficiency, we study injection and early-stage migration of CO₂ in 54 different realizations of a shallow-marine reservoir.

1 INTRODUCTION

Academic studies of CO₂ injection frequently employ simplified or conceptualized reservoir descriptions in which the medium is considered nearly homogeneous. However, geological knowledge and experience from petroleum production show that the petrophysical characteristics of potential CO₂ sequestration sites can be expected to be heterogeneous on the relevant physical scales, regardless of whether the target formation is an abandoned petroleum reservoir or a pristine aquifer. Geological uncertainty introduces tortuous subsurface flow paths, which in turn influence reservoir behavior during injection. It is paramount that the effect of the geological heterogeneity is quantified by the research community. This will facilitate both improved understanding of subsurface flow at operational CO₂ injection sites, and allow comparison with simulated flow in ideal homogeneous models and upscaled versions of these.

Within oil recovery, the impact of geological uncertainty on production forecast has been thoroughly investigated in the SAIGUP project [2, 3, 4] focusing on shallow-marine reservoirs. To study different factors, synthetic realistic models were made and several thousand cases were run for different production scenarios. The results showed that realistic heterogeneity in the structural and sedimentological description had a strong influence on the production responses.

Meisam Ashraf, Knut-Andreas Lie, Halvor M. Nilsen, Jan M. Nordbotten and Arne Skorstad

The main objectives of CO₂ storage studies are to maximize the injection volume/rate and to minimize the risk of leakage [1]. The problem of CO₂ storage differs from oil recovery prediction not only in the objectives of study, but also in the time scales considered for the process (thousands of years compared to tens of years for CO₂ migration). In addition, the characteristic length scale of the flow is much larger. Working with long temporal and spatial scales and huge amounts of uncertainties poses the question of how detailed the geological description should be. The motivation of this work is mainly to answer two questions related to CO₂ storage:

- How sensitive is the injection and early-stage migration to uncertainty and variability in the geological description?
- What simplifying assumptions are allowed in averaging the geological attributes over scales?

To this end, we use a subset of the synthetic models from the SAIGUP study to perform a preliminary sensitivity analysis for CO₂ sequestration in aquifers. Heterogeneity classes are defined based on different sequence-stratigraphy parameters and levels of shale barriers. We assume two-phase flow with slight compressibility for supercritical CO₂. The injection scenarios are defined based on the objectives outlined above, and important responses are discussed to evaluate the efficiency and risk of the process.

2 Geological descriptions

In this work we question the widespread use of simplified geological descriptions that ignore the detailed heterogeneity in modeling. Our hypothesis is that heterogeneity features like channels, barriers, sequence stratigraphy of facies, and fault intensity/geometry all have a particular effect on flow behavior, both locally and globally, and may significantly alter the injection and migration of CO₂ plumes.

Sound geological classifications and descriptions of key geological features are important to give a realistic description of the sensitivity of CO₂ storage performance. To this end, we have selected four parameter spaces of geological variations from the SAIGUP study [2, 3, 4]. The parameters span realistic intervals for progradational shallow-marine depositional systems with limited tidal influence. In the following, we give a brief description of each.

Lobosity: Lobosity is defined by the plan-view shape of the shore-line. As a varying parameter, lobosity indicates the level at which the shallow-marine system is dominated by each of the main depositional processes. Two depositional processes are considered in the SAIGUP study: fluvial and wave processes. The higher amount of sediment supply from rivers relative to the available accommodation space in the shallow sea, the more fluvial dominant the process will be. As the river enters the mouth of the sea, it can divide into different lobes and branches. Wave processes from the sea-side smear this effect and flatten the shoreline shape. Less wave effect produces more pronounced lobe shapes around the river mouths. Very high permeability and porosity can be found in

Meisam Ashraf, Knut-Andreas Lie, Halvor M. Nilsen, Jan M. Nordbotten and Arne Skorstad

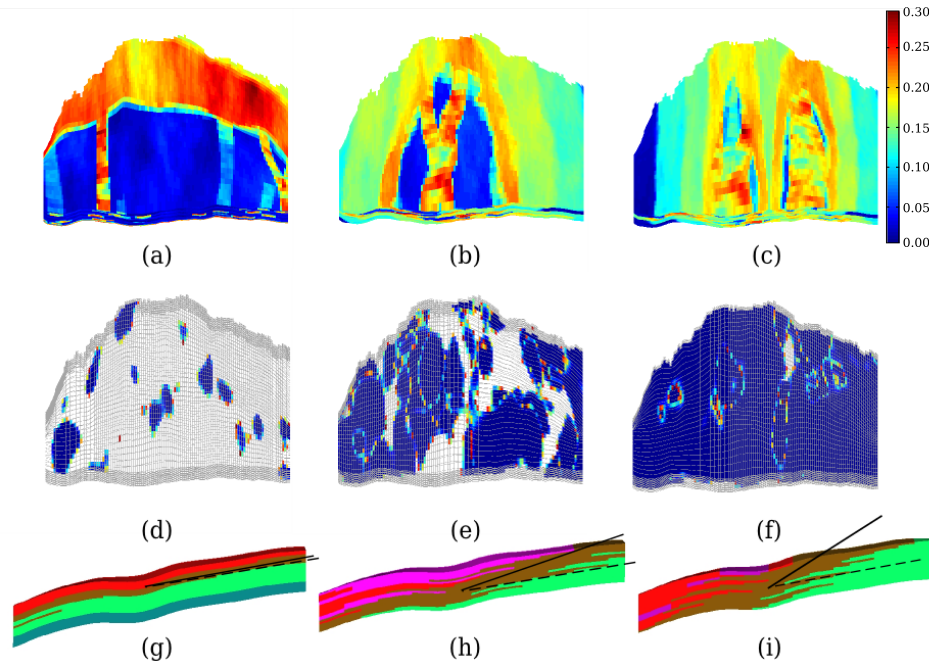


Figure 1: Different geological features considered in this study. Top row shows ‘lobosity’ in porosity distribution: (a) flat shore-line, (b) one lobe, (c) two lobes. The middle row shows ‘barrier’ by the distribution of zero transmissibility multipliers: (d) low, (e) medium, (f) high. The lower row shows ‘aggradation’ in rock-type distribution: (g) low angle of interface between the transitional rock-types leads to parallel layers; this angle is increasing in cases (h) and (i), which correspond to higher levels of aggradation. An up-dip progradation direction is shown in (b), and if the lobe flips over the long axis, we will have down-dip progradation.

the channeling branches, while dense rock with low permeability fills the space between them. Reservoir quality decreases with distance from the shoreface. We expect that the level of lobosity can have a considerable effect on the CO₂ injection and plume size in the aquifer. In this study, models of three levels of lobosity are used: flat shoreline, one lobe and two lobes, see Fig. 1.

Barriers: Periodic floods result in a sheet of sandstone that dips, thins, and fines in a seaward direction. In the lower front, thin sheets of sandstone are interbedded with the mudstones deposited from suspension. These mud-draped surfaces are potential significant barriers to both horizontal and vertical flow. In the SAIGUP domain used here, these barriers were modeled by transmissibility multipliers in three levels of zero value percentage: low (10%), medium (50%), and high (90%). We use the same variations in this study, see Fig. 1.

Aggradation: In shallow-marine systems, two main factors control the shape of the transition zone between the river and the basin: amount of deposition supplied by the river and the accommodation space that the sea provides for these depositional masses. One can imagine a constant situation in which the river is entering the sea and the flow

Meisam Ashraf, Knut-Andreas Lie, Halvor M. Nilsen, Jan M. Nordbotten and Arne Skorstad

slows down until stagnation. The deposition happens in a spectrum from larger grains depositing earlier in the land side to fine deposits in the deep basin. If the river flux or sea level fluctuates, the equilibrium changes into a new bedding shape based on the balance of these factors.

In the SAIGUP study, the progradational cases are considered in which, for example, the river flux increases and shifts the whole depositional system into the sea. The angle at which the transitional deposits are stacked on each-other because of this shifting, is called aggradation angle. Three levels of aggradation are modeled here: low, medium and high (Fig. 1). As we will observe later, aggradation can have a dramatic influence on the injection and migration process.

Progradation: The final factor varied is the progradation or the depositional-dip direction. Two types are considered here: up and down the dominant structural dip. Since the model is tilted a little, this corresponds to the lobe direction from flank to the crest or vice-versa (Fig. 1). This has a potential influence on the CO₂ flow from the injection point up to the crest.

3 Simulation workflow

A fully automated workflow was designed for this study, starting from variational parameters in the SAIGUP models and ending into comprehensive result outputs based on the objective of the work. As a first step, 54 representative cases are studied using a commercial simulator (Eclipse). However, the parallel aim of future work is to develop fast simulation methods that are suitable for performing thousands of runs, using e.g., a vertically-averaged formulation [5].

4 Scenario design

After studying several scenarios for a typical CO₂ injection, we ended up using an injector down in the flank and hydrostatic boundary conditions on the sides, except the faulted side on the crest (Fig. 2). No-flow boundary conditions are imposed on the top and bottom surfaces of the model. The well is completed only in the last three layers.

Simple linear saturation functions with zero capillarity are used. This can be justified because the permeability contrast in channels has the dominating effect on the flow. Also, simple PVT data for a slightly compressible supercritical CO₂ is used. To model the hydrostatic boundaries in Eclipse, high multipliers are used to magnify the pore volume of the outer cells in the model. About 40MM m³ of supercritical CO₂ is injected for thirty years, which amounts to 20% of the models' pore volumes. After the injection period, seventy years of early plume migration is simulated.

5 Results

As our objective function, we seek to maximize the CO₂ storage volume and minimize the risk of leakage. These quantities are measured indirectly by various simulation outputs

Meisam Ashraf, Knut-Andreas Lie, Halvor M. Nilsen, Jan M. Nordbotten and Arne Skorstad

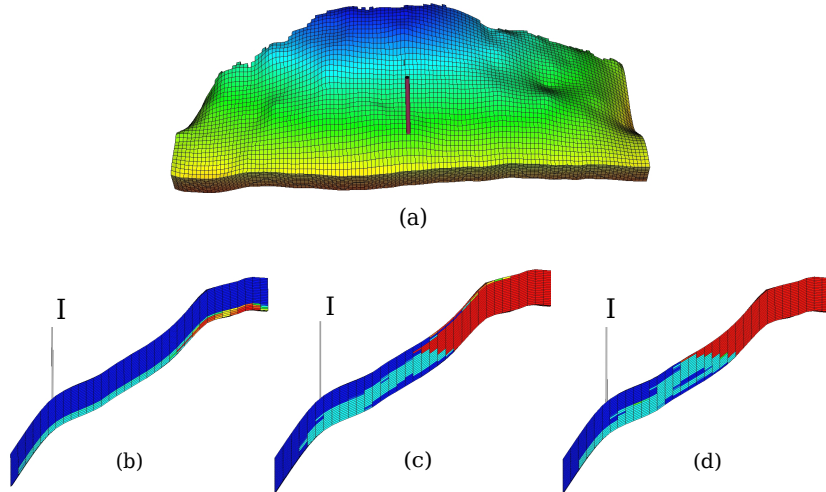


Figure 2: (a) Model geometry and well position. Model dimensions are 3km×9km×80m with 20 layers. The bottom row shows the side view of CO₂ distribution (in red) at the end of simulation in different aggradation cases, from low (b) to high (d). The vertical direction is exaggerated.

that are discussed below.

In all outputs, we recognize the effect of aggradation. Cases with low aggradation have continuous facies layering parallel to the horizontal direction of the grid. Because the three lowest layers, in which the well is completed, are sealing in the cross-layering direction, the flow is forced to stay in the same layers rather than accumulating in the crest (Fig. 2).

Reservoir pressure: The pressure response in general shows a sharp jump at the start of injection and a declining trend during the injection and plume migration. Pressure behavior of different cases at the end of the injection period is shown in Fig. 3. Low aggradation cases show higher pressure.

Boundary fluxes: The flux out of the open boundaries is a measure of the sweep efficiency of the CO₂ plume. As channeling can lead to early CO₂ breakthrough at boundaries, we prefer cases with less fluxes out of the boundaries. The down boundary that is closer to the injector is a potential loss for the injected volume (Fig. 4). Again, the flow is led readily to the boundaries in cases with low aggradations .

Total mobile/residual CO₂: If the CO₂ saturation is below the critical value, it will be immobile in the bulk flow, although not in the molecular sense. Less mobile CO₂ means less risk of leakage and more residual volumes (with saturations less than the critical) resulting from a more efficient volume sweep as preferable (Fig. 4). We use critical saturation of 0.2 for both water and CO₂.

Connected CO₂ volumes: To estimate the risk of leakage from the caprock, we

Meisam Ashraf, Knut-Andreas Lie, Halvor M. Nilsen, Jan M. Nordbotten and Arne Skorstad

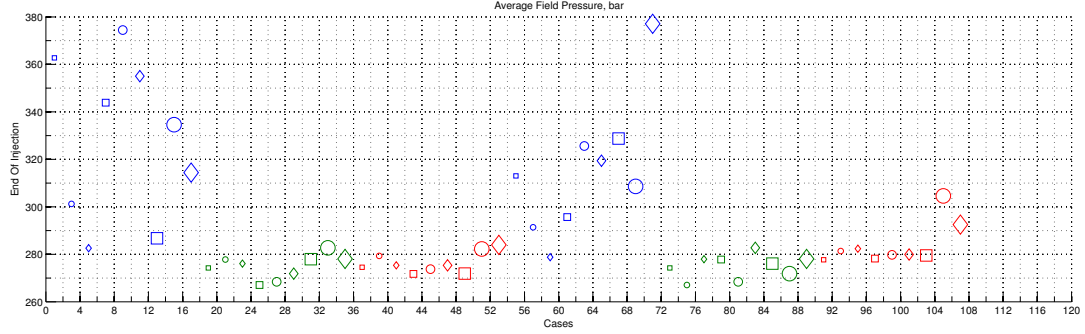


Figure 3: Average reservoir pressure plot for all cases. Colors represent 'aggradation' level: blue for low, green for medium, and red for high levels. Size represents 'barrier': small for low, medium for medium, and large for high level of barrier. Marker shape represents 'lobosity': square for flat shore-line, circle for one lobe, and diamond for two lobes. The first half of the case numbers refer to 'progradation' up-dip towards the crest, and the second half represent 'progradation' down-dip.

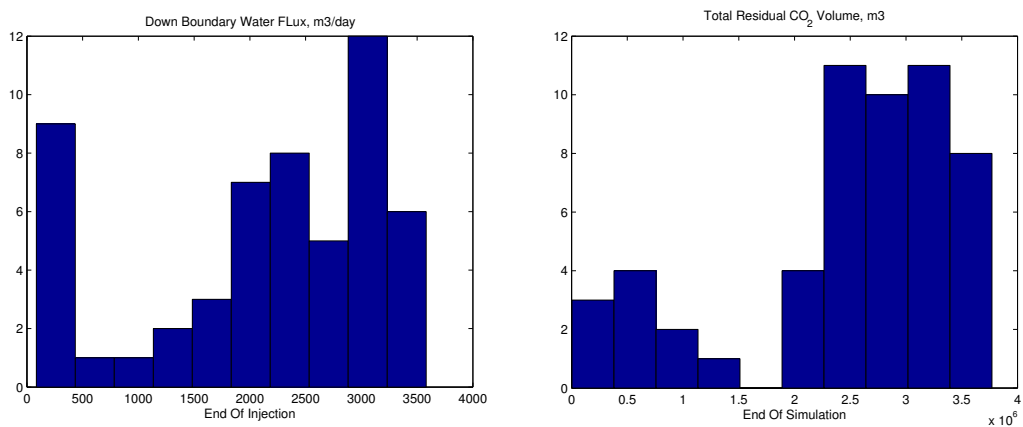


Figure 4: (a) Flux histogram for down boundary: cases with low aggradation show high values. (b) Total residual CO₂ volume; cases with low aggradation show less values in a separate family.

Meisam Ashraf, Knut-Andreas Lie, Halvor M. Nilsen, Jan M. Nordbotten and Arne Skorstad

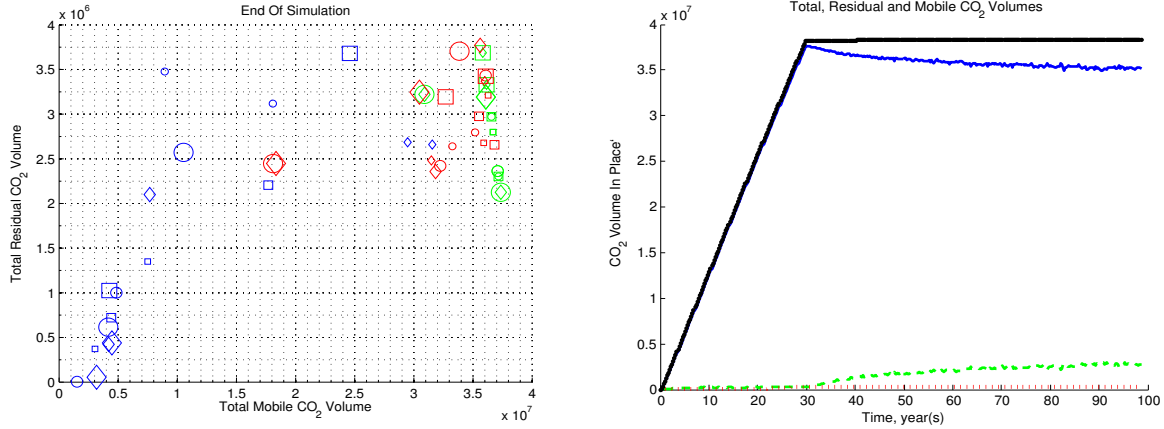


Figure 5: CO₂ volumes. Left: residual versus mobile volume at the end of simulation. Most of the green colored cases follow a linear trend, which is expected because the injected CO₂ must be conserved if no CO₂ leaves the system. For the rest of the cases, some CO₂ goes out of boundaries. Right: Total CO₂ volumes with time plotted for one case. Green curve is the residual volumes, dotted red denotes volumes that have left the domain, solid blue is mobile volumes, and the solid black shows the summation, which is the total volume and stays constant after injection because no more CO₂ is added to the system.

assume that all mobile CO₂ connected to a leakage point will escape out of the reservoir. Hence, it is preferable if the total mobile CO₂ volume is split into smaller plumes rather than forming a big mobile plume. Though the area exposed to potential leakage points will increase by splitting the plume, yet the volume reduction is overtaking the area effect.

On the other hand, the split CO₂ plumes can sweep more cross-areas than a big single plume. The no-flow faulted side can be considered to be connected to an imaginary large volume available for long-term plume migration. Thus, it makes sense to talk about plume sweeping cross area. Larger areas leave more residual CO₂ in the tail of the plume. Hence, we looked at the largest plume size, the number of plumes, and other statistical parameters. The number of plumes at the end of simulation for all cases are given in Fig. 6. Two-lobed cases include more branching channels which result in more plume numbers. Also barrier effect increases the lateral distribution of the plume.

6 Conclusions

Herein, we have reported on a preliminary study of the influence of various geological parameters on the injection and early-stage migration of CO₂ in progradational shallow-marine systems. Large variations in the flow responses show the importance of considering uncertainty in the geological parameters. In particular, our results highlight how variation in aggradation and barriers significantly change the flow direction within the medium. Therefor we believe that effort should be put into detailed geological modeling of potential injection sites. This way, one can better balance the influence of simplifications made in the models of geology and flow physics.

Meisam Ashraf, Knut-Andreas Lie, Halvor M. Nilsen, Jan M. Nordbotten and Arne Skorstad

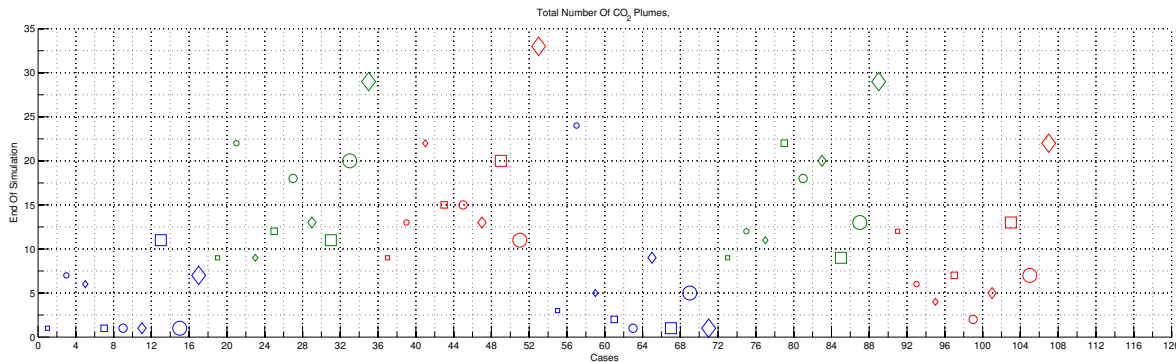


Figure 6: CO₂ plume number at end of simulation, see explanation in Fig. 3.

Finally, we stress that these are very preliminary conclusions drawn from a limited number of simulations performed on a suite of synthetic models that were made to study petroleum production. A more thorough investigation should generate new synthetic geological realizations that are more representative of typical injection sites.

REFERENCES

- [1] J. M. Nordbotten: *Sequestration of Carbon in Saline Aquifers: Mathematical and Numerical Analysis*, Doctor Scientiarum Thesis, Department of Mathematics, University of Bergen, (2004).
- [2] J. A. Howel, A. Skorstad, A. MacDonald, A. Fordham, S. Flint, B. Fjellvoll, and T. Manzocchi: *Sedimentological parameterization of shallow-marine reservoirs*, Petroleum Geoscience, Vol. 14, No. 1, pp. 17-34, (2008).
- [3] T. Manzocchi, J. N. Carter, A. Skorstad, B. Fjellvoll, K. D. Stephen, J. A. Howell, J. D. Matthews, J. J. Walsh, M. Nepveu, C. Bos, J. Cole, P. Egberts, S. Flint, C. Hern, L. Holden, H. Hovland, H. Jackson, O. Kolbjørnsen, A. MacDonald, P. A. R. Nell, K. Onyeagoro, J. Strand, A. R. Syversveen, A. Tchistiakov, C. Yang, G. Yielding, and R. W. Zimmerman: *Sensitivity of the impact of geological uncertainty on production from faulted and unfaulted shallow-marine oil reservoirs: objectives and methods*, Petroleum Geoscience, Vol. 14, No. 1, pp. 3-15, (2008).
- [4] J. D. Matthews, J. N. Carter, K. D. Stephen, R. W. Zimmerman, A. Skorstad, T. Manzocchi, and J. A. Howell: *Assessing the effect of geological uncertainty on recovery estimates in shallow-marine reservoirs: the application of reservoir engineering to the SAIGUP project*, Petroleum Geoscience, Vol. 14, No. 1, pp. 33-44, (2008).
- [5] S. E. Gasda, J. M. Nordbotten, and M. A. Celia: *Vertical equilibrium with sub-scale analytical methods for geological CO₂ sequestration*, Computational Geosciences, Volume 13, Number 4, pp. 469-481, (2009).

Paper B

A.2 Impact of geological heterogeneity on early-stage CO₂ plume migration: sensitivity study

Ashraf, M., Lie, K.A., Nilsen, H.M., and Skorstad, A.

Presented and published in the proceedings of the ECMOR XII in Oxford, 2010.

IMPACT OF GEOLOGICAL HETEROGENEITY ON EARLY-STAGE CO₂ PLUME MIGRATION: SENSITIVITY STUDY

M. Ashraf^a, K.A. Lie^a, H.M. Nilsen^a & A. Skorstad^{bc}

^a SINTEF ICT, Department of Applied Mathematics, NO-0314 Oslo, Norway

^b Norwegian Computing Center, NO-0314 Oslo, Norway.

^c Present address Roxar Software Solutions, Lysaker Torg 45, NO-1366 Lysaker, Norway

July 30, 2010

Introduction

Academic studies of CO₂ injection frequently employ simplified or conceptualized reservoir descriptions in which the medium is considered nearly homogeneous. However, geological knowledge and experience from petroleum production show that the petrophysical characteristics of potential CO₂ sequestration sites can be expected to be heterogeneous on the relevant physical scales, regardless of whether the target formation is an abandoned petroleum reservoir or a pristine aquifer. Geological uncertainty introduces tortuous subsurface flow paths, which in turn influence reservoir behaviour during injection. It is paramount that the effect of the geological heterogeneity is quantified by the research community. This will facilitate both improved understanding of subsurface flow at operational CO₂ injection sites, and allow comparison with simulated flow in ideal homogeneous models and upscaled versions of these.

Within oil recovery, the impact of geological uncertainty on production forecast has been thoroughly investigated in the SAIGUP project [3, 4, 5] focusing on shallow-marine reservoirs. To study different factors, synthetic realistic models were made and several thousand cases were run for different production scenarios. The results showed that realistic heterogeneity in the structural and sedimentological description had a strong influence on the production responses.

The main objectives of CO₂ storage studies are to maximize the injection volume/rate and to minimize the risk of leakage [1, 2]. The problem of CO₂ storage differs from oil recovery prediction not only in the objectives of study, but also in the time scales considered for the process (thousands of years compared to tens of years for CO₂ migration). In addition, the characteristic length scale of the flow is much larger. Working with long temporal and spatial scales and huge amounts of uncertainties poses the question of how detailed the geological description should be. The motivation of this work is mainly to address two questions related to CO₂ storage:

- How sensitive is the injection and early-stage migration to uncertainty and variability in the geological description?
- What simplifying assumptions are allowed in averaging the geological attributes over scales?

To this end, we use a subset of the synthetic models from the SAIGUP study to perform a preliminary sensitivity analysis for CO₂ sequestration in aquifers. Heterogeneity classes are defined based on different sequence-stratigraphy parameters and levels of shale barriers. We assume two-phase flow with slight compressibility for supercritical CO₂. The injection scenarios are defined based on the objectives outlined above, and important responses are discussed to evaluate the efficiency and risk of the process.

Geological descriptions

In this work we question the widespread use of simplified geological descriptions that ignore the detailed heterogeneity in modelling. Our hypothesis is that heterogeneity features like channels, barriers, sequence stratigraphy of facies, and fault intensity/geometry all have a particular effect on flow behaviour, both locally and globally, and may significantly alter the injection and migration of CO₂ plumes.

Sound geological classifications and descriptions of key geological features are important to give a realistic description of the sensitivity of CO₂ storage performance. To this end, we have selected four parameter spaces of geological variations from the SAIGUP study [3, 4, 5]. The parameters span realistic intervals for progradational shallow-marine depositional systems with limited tidal influence. In the following, we give a brief description of each.

Lobosity: Lobosity is defined by the plan-view shape of the shore-line. As a varying parameter, lobosity indicates the level at which the shallow-marine system is dominated by each of the main depositional

processes. Two depositional processes are considered in the SAIGUP study: fluvial and wave processes. The higher amount of sediment supply from rivers relative to the available accommodation space in the shallow sea, the more fluvial dominant the process will be. As the river enters the mouth of the sea, it can divide into different lobes and branches. Wave processes from the sea-side smear this effect and flatten the shoreline shape. Less wave effect produces more pronounced lobe shapes around the river mouths. Very high permeability and porosity can be found in the channelling branches, while dense rock with low permeability fills the space between them. Reservoir quality decreases with distance from the shore-face. We expect that the level of lobosity can have a considerable effect on the CO₂ injection and plume size in the aquifer. In this study, models of three levels of lobosity are used: flat shoreline, one lobe and two lobes, see Fig. 1.

Barriers: Periodic floods result in a sheet of sandstone that dips, thins, and fines in a seaward direction. In the lower front, thin sheets of sandstone are interbedded with the mudstones deposited from suspension. These mud-draped surfaces are potential significant barriers to both horizontal and vertical flow. In the SAIGUP domain used here, these barriers were modelled by transmissibility multipliers in three levels of coverage of barrier sheet: low (10%), medium (50%), and high (90%). We use the same variations in this study, see Fig. 1.

Aggradation: In shallow-marine systems, two main factors control the shape of the transition zone between the river and the basin: amount of deposition supplied by the river and the accommodation space that the sea provides for these depositional masses. One can imagine a constant situation in which the river is entering the sea and the flow slows down until stagnation. The deposition happens in a spectrum from larger grains depositing earlier in the land side to fine deposits in the deep basin. If the river flux or sea level fluctuates, the equilibrium changes into a new bedding shape based on the balance of these factors.

In the SAIGUP study those cases are considered in which, for example, the river flux increases and shifts the whole depositional system into the sea. The angle at which the transitional deposits are stacked on each-other because of this shifting, is called aggradation angle. Three levels of aggradation are modelled here: low, medium and high (Fig. 1). As we will observe later, aggradation can have a dramatic influence on the injection and migration process.

Progradation: The next factor varied is the progradation or the depositional-dip direction. Two types are considered here: up and down the dominant structural dip. Since the model is tilted a little, this corresponds to the lobe direction from flank to the crest or vice-versa (Fig. 1). This has a potential influence on the CO₂ flow from the injection point up to the crest.

Fault: There are three variational dimensions considered for faults in the SAIGUP study: fault type, intensity and transmissibility. However we did not include all of these variations in our work and confined this step to two transmissibilities of almost open and closed faults. Fig. 2 shows the effect of fault transmissibility on the flow pattern. Here we took the compartment type of faults of medium intensity ([3, 5]).

Simulation workflow

A fully automated workflow was designed for this study, starting from variational parameters in the SAIGUP models and ending into comprehensive result outputs based on the objective of the work. As a first step, 54 representative cases are studied using a commercial simulator. However, the parallel aim of future work is to develop fast simulation methods that are suitable for performing thousands of runs, using e.g., a vertically-averaged formulation [6].

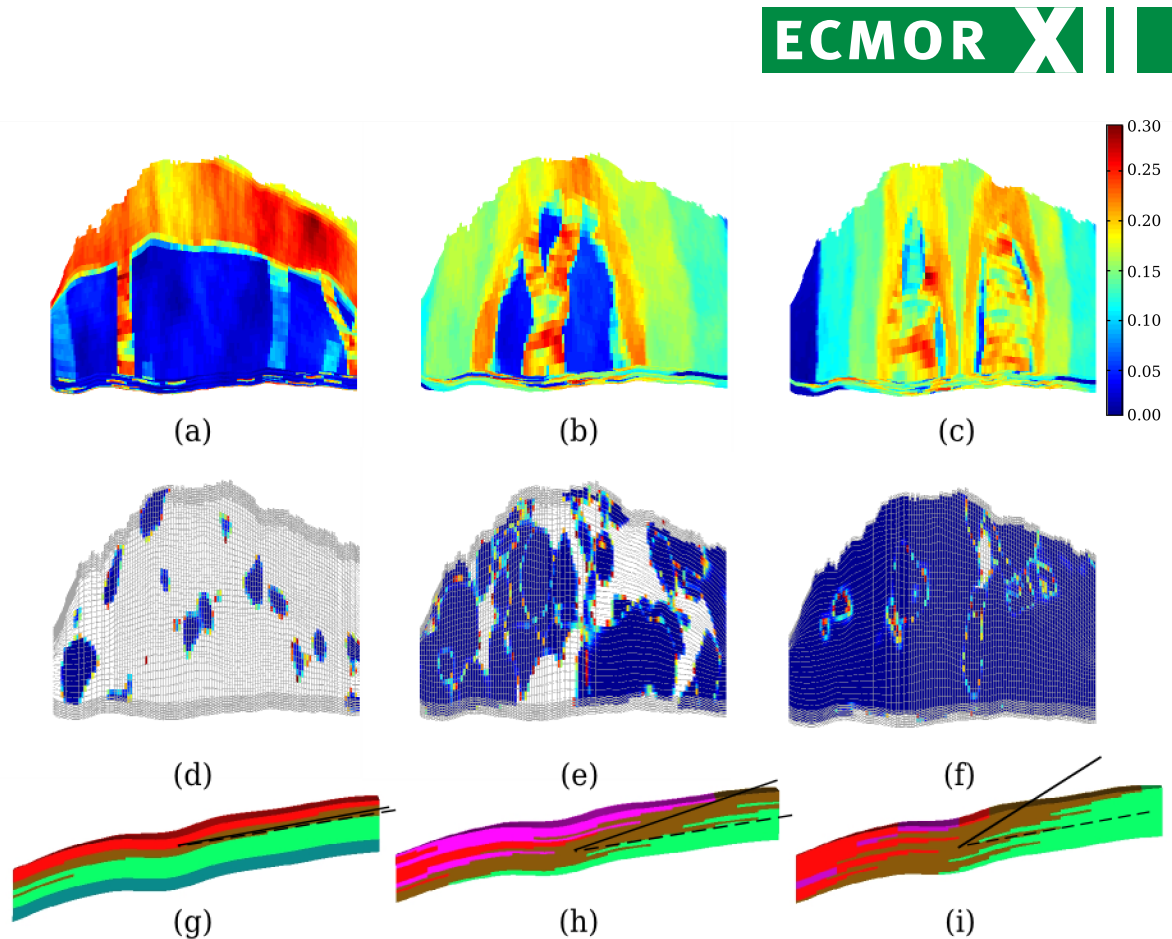


Figure 1 Different geological features considered in this study. Top row shows 'lobosity' in porosity distribution: (a) flat shore-line, (b) one lobe, (c) two lobes. The middle row shows 'barrier' by the distribution of zero transmissibility multipliers: (d) low, (e) medium, (f) high. The lower row shows 'aggradation' in rock-type distribution: (g) low angle of interface between the transitional rock-types leads to parallel layers; this angle is increasing in cases (h) and (i), which correspond to higher levels of aggradation. An up-dip progradation direction is shown in (b), and if the lobe flips over the long axis, we will have down-dip progradation.

Scenario design

We are using an injector down in the flank and hydrostatic boundary conditions on the sides, except the faulted side on the crest (Fig. 3). No-flow boundary conditions are imposed on the top and bottom surfaces of the model. The well is completed only in the last three layers.

Simple linear saturation functions with zero capillarity are used. This can be justified because the permeability contrast in channels has the dominating effect on the flow. Also, simple PVT data for a slightly compressible supercritical CO₂ is used. To model the hydrostatic boundaries in used simulator, high multipliers are used to magnify the pore volume of the outer cells in the model. About 40MM m³ of supercritical CO₂ is injected for thirty years, which amounts to 20% of the models' pore volumes. After the injection period, seventy years of early plume migration is simulated.

Results

As our objective function, we seek to maximize the CO₂ storage volume and minimize the risk of leakage. The results are discussed in three parts: first we look at model responses, then correlation between these responses. Afterwards we consider the sensitivity of each response to the studied geological feature.

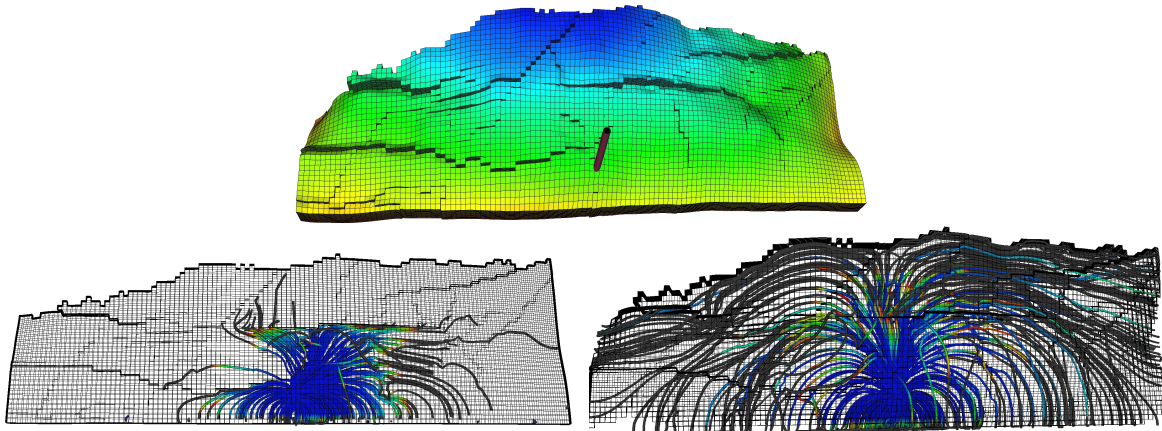


Figure 2 The studied fault features: the picture on the top shows the orientations and intensity of the faults, down left picture shows the flow path in almost closed faults case and the one on the right is showing the flow in the almost open faulted medium. The streamlines are shown for the same time step in both pictures. Notice that the flow is confined in the closed faults model.

In all outputs, we recognize the effect of aggradation. Cases with low aggradation have continuous facies layering parallel to the horizontal direction of the grid. Because the three lowest layers, in which the well is completed, are sealing in the cross-layering direction, the flow is forced to stay in the same layers rather than accumulating in the crest (Fig. 3).

Important responses

Reservoir pressure: The pressure response in general shows a sharp jump at the start of injection and a declining trend during the injection and plume migration. Pressure behaviour of different cases at the end of the injection period is shown in Fig. 4. Low aggradation cases show higher pressure.

Boundary fluxes: The flux out of the open boundaries is a measure of the sweep efficiency of the CO₂ plume. As channelling can lead to early CO₂ breakthrough at boundaries, we prefer cases with less fluxes out of the boundaries. The down boundary that is closer to the injector is a potential loss for the injected volume (Fig. 5(a)). Again, the flow is led to the boundaries in cases with low aggradations.

Total mobile/residual CO₂: If the CO₂ saturation is below the critical value, it will be immobile in the bulk flow, although not in the molecular sense. Less mobile CO₂ means less risk of leakage and more residual volumes (with saturations less than the critical) resulting from a more efficient volume sweep as preferable (Fig. 5(b)). We use critical saturation of 0.2 for both water and CO₂.

Connected CO₂ volumes: To estimate the risk of leakage from the cap-rock, we assume that all mobile CO₂ connected to a leakage point will escape out of the reservoir. Hence, it is preferable if the total mobile CO₂ volume is split into smaller plumes rather than forming a big mobile plume. Though the area exposed to potential leakage points will increase by splitting the plume, yet the volume reduction is overtaking the area effect.

On the other hand, the split CO₂ plumes can sweep more cross-areas than a big single plume. The no-flow faulted side can be considered to be connected to an imaginary large volume available for long-term plume migration. Thus, it makes sense to talk about plume sweeping cross area. Larger areas leave more residual CO₂ in the tail of the plume. Hence, we looked at the largest plume size, the number of plumes, and other statistical parameters. The number of plumes at the end of simulation for all cases are given

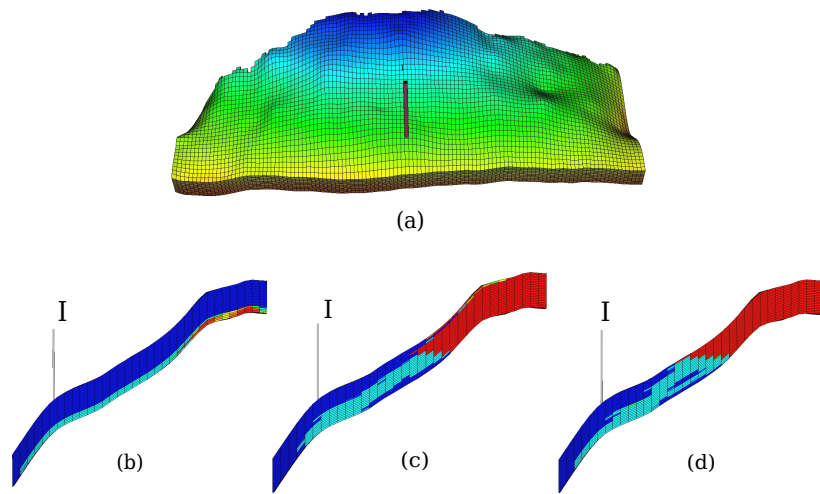


Figure 3 (a) Model geometry and well position. Model dimensions are 3km×9km×80m with 20 layers. The bottom row shows the side view of CO₂ distribution (in red) at the end of simulation in different aggradation cases, from low (b) to high (d). The vertical direction is exaggerated.

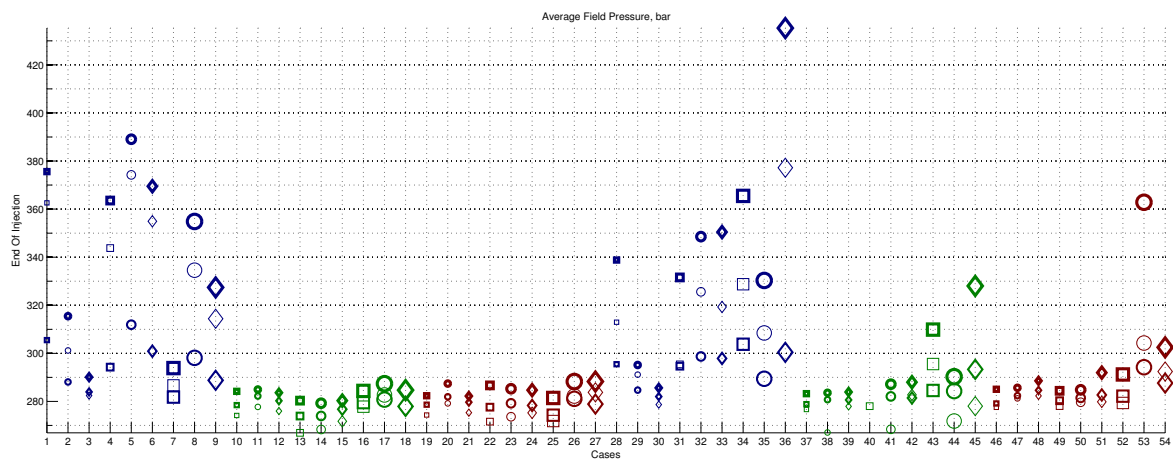


Figure 4 Average reservoir pressure plot for all cases. Colours represent 'aggradation' level: blue for low, green for medium, and red for high levels. Size represents 'barrier': small for low, medium for medium, and large for high level of barrier. Marker shape represents 'lobosity': square for flat shore-line, circle for one lobe, and diamond for two lobes. The first half of the case numbers refer to 'progradation' up-dip towards the crest, and the second half represent 'progradation' down-dip. Thickness shows the fault criteria: thin for unfaulted, medium for open faulted and thick for closed faulted cases.

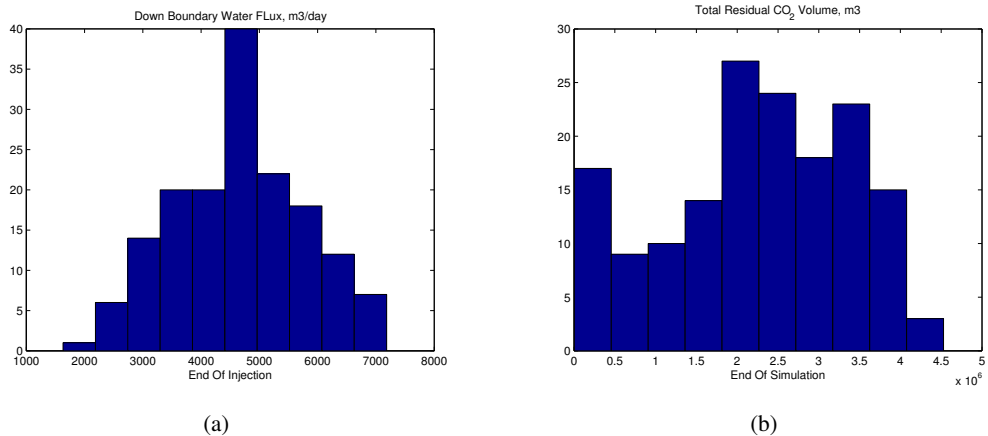


Figure 5 (a) Flux histogram for down boundary (b) Total residual CO₂ volume; cases with low aggradation show less values in a separate family.

in Fig. 7. Two-lobed cases include more branching channels which result in more plume numbers. Also barrier effect increases the lateral distribution of the plume.

Correlation between responses

Here we relate the responses by plotting them against each other. This helps in understanding the degree of correlations between the responses. By looking at these plots we can relate the trends to geological features. This in turn helps in evaluating the effect of uncertainty of each feature on the uncertainty of the simulation outputs.

Fig. 8 shows down boundary CO₂ flux versus average field pressure at the end of injection. Two linear trends can be recognized in the plot: first one starting from 280 bar going until 290 bar in a near vertical slope. The other one starts from 290 bar on the pressure axis and goes about 400 bar in a lower slope. The first trend shows that average pressure is not changing a lot with the increase of CO₂ out-flux. But the second trend shows a dramatic change in pressure corresponding to the change in the down flux rate.

The second trend is made mainly by the cases of blue colour. This is again showing the effect of low aggradation in the flow and pressure behaviour. In low aggradation cases, as the CO₂ flux out of the down boundary increases, the average pressure also increases in the aquifer. Effect of other geological features combined with the low aggradation dictates the amount of CO₂ which goes up to the crest or stays in the bottom-most layers going out from the down boundary. Since the lower layers have poor quality rock, more flow through these layers towards down boundary result in higher pressure in the aquifer.

In Fig. 9, the total number of CO₂ plumes are plotted against total residual CO₂ volumes at end of simulation. The general trend shows positive correlation between these two responses. This is consistent with our discussion in the previous section about the plume size and sweep efficiency. Split plume introduces more residual CO₂. On the other hand, there is a separation in the plotted cases based on the fault criteria. Thin signs are clustered in the lower part of the graph. The medium thickness markers are clustered on the higher part of the graph and the very thick signs are sitting in between. This implies that the unfaulted cases show higher residuals with lower number of plumes, and the open faulted cases introduce more number of plumes. This can be justified by looking at a flow pattern in unfaulted and open faulted case which are shown in Fig. 10. In the open faulted cases, the flow is more laterally distributed. The closed faulted cases restrict the plume migration in the fault compartments and this

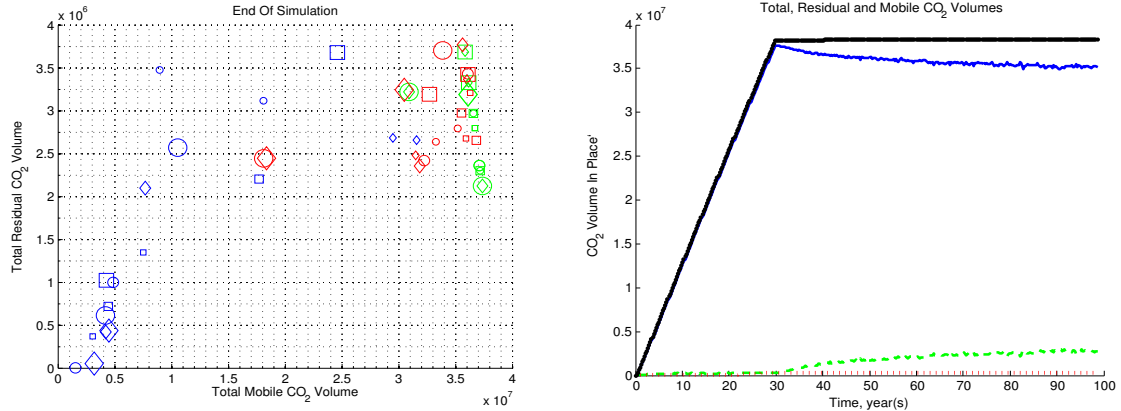


Figure 6 CO₂ volumes. Left: residual versus mobile volume at the end of simulation. Most of the green coloured cases follow a linear trend, which is expected because the injected CO₂ must be conserved if no CO₂ leaves the system. For the rest of the cases, some CO₂ goes out of boundaries. Right: Total CO₂ volumes with time plotted for one case. Green curve is the residual volumes, dotted red denotes volumes that have left the domain, solid blue is mobile volumes, and the solid black shows the summation, which is the total volume and stays constant after injection because no more CO₂ is added to the system. The faulted cases are not included in this figure.

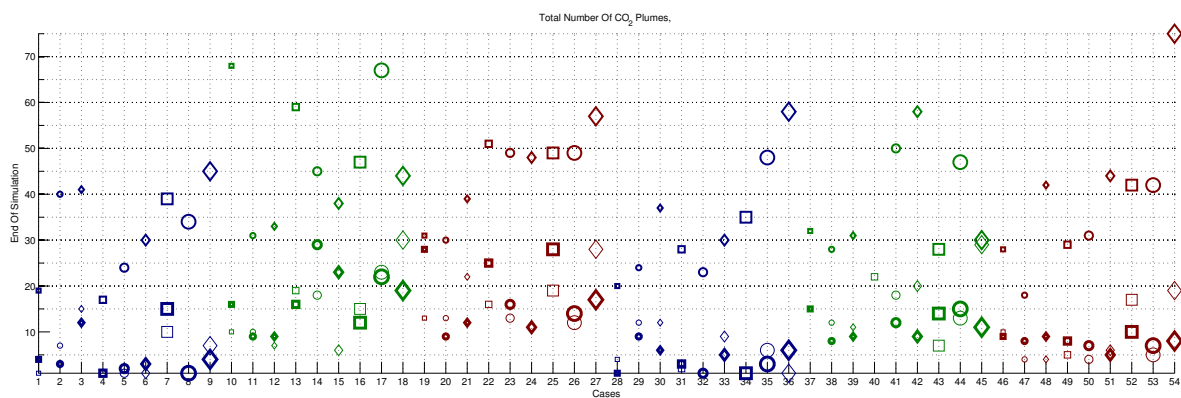


Figure 7 CO₂ plume number at end of simulation, see explanation in Fig. 4.

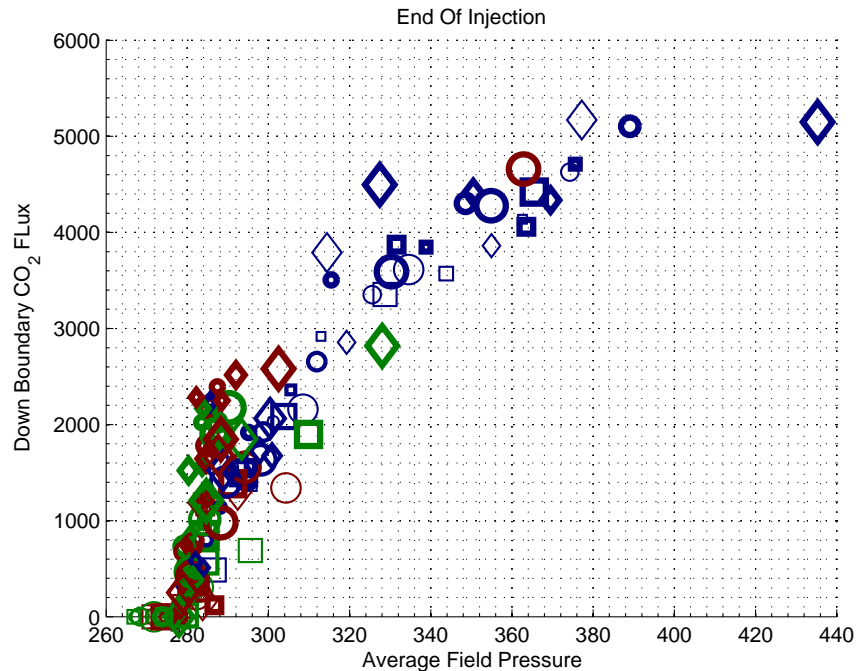


Figure 8 Down boundary CO₂ flux versus average pressure, at end of injection.

introduces lower number of plumes with lower volumes of residuals which make these cases to fall in between (Fig. 2).

Finally we look at total CO₂ residuals versus down boundary CO₂ fluxes at end of injection. We can recognize a negative correlation in an almost linear trend in Fig. 11. Higher out-flux through the down boundary leaves less CO₂ in the domain to migrate and this lowers the residual volumes in the domain.

Sensitivity of responses

In this section, we try to quantify the sensitivity of flow responses to each of the geological features. To achieve this, we define a gradient for each of the features. To make it clear, we use the example of barriers which are easier to explain.

We have three levels of barrier: low, medium and high. Suppose that we are interested in calculating the gradient of average field pressure with respect to barriers. We do this in two steps: first we average the average field pressure for cases of the same level of barriers. This results in three averaged pressure values corresponding to each level of barriers. In the next step, we fit a line through these three points and calculate the tangent of this line. This represents the average pressure increase due to one level increase in barriers.

For other features like fault and lobosity, we follow the same procedure. Though the feature variation is not apparent like barrier, that points to change in the type of the feature. For example, first level of fault criteria relates to unfaulted cases, the second relates to the open faulted and the third one is for the closed faulted cases. Or regarding progradation, we have two levels: up-dip and down-dip direction. The positive and negative gradient is defined based on the way we vary the defined levels.

Fig. 12 shows the average pressure sensitivity to different features at end of injection and end of sim-

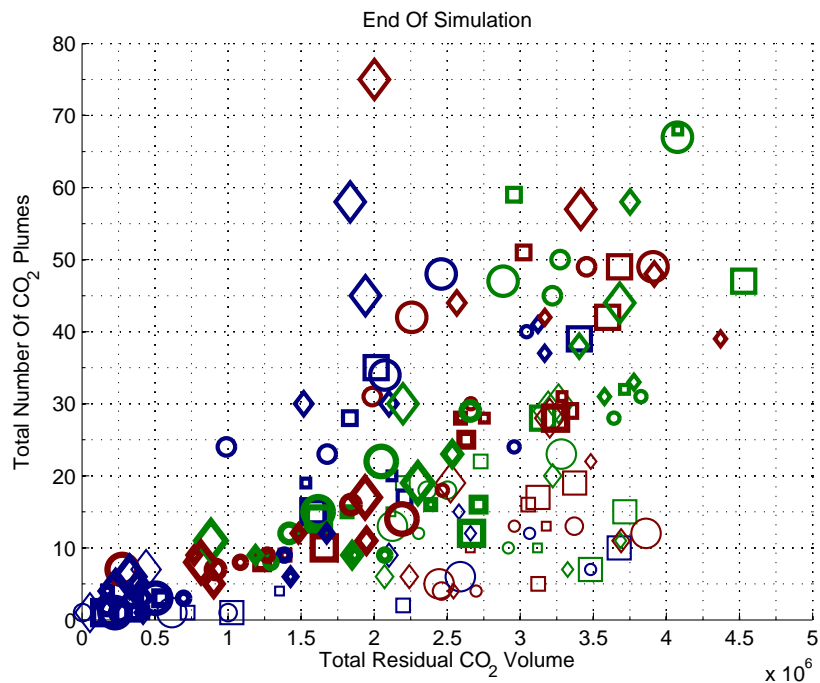


Figure 9 Plume number versus residuals at end of simulation.

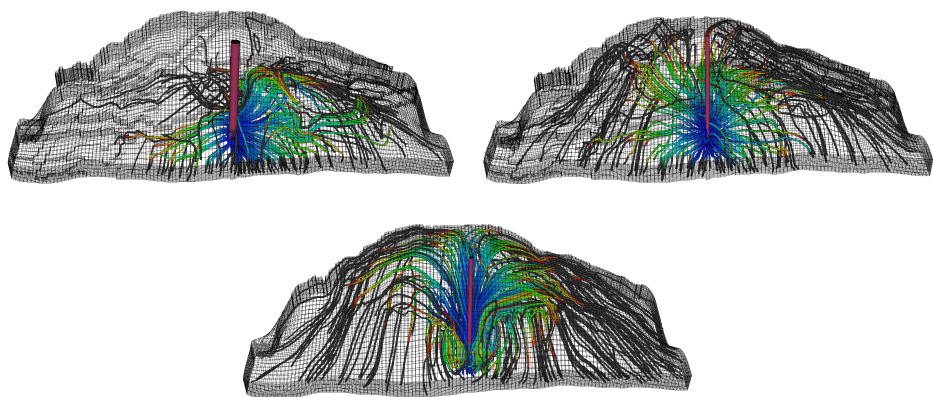


Figure 10 Effect of fault structure on the flow pattern: top left picture shows the closed faulted case, top right picture shows the open faulted case and the bottom picture shows the unfaulted case. Open faults enhance the lateral flow, while the flow in the unfaulted case is mainly upward heading the crest.

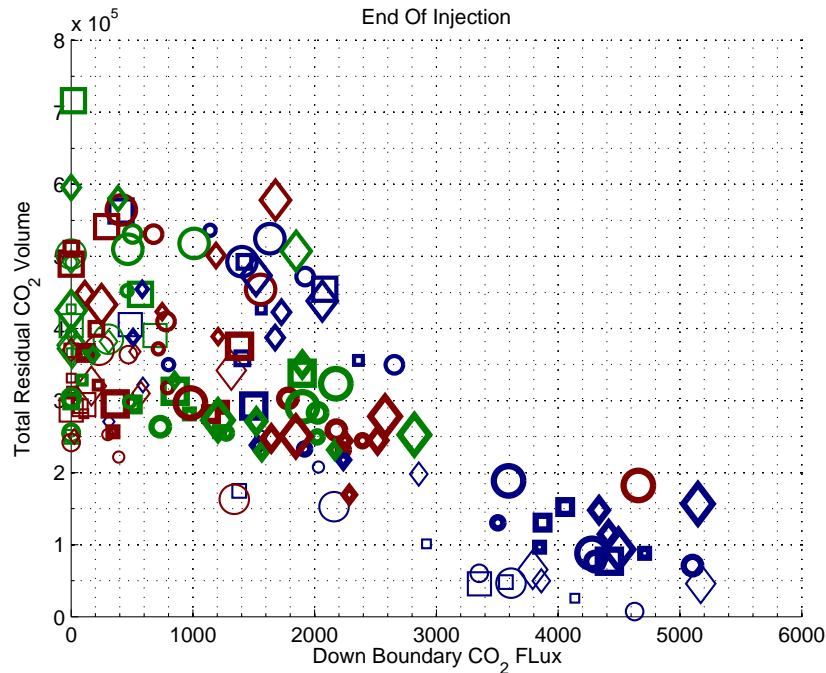


Figure 11 CO₂ residual volume versus down boundary CO₂ flux.

ulation. These results show that in the injection period the dominating effect is related to aggradation, while at end of simulation the most influential feature is the fault criteria. During injection, the flow is dictated by the viscous force imposed by the injector. This force is more sensitive to the feature. In the low aggradation cases, flow is forced to stay in the lower layers with lower permeability values. This increase the pressure in the aquifer. In the higher aggradation level, CO₂ can flow upward through channels with higher permeabilities. This lowers the average pressure in the domain. This is why the gradient is negative for aggradation at end of injection, since lower aggradation level introduces higher pressure.

After stopping the injection, the dominating force is the gravity. The main flow direction is vertical and the pressure is now more sensitive to fault criteria. This is what we see in Fig. 12(b).

The effect of progradation switches from positive to negative after stopping the injection. During injection period, injecting in up-dip direction is easier than injecting in down-dip direction, while for the plume migration after injection the down-dip opens more conductive medium in front of the plumes moving towards the crest.

In Fig. 13 plume number sensitivity is shown. During injection (Fig. 13(a)), barriers are the most influential features. They enhance the lateral flow and the plume splits rather than accumulating in the crest. At end of simulation (Fig. 13(b)), progradation plays an important role relatively. Note that at this time, the open faults are introducing large number of plumes, while the unfaulted and closed faulted cases introduce small number of plumes which in average cancels out to a low gradient.

Finally Fig. 14 shows gradients for total CO₂ residuals. During injection (Fig. 14(a)) aggradation is the most influential feature. Fault criteria is playing the most important role in the plume migration period after injection (Fig. 14(b)).

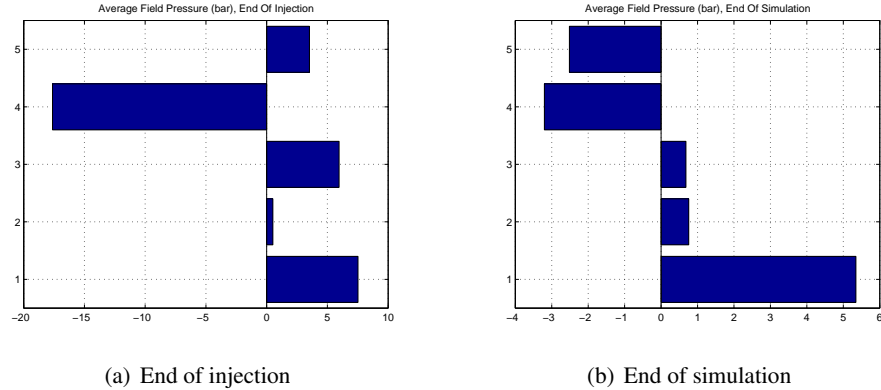


Figure 12 Average pressure sensitivity to different geological features. In these pictures, the vertical axis shows the different geological features from bottom to top: 1-fault, 2-lobosity, 3-barrier, 4-aggradation and 5-progradation. Notice the different range in the horizontal axis at end of injection and end of simulation.

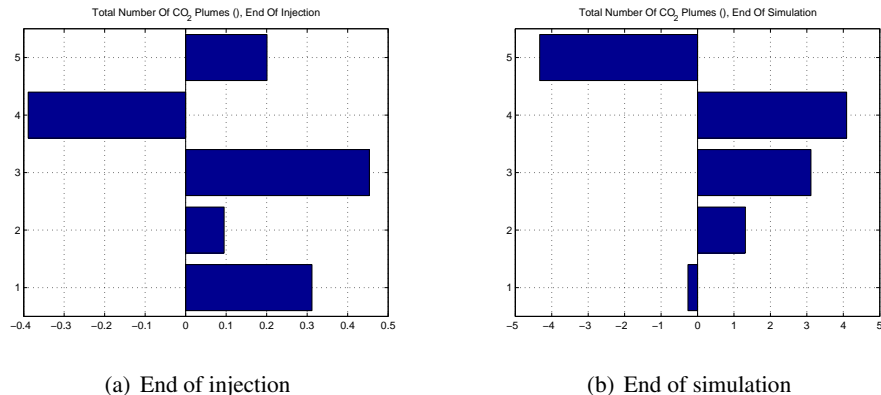


Figure 13 CO₂ plume number sensitivity to different geological features. See Fig. 12 for the vertical axis explanation.

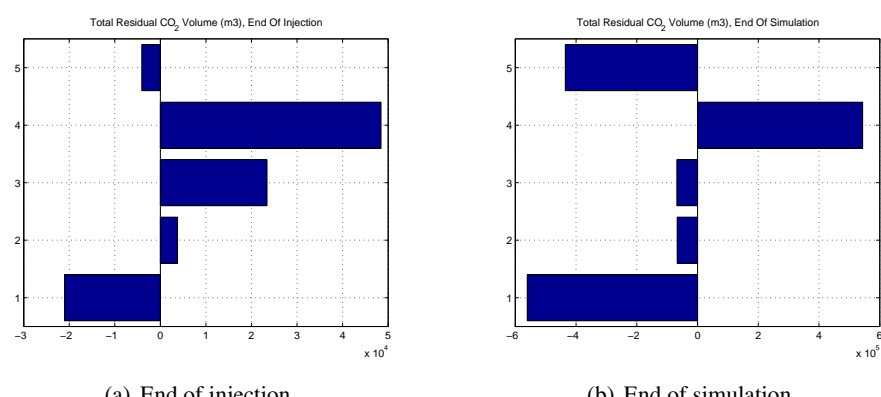


Figure 14 Total residual CO₂ sensitivity to different geological features.

Conclusions

Herein, we have reported on a preliminary study of the influence of various geological parameters on the injection and early-stage migration of CO₂ in progradational shallow-marine systems. The important responses related to storage capacity and risk of leakage are calculated for all the cases and discussed accordingly. The correlations between responses are investigated and a sensitivity measure is introduced and discussed for different responses.

Large variations in the flow responses show the importance of considering uncertainty in the geological parameters. Moreover, we have demonstrated that different geological parameters can have a different impact on the CO₂ migration during injection and during the later migration. In particular, our results highlight how variation in aggradation, fault criteria and barriers significantly change the flow direction within the medium. Therefore we believe that effort should be put into detailed geological modelling of potential injection sites. This way, one can better balance the influence of simplifications made in the models of geology and flow physics.

References

- [1] J. M. Nordbotten: *Sequestration of Carbon in Saline Aquifers: Mathematical and Numerical Analysis*, Doctor Scientiarum Thesis, Department of Mathematics, University of Bergen, (2004).
- [2] S. Bachu: *CO₂ storage in geological media: Role, means, status and barriers to deployment*, Progress in Energy and Combustion Science, ELSEVIER, (2008).
- [3] J. A. Howell, A. Skorstad, A. MacDonald, A. Fordham, S. Flint, B. Fjellvoll, and T. Manzocchi: *Sedimentological parameterization of shallow-marine reservoirs*, Petroleum Geoscience, **14** (1), pp. 17-34, (2008).
- [4] T. Manzocchi, J. N. Carter, A. Skorstad, B. Fjellvoll, K. D. Stephen, J. A. Howell, J. D. Matthews, J. J. Walsh, M. Nepveu, C. Bos, J. Cole, P. Egberts, S. Flint, C. Hern, L. Holden, H. Hovland, H. Jackson, O. Kolbjørnsen, A. MacDonald, P. A. R. Nell, K. Onyeagoro, J. Strand, A. R. Syversveen, A. Tchistiakov, C. Yang, G. Yielding, and R. W. Zimmerman: *Sensitivity of the impact of geological uncertainty on production from faulted and unfaulted shallow-marine oil reservoirs: objectives and methods*, Petroleum Geoscience, **14** (1), pp. 3-15, (2008).
- [5] J. D. Matthews, J. N. Carter, K. D. Stephen, R. W. Zimmerman, A. Skorstad, T. Manzocchi, and J. A. Howell: *Assessing the effect of geological uncertainty on recovery estimates in shallow-marine reservoirs: the application of reservoir engineering to the SAIGUP project*, Petroleum Geoscience, **14** (1), pp. 33-44, (2008).
- [6] S. E. Gasda, J. M. Nordbotten, and M. A. Celia: *Vertical equilibrium with sub-scale analytical methods for geological CO₂ sequestration*, Computational Geosciences, **13** (4), pp. 469-481, (2009).

Paper C

A.3 Field-case simulation of CO₂ plume migration using vertical-equilibrium models.

Nilsen , H.M., Herrera , P.A., Ashraf, M., Ligaarden , I.S., Iding , M., Hermanrud , C., Lie , K.A., Nordbotten , J.M., Dahle , H.K., and Keilegavlen , E.

Presented in GHGT10, Amsterdam, 2011. Published in 2011, Energy Procedia 4 (2011): 3801-3808.



Available online at www.sciencedirect.com



Energy
Procedia

Field-case simulation of CO₂-plume migration using vertical-equilibrium models www.elsevier.com/locate/procedia

Halvor Møll Nilsen^{a,*}, Paulo A. Herrera^b, Meisam Ashraf^{a,e}, Ingeborg Ligaarden^a, Martin Iding^d, Christian Hermanrud^{d,e}, Knut-Andreas Lie^{a,e}, Jan M. Nordbotten^{e,f}, Helge K. Dahle^e, Eirik Keilegavlen^e

^aSINTEF ICT, Dept. Applied Math., Oslo, Norway

^bCentre for Integrated Petroleum Research, Uni Research, Bergen, Norway

^cDepartment of Mathematics, University of Bergen, Norway

^dStatoil ASA, Trondheim, Norway

^eDepartment of Mathematics, University of Bergen, Norway

^fDepartment of Civil and Environmental Engineering, Princeton University, USA

Abstract

When injected in deep saline aquifers, CO₂ moves radially away from the injection well and progressively higher in the formation because of buoyancy forces. Analyses have shown that after the injection period, CO₂ will potentially migrate over several kilometers in the horizontal direction but only tens of meters in the vertical direction, limited by the aquifer caprock [1, 2]. Because of the large horizontal plume dimensions, three-dimensional numerical simulations of the plume migration over long periods of time are computationally intensive. Thus, to get results within a reasonable time frame, one is typically forced to use coarse meshes and long time steps which result in inaccurate results because of numerical errors in resolving the plume tip.

Given the large aspect ratio between the vertical and horizontal plume dimensions, it is reasonable to approximate the CO₂ migration using vertically averaged models. Such models can, in many cases, be more accurate than coarse three-dimensional computations. In particular, models based on vertical equilibrium (VE) [3] are attractive to simulate the long-term fate of CO₂ sequestered into deep saline aquifers. The reduced spatial dimensionality resulting from the vertical integration ensures that the computational performance of VE models exceeds the performance of standard three-dimensional models. Thus, VE models are suitable to study the long-time and large-scale behavior of plumes in real large-scale CO₂-injection projects [4, 1, 2, 5]. We investigate the use of VE models to simulate CO₂ migration in a real large-scale field case based on data from the Sleipner site in the North Sea. We discuss the potential and limitations of VE models and show how VE models can be used to give reliable estimates of long-term CO₂ migration. In particular, we focus on a VE formulation that incorporates the aquifer geometry and heterogeneity, and that considers the effects of hydrodynamic and residual trapping. We compare the results of VE simulations with standard reservoir simulation tools on test cases and discuss their advantages and limitations and show how, provided that certain conditions are met, they can be used to give reliable estimates of long-term CO₂ migration. © 2011 Published by Elsevier Ltd.

1. Introduction

Carbon capture and storage (CCS) is a promising technology for reducing CO₂ emissions to the atmosphere. To become an effective part of the solution to the climate problem, CCS technology will have to be applied at a very large scale to store a significant part of the increasing CO₂ emissions [6]. CO₂ injection into deep saline aquifers would provide large volumes to store CO₂. Investigations of the risk of CO₂ leakage from the aquifers will require simulations that consider large temporal and spatial scales and because of the inherent uncertainty of geological characterizations, simulation of multiple realizations of a given storage scenario will be required for risk analysis. This is the main motivation for the development of fast simulation tools.

The CO₂-brine system is simpler than the fluid system used in the oil industry, where black-oil or component-based formulations are standard. In particular, it is expected that at typical injection conditions, strong gravity segregation will occur over relatively short time-scales because of the large density differences between the resident brine and the injected supercritical CO₂. This feature of the flow system can be used to develop fast simulation tools particularly tuned for simulating the long-term migration of the injected CO₂.

Models based on a vertical equilibrium (VE) assumption have been used for long time to describe flow in porous media. Dupuit's approximation, which is commonly used in groundwater hydrology, is an example of this kind of models. In the oil industry, VE models were extended during the 50's and 60's to simulate two-phase and

* Corresponding author

Email addresses: Halvor.M.Nilsen@ntef.no (Halvor Møll Nilsen), paul.o.herrera@ni.no (Paulo A. Herrera), jan.nordbotten@at.h.uib.no (Jan M. Nordbotten), helge.dahle@at.h.uib.no (Helge K. Dahle)

three-phase vertically segregated flows [7, 8, 9]. The interest in VE models diminished as computational resources increased. However, interface models for scenarios with strong gravity segregation (like steam injection) were also an active research area in the 80's and 90's [10, 11].

In recent years, there has been a renewed interest in VE methods as a means to simulate large-scale CO₂ migration, for which a sharp-interface assumption with vertical equilibrium may be reasonable. Many authors have developed analytical solutions to study different aspects of CO₂ injection, assuming rapid vertical segregation and vertical equilibrium [12, 4, 1, 13, 14, 15, 16]. In particular Gasda et al. [17], extended a VE formulation with sub-scale analytic functions and demonstrated the potential of using a VE formulation to speed up simulations of CO₂ migration. Numerical calculations using a VE formulation compared well with full 3D simulations in a recent benchmark study [18].

Herein, we investigate the use of VE models for a realistic large-field case based on data from the Sleipner site. Our calculations consider the effects of hydrodynamic and residual trapping. We discuss the potential and limitations of VE models and show how VE models can be combined with standard methods to give reliable results both for the plume development (injection stage) and plume migration (post injection). Particularly, we focus on a model that incorporates the aquifer geometry and heterogeneity in a flexible way that enables us to utilize 3D simulations whenever needed, for example, for the injection period in heterogeneous reservoirs. To investigate large-scale CO₂-injection projects with realistic rock properties over long time periods, it is crucial to reduce the computational cost. VE models enables this by using analytical solutions to capture the vertical features in the flow system, thereby reducing the dimensionality of the problem. Achieving the same in a three dimensional simulation requires prohibitively high vertical resolution.

The main objective of this paper is to compare simulations of CO₂ migration in the Utsira formation in the North Sea using a standard three-dimensional reservoir simulator and two-dimensional VE formulations. To our knowledge, this is one of the first comparisons between full-3D and VE calculations for a real CO₂ injection site. Our aims are to demonstrate the benefits of using a VE model to simulate CO₂ migration in a realistic setting and to discuss how VE models can be used to develop fast techniques to simulate CO₂ injection at the basin scale.

2. Mathematical formulation

In this section we present a brief summary of the derivation of a vertical equilibrium formulation. A more thorough derivation can be found in [19]. First, we assume that CO₂ migration in saline aquifers can be modeled as a two-phase problem with brine and CO₂ as the wetting (*w*) and non-wetting (*n*) fluids, respectively. Furthermore, we consider the evolution of a CO₂ plume in an aquifer whose mean direction makes a constant dip angle θ with the horizontal plane as shown in Figure 1. We start the derivation by writing a mass conservation

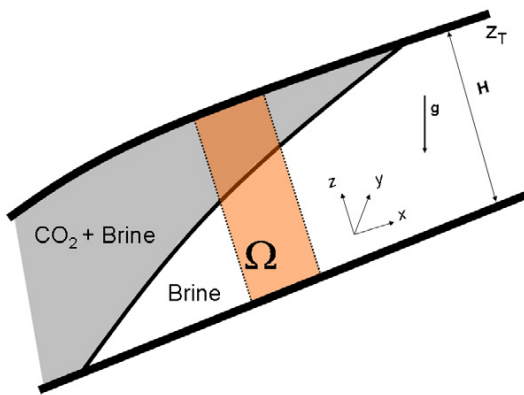


Figure 1: Schematic of the CO₂ plume and aquifer considered to derive a vertical equilibrium formulation for CO₂ migration.

equation for each fluid phase inside control volume $\Omega = \Delta x \Delta y H$ to obtain

$$\frac{\partial}{\partial t} \int_{\Omega} \phi s_{\alpha} + \int_{\partial\Omega} \mathbf{f}_{\alpha} = \int_{\Omega} q_{\alpha}, \quad (1)$$

where s_{α} is the core-scale saturation of phase α , ϕ is the rock porosity, \mathbf{f}_{α} are the fluid fluxes that pass through the control volume boundaries and q_{α} represents source and/or sink terms. Taking the limit $\Delta x, \Delta y \rightarrow 0$ and

assuming no flow perpendicular to the top and bottom of the aquifer, we obtain

$$\frac{\partial}{\partial t} \int_0^H \phi s_\alpha dz + \nabla_{\parallel} \cdot \int_0^H \mathbf{u}_\alpha^H dz = \int_0^H q_\alpha dz, \quad (2)$$

where $\mathbf{u}_\alpha^H = (u_\alpha^x, u_\alpha^y)$ and $\nabla_{\parallel} = (\partial/\partial x, \partial/\partial y)$ are two-dimensional vectors in the aquifer plane. The second term on the left hand side includes the vertical integral of the horizontal velocity of the fluid. Applying the generalized Darcy's law we have that $\mathbf{u}_\alpha^H = -k\lambda_\alpha (\nabla_{\parallel} p_\alpha - \rho_\alpha \mathbf{g}^H)$, so that,

$$\int_0^H \mathbf{u}_\alpha^H dz = - \int_0^H k\lambda_\alpha (\nabla_{\parallel} p_\alpha - \rho_\alpha \mathbf{g}^H) dz. \quad (3)$$

Here k is the permeability of the medium, λ_α and ρ_α are the mobility and density of phase α , respectively; and \mathbf{g}^H is the projection of gravity onto the aquifer plane. To evaluate (3), we assume that [3]: i) the velocity component perpendicular to the aquifer plane is very small, and ii) the fluid density in each phase is constant. Hence the fluids are in hydrostatic equilibrium in the vertical direction. Then, pressure in each fluid phase can be written in terms of the fluid pressure at the top of the aquifer and the elevation of the top of the aquifer (z_T), i.e. we take the caprock surface as a datum level to measure fluid pressures. Then, the pressure gradient in the aquifer plane can be evaluated as,

$$\nabla_{\parallel} p_\alpha = \nabla_{\parallel} P_\alpha - g_z \rho_\alpha \nabla_{\parallel} z_T. \quad (4)$$

Next, we define the set of vertically integrated variables and parameters listed in Table 2. Substituting (4)

Table 1: Vertically-averaged variables and parameters.

Parameter	Expression	Parameter	Expression
Gravity	$\mathbf{G} = g_z \nabla_{\parallel} z_T + \mathbf{g}^H$	Velocities	$\mathbf{U}_\alpha = \frac{1}{H} \int_0^H \mathbf{u}_\alpha^H dz$
Porosity	$\Phi = \frac{1}{H} \int_0^H \phi dz$	Saturations	$S_\alpha = \frac{1}{\Phi H} \int_0^H \phi s_\alpha dz$
Permeability	$K = \frac{1}{H} \int_0^H k dz$	Pressures	$P_\alpha = p_\alpha(z_T)$
Mobilities	$\Lambda_\alpha = \frac{1}{KH} \int_0^H k \lambda_\alpha dz$	Sources/Sinks	$Q_\alpha = \frac{1}{H} \int_0^H q_\alpha dz$

into (3) and the vertically integrated parameters into (2), we obtain a mass conservation equation for the vertically integrated fluid saturations S_α . Table 2 shows a comparison between the original 3D equations and their vertically integrated equivalents.

Table 2: Equations that define the full 3D and 2D vertical equilibrium (VE) models.

3D	2D
$\frac{\partial(\phi s_\alpha)}{\partial t} + \nabla \cdot \mathbf{u}_\alpha = q_\alpha$	$\Phi \frac{\partial S_\alpha}{\partial t} + \nabla_{\parallel} \cdot \mathbf{U}_\alpha = Q_\alpha$
$\mathbf{u}_\alpha = -k\lambda_\alpha (\nabla_{\parallel} p_\alpha - \rho_\alpha \mathbf{g}^H)$	$\mathbf{U}_\alpha = -K\Lambda_\alpha (\nabla_{\parallel} P_\alpha - \rho_\alpha \mathbf{G})$
$s_w + s_n = 1$	$S_w + S_n = 1$
$\lambda_\alpha = \lambda_\alpha(s_w)$	$\Lambda_\alpha = \Lambda_\alpha(S_w)$
$p_c = p_n - p_w = p_c(s_w)$	$P_c = P_n - P_w = P_c(S_w)$

The last step in the derivation of the vertically integrated model is to evaluate the vertically integrated mobilities (Λ_α) and capillary pressure (P_c) as function of the vertically integrated saturations (S_α). Assuming hydrostatic pressure distribution, so that $p_n(z) = P_n - \rho_n g_z(z_T - z)$ and $p_w(z) = P_w - \rho_w g_z(z_T - z)$, we have that by definition capillary pressure as function of elevation can be computed as [3],

$$p_c(z) = p_n(z) - p_w(z) = P_n - P_w - \Delta \rho g_z(z_T - z) \quad (5)$$

where the capillary pressure at the top of the aquifer is a function of the wetting saturation at z_T , $P_c = P_n - P_w = p_c(s_w(z_T))$. Then, given the wetting saturation at the top of the aquifer, $s_w^T = s_w(z_T)$, we can get a reconstruction of the fine scale saturation as function of z evaluation the inverse function of $p_c(z)$, to obtain,

$$\hat{s}_\alpha(z) = p_c^{-1}(p_c(z; s_w^T)) \quad (6)$$

Notice that $\hat{s}_w(z)$ is not the true fine scale saturation but the one by assuming hydrostatic fluid pressure distribution in the vertical direction. Now, the vertically integrated constitutive relations can be directly computed by evaluating, $S_\alpha = S_\alpha(\hat{s}_\alpha(s))$, $\Lambda_\alpha = \frac{1}{KH} \int_0^H k \lambda_\alpha(\hat{s}_w) dz$ and $P_c = p_c(s_w^T)$.

3. Numerical simulations

In this section we compare a 3D and a VE model to simulate CO₂ migration in the Utsira Sand aquifer, which is a major saline aquifer in the North Sea, into which CO₂ separated from gas extracted from the overlying Sleipner field has been injected at a rate of approximately 1 Mt/year since 1996 [20, 21]. The Utsira Sand extends for more than 400 km in north-south direction and between 50 and 100 km in the east-west axis, covering an area of approximately $2.6 \cdot 10^4$ km² [21]. The geometry of the aquifer is irregular and complex. While the top surface is undulatory and varies smoothly in the depth range of 550–1500 m, the bottom is more complex with multiple domes of up to 100 m high and 1–2 km wide. The aquifer thickness ranges from 300 m near the CO₂ injection site to 200 m farther north (200 km from the injection site). The reservoir caprock is several hundred meters thick and comprises several units of low permeability materials (shales, glacio-marine clay, and glacial till) [21]. Geophysical logs indicate that the main reservoir has a proportion of clean sand between 0.7 and 1.0 with a small shale fraction composed by multiple thin (~ 1 m) layers that constitute vertical flow barriers. The interpretation of seismic surveys, performed periodically since the CO₂ injection started, indicate that such shale layers have a major impact on the CO₂ migration because a significant part of the rising CO₂ has been trapped underneath these low permeability layers forming multiple quasi-independent plumes [20, 22]. Analyses of core samples of the Utsira formation sand have estimated porosity values between 35 % and 40 % and permeability in the range 1000–3000 mD [21].

Model setup

Numerical simulations were performed using a preliminary numerical model setup by the Statoil R&D group [23] to study how CO₂ migrates once it reaches the upper-most sand layer. Thus, the model includes the section of the aquifer immediately underneath the caprock and above the upper most shale layer as shown in Figure 2. The domain covers an area of approximately 60 km² and has an average thickness of 25 m. The numerical grid includes 120,000 hexahedral cells with constant 50 m spacing in the horizontal directions and average 5 m spacing in the vertical direction. Estimated permeability values for the top sand layer and caprock are shown in Figure 2. In the model the horizontal components of the permeability tensor are assumed isotropic and vary between 1789 and 2018 mD, while the vertical component is assigned as equal to 1/10th of the horizontal value. Because of the relative low permeability of the caprock and the underlying shale relative to the main sand aquifer, they are modeled as impermeable boundaries. The porosity of the aquifer sand was set according to a linear correlation with the permeability and has a mean value equal to 0.36. The amount of CO₂ that reaches the top of the aquifer was simulated as a point source with specified injection rates that increase from 0 to $5 \cdot 10^6$ m³/year during the first 32 years and then set to zero until the end of the simulation (132 years). The total amount of CO₂ injected is $5.3 \cdot 10^6$ m³ at reservoir conditions.

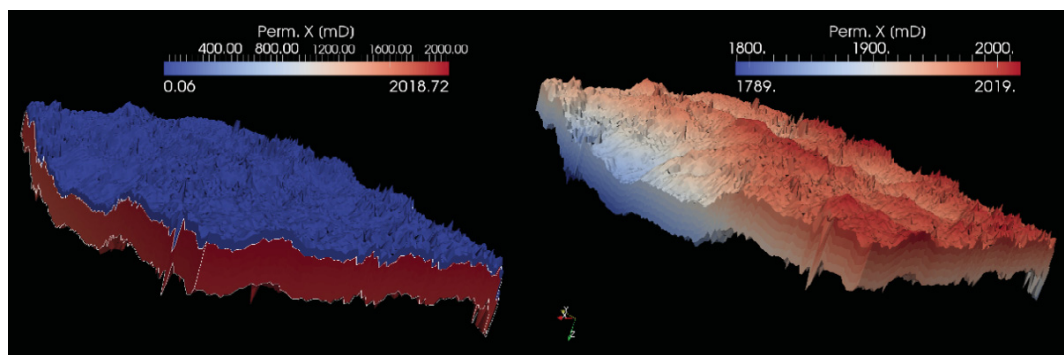


Figure 2: Estimated horizontal permeability for the upper 25 m of the Utsira Sand aquifer and lower 10 m of the caprock. There are large contrasts in permeability between the main aquifer and the caprock (left), but only moderated differences within the aquifer itself (right).

Simulation results

We present results of 3D and VE simulations carried out with the commercial ECLIPSE Reservoir simulator [24] and the VE module of the open-source Matlab Reservoir Simulation Toolbox (MRST) developed at SINTEF ICT and available at <http://www.sintef.no/Projectweb/MRST/>. In the following discussion we will refer to the different numerical solutions as ECLIPSE-3D, ECLIPSE-VE and MRST-VE. To test the sensitivity of the 3D solution with respect to the vertical discretization, we run the ECLIPSE-3D simulations using the original grid (coarse) and a refined grid (fine) that has five times more horizontal layers than the original one. Capillary forces were not included in the simulations presented below, however, as explained above, they can be easily included in the VE formulation without introducing additional computational complexity [9, 25]. The 3D simulations

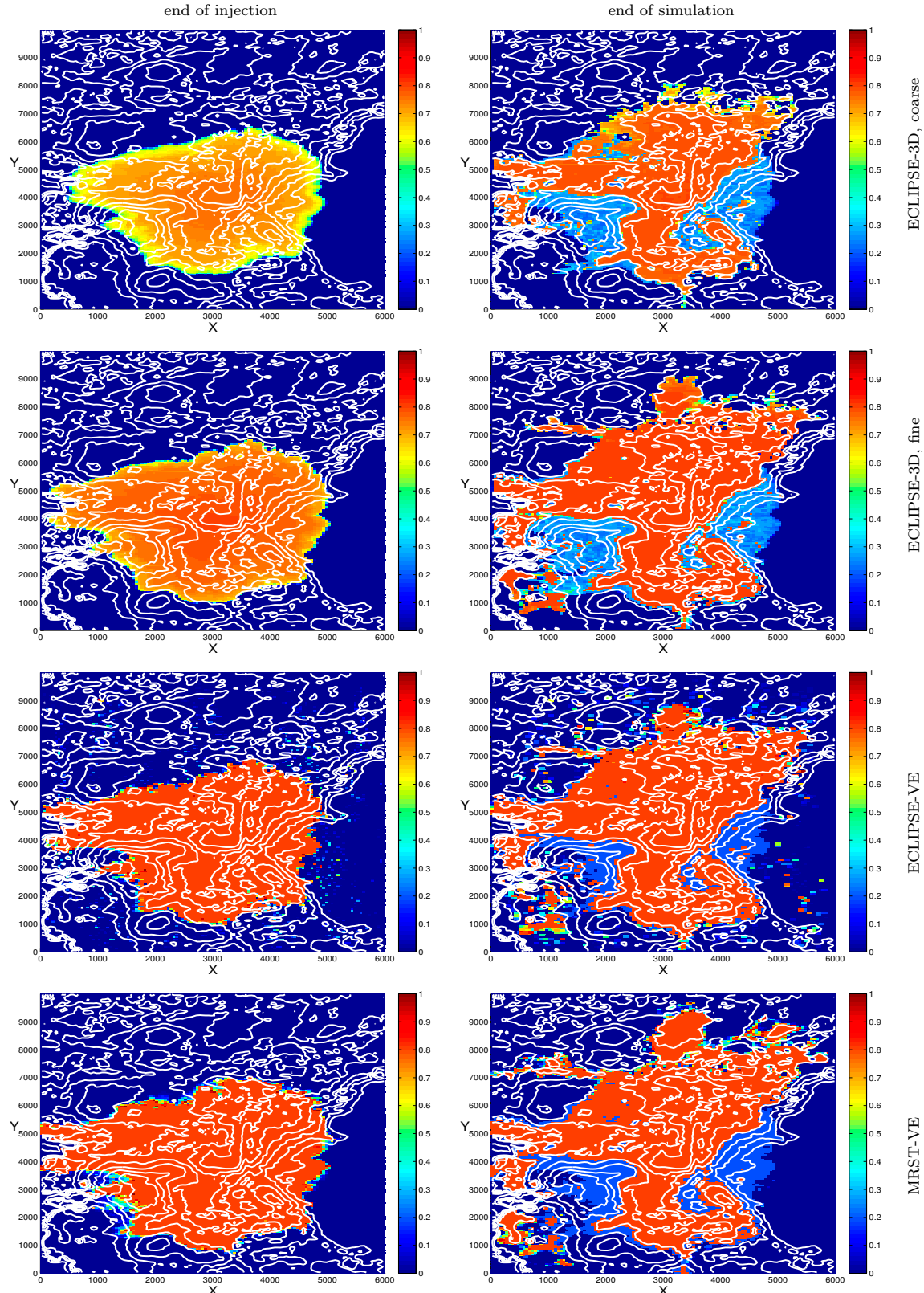


Figure 3: CO₂ saturation in the top cells at the end of injection (left column) and at the end of simulation (right column). Saturations computed with ECLIPSE-3D with coarse grid (first row), ECLIPSE-3D with fine grid (second row), ECLIPSE-VE (third row), and MRST-VE (fourth row). The white lines are contour lines of the height of the top of the aquifer with height distance 5 m.

3806

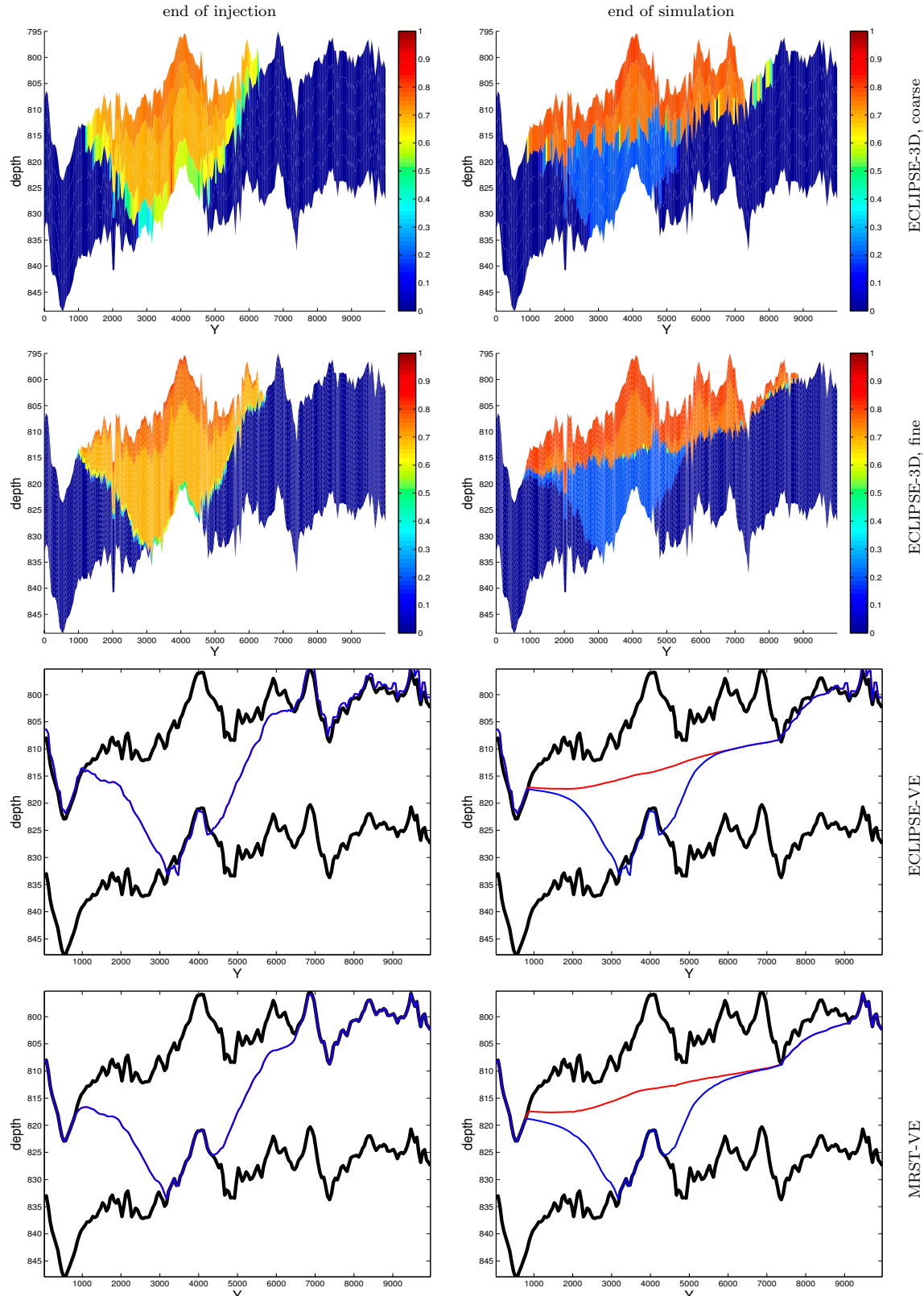
H. Møll Nilsen et al. / Energy Procedia 4 (2011) 3801–3808

Figure 4: CO₂ saturation along vertical cross-section parallel to the x-axis that passes through injection point. Saturation profiles at the end of the injection period (left column) and at the end of simulation (right column). Saturations were computed with ECLIPSE-3D with coarse grid (first row), ECLIPSE-3D with fine grid (second row), ECLIPSE-VE (third row) and MRST-VE (fourth row) simulators. Blue and red lines in the last two rows show contours of trapped and mobile CO₂, respectively; black lines show the position of the bottom and top of the aquifer at the center of the cell.

were performed using both a fully implicit and an implicit-pressure, explicit-saturation (IMPES) formulation. For the coarse grid, the implicit simulation took 14 hours while the IMPES simulation took 36 minutes. The fine-grid 3D simulation took 14 hours using the IMPES option. For ECLIPSE-VE, the fully implicit option was fastest and used 19 minutes, while the IMPES time-stepping scheme used 2 hours. MRST-VE is based on a sequential splitting approach and took 12 minutes.

Figure 3 shows CO₂ saturation in the top cells of the model at the end of injection (32 years) and end of the simulation (132 years). Overall there is a very good agreement between the solution computed with the ECLIPSE-3D simulator in a fine grid and the two VE solutions. The difference between the two ECLIPSE-3D simulations are due to numerical errors that diminish as the grid is refined in the vertical direction. In particular, the CO₂ plume simulated with the coarse grid moves slower than the one simulated with the fine grid. This observation is confirmed by Figure 4, which shows simulated CO₂ saturations in a vertical cross-section that passes through the injection point and is parallel to the x-axis. The difference in plume speed between the coarse and fine grids is caused by CO₂ moving more rapidly for higher saturation values. The large cell size of the coarse grid results in a large difference between the average of the nonlinear relative permeability functions and the relative permeability functions evaluated in the average saturation. The smaller size of the cells in the refined grid reduce this effect and the CO₂ plume expands faster. As the CO₂ plume moves away from the injection area following the top of the numerical domain, it becomes thinner and the numerical errors due to poor vertical discretization become more important. This source of error is absent in the VE models because the vertical geometry of the plume is implicitly accounted for.

Figure 4 also confirms that vertical segregation of CO₂ and brine occurs in relatively short time and that the system reaches vertical equilibrium even before the end of the injection period. Similar patterns were observed in several other cross-sections that are not shown here. If capillary forces were included, they would not change the time required to reach vertical equilibrium, but would introduce a capillary fringe. If the capillary fringe is smaller than the vertical resolution, the vertically-averaged model will still give a better description of the system than the 3D model. Introducing capillary forces in the vertically-averaged model for our homogeneous system, however introduces very little extra computational complexity. If capillary forces were included in the simulations discussed here, the thickness of the capillary fringe would be smaller than the vertical cell spacing, hence the VE models would also give a better representation of the system than the full 3D models.

4. Conclusions

We have presented results of full 3D and 2D vertical-equilibrium simulations of the migration of CO₂ in a realistic model of a site where CO₂ has been stored for more than a decade. The analysis of these results demonstrates that for the specific case of CO₂ migration in the Utsira Sand aquifer, VE models provide solutions that are more accurate. The VE model is much faster than corresponding 3D simulations that resolve the same dynamics. VE models are also more accurate than 3D models when full local segregation is achieved, because the vertical extension of the CO₂ plume is implicitly included in the model so that the VE results are independent of the vertical resolution. This is particularly important for simulations of long-term migration of CO₂, where the plume thins out as it moves farther from the injection site. The VE models have reduced dimensionality compared with full 3D models and also avoid thin cells, thereby gaining a computational advantage. In addition, VE models perform better because of the weaker coupling between the pressure and transport equations [26] which make them more suitable for sequential splitting approaches. Such splitting approaches can be troublesome in three-dimensional simulations of CO₂ migration because of the strong coupling between the pressure and saturation equations caused by gravity.

Based on the results discussed above, we recommend that more effort should go into developing more accurate and faster VE models for simulating CO₂ migration. Moreover, we anticipate that the renewed interest in vertical equilibrium models will result in the development of new simulators that would be able to represent more complex physical mechanisms that affect CO₂ migration such as capillary pressure and CO₂ dissolution into brine.

References

- [1] M. A. Hesse, F. M. Orr, H. A. Tchelepi, Gravity currents with residual trapping, *J. Fluid Mech.* 611 (2008) 35–60.
- [2] R. Juanes, C. W. MacMinn, M. L. Szulczewski, The footprint of the CO₂ plume during carbon dioxide storage in saline aquifers: storage efficiency for capillary trapping at the basin scale, *Tran. Porous Media* 82 (1) (2010) 19–30.
- [3] L. W. Lake, Enhanced oil recovery, Prentice-Hall, 1989.

3808

H. Møll Nilsen et al./Energy Procedia 4 (2011) 3801–3808

- [4] M. A. Hesse, H. A. Tchelepi, B. J. Cantwell, F. M. Orr, Gravity currents in horizontal porous layers: transition from early to late self-similarity, *J. Fluid. Mech.* 577 (2007) 363–383.
- [5] J. M. Nordbotten, M. A. Celia, D. Kavetski, S. Bachu, A semi-analytical model estimating leakage associated with CO₂ storage in large-scale multi-layered geological systems with multiple leaky wells, *Environmental Science and Technology* 43 (3) (2009) 743–749.
- [6] B. Metz, O. Davidson, H. de Coninck, M. Loos, L. Meyer, *Special Report on Carbon Capture and Storage*, Cambridge University Press, UK, 2005.
- [7] J. C. Martin, Some mathematical aspects of two phase flow with application to flooding and gravity segregation, *Prod. Monthly* 22 (6) (1958) 22–35.
- [8] K. H. Coats, R. L. Nielsen, M. H. Terune, A. G. Weber, Simulation of three-dimensional, two-phase flow in oil and gas reservoirs, *Soc. Pet. Eng. J. Dec* (1967) 377–388.
- [9] J. C. Martin, Partial integration of equation of multiphase flow, *Soc. Pet. Eng. J. Dec* (1968) 370–380.
- [10] R. Godderij, J. Bruining, J. Molenaar, A fast 3d interface simulator for steamdrives, *SPE Journal* 4 (4) (1999) 400–408.
- [11] C. H. Neuman, A gravity override model of steamdrive, *J. Petrol. Tech.* 37 (1) (1985) 163–189.
- [12] M. A. Celia, S. Bachu, J. M. Nordbotten, D. Kavetski, S. Gasda, A risk assessment tool to quantify CO₂ leakage potential through wells in mature sedimentary basins, in: *Proceedings of the 8th Conference on Greenhouse Gas Technologies*, 2006.
- [13] C. W. MacMinn, R. Juanes, Post-injection spreading and trapping of CO₂ in saline aquifers: Impact of the plume shape at the end of injection, *Comput. Geosci.* 13 (2009) 483–491.
- [14] H. E. Huppert, A. E. Woods, Gravity-driven flows in porous layers, *J. Fluid Mech.* 292 (1995) 55–69.
- [15] S. Lyle, H. E. Huppert, M. Hallworth, M. Bickle, A. Chadwick, Axisymmetric gravity currents in a porous media, *J. Fluid. Mech.* 543 (2005) 293–302. doi:[10.1017/S0022112005006713](https://doi.org/10.1017/S0022112005006713).
- [16] D. Vella, H. E. Huppert, Gravity currents in a porous medium at an inclined plane, *J. Fluid Mech.* 292 (1995) 59–65.
- [17] S. E. Gasda, J. M. Nordbotten, M. A. Celia, Vertical equilibrium with sub-scale analytical methods for geological CO₂ sequestration, *S. of Comput. Geosci.* 13 (4) (2009) 469–481.
- [18] H. Class, A. Ebigbo, R. Helmig, H. K. Dahle, J. M. Nordbotten, M. A. Celia, P. Audigane, M. Darcis, J. Ennis-King, Y. Fan, B. Flemisch, S. E. Gasda, M. Jin, S. Krug, D. Labregere, A. N. Beni, R. J. Pawar, A. Sbai, S. G. Thomas, L. Trenty, L. Wei, A benchmark study on problems related to CO₂ storage in geologic formations, *Comput. Geosci.* 13 (4) (2009) 409–434. doi:[10.1007/s10596-009-9146-x](https://doi.org/10.1007/s10596-009-9146-x).
- [19] J. M. Nordbotten, M. A. Celia, *Geological Storage of CO₂: Modeling Approaches for Large-Scale Simulation*, for publication with John Wiley, 2010.
- [20] M. Bickle, A. Chadwick, H. E. Huppert, M. Hallworth, S. Lyle, Modelling carbon dioxide accumulation at Sleipner: Implications for underground carbon storage, *Earth Planet. Sci. Lett.* 255 (1-2) (2007) 164–176.
- [21] R. A. Chadwick, P. Zweigle, U. Gregersen, G. A. Kirby, S. Holloway, P. N. Johannessen, Geological reservoir characterization of a CO₂ storage site: The Utsira Sand, Sleipner, Northern North Sea, *Energy* 29 (9-10) (2004) 1371–1381.
- [22] R. Arts, O. Eiken, A. Chadwick, P. Zweigle, L. van der Meer, B. Zinszner, Monitoring of CO₂ injected at Sleipner using time-lapse seismic data, *Energy* 29 (9-10) (2004) 1383–1392.
- [23] V. Singh, A. Cavanagh, H. Hansen, B. Nazarian, M. Iding, P. Ringrose, Reservoir modeling of CO₂ plume behavior calibrated against monitoring data from Sleipner, Norway (2010).
- [24] Schlumberger Information Systems, Eclipse technical description, Report Houston, TX (2007).
- [25] J. Nordbotten, H. Dahle, Impact of the capillary fringe in vertically integrated models for CO₂ storage, Under review.
- [26] I. Ligaarden, H. M. Nilsen, Numerical aspects of using vertical equilibrium models for simulating CO₂ sequestration, in: *Proceedings of ECMOR XII–12th European Conference on the Mathematics of Oil Recovery*, EAGE, Oxford, UK, 2010.

Bibliography

- [1] NILSEN, H.M., SYVERSVEEN, A.R., LIE, K.A., TVERANGER, J., AND NORDBOTTEN, J.M. Impact of top-surface morphology on CO₂ storage capacity. *International Journal of Greenhouse Gas Control* 11 (2012), 221–235.
- [2] SYVERSVEEN, A.R., NILSEN, H.M., LIE, K.A., TVERANGER, J., AND ABRAHAMSEN, P. A Study on How Top-Surface Morphology Influences the Storage Capacity of CO₂ in Saline Aquifers. *Geostatistics* (2012), 481–492.